

1475A-CR-141,120

JOINT INSTITUTE FOR AERONAUTICS AND ACOUSTICS

NASA
National Aeronautics and
Space Administration
Ames Research Center

NASA-CR-169128
19820021235



Stanford University

JIAA TR - 45

THE EFFECT OF BARRIERS ON WAVE PROPAGATION PHENOMENA: WITH APPLICATION FOR AIRCRAFT NOISE SHIELDING

**C.V.M. Mgana
and I-Dee Chang**

LIBRARY COPY

MAY 15 1982

LANGLEY RESEARCH CENTER
LIBRARY, NASA
HAMPTON, VIRGINIA

STANFORD UNIVERSITY
Department of Aeronautics and Astronautics
Stanford, California 94305

MAY 1982



JIAA TR - 45

THE EFFECT OF BARRIERS ON WAVE PROPAGATION PHENOMENA:
WITH APPLICATION FOR AIRCRAFT NOISE SHIELDING

C. V. M. Mgana and I-Dee Chang

The work here presented has been supported by the
National Aeronautics and Space Administration under
Grant No. NASA NCC 2-76.

N82-29111 #



ACKNOWLEDGEMENTS

This work was carried out in part with the support of NASA Grant NASA NCC 2-76. The authors wish to thank Professor K. Karamcheti, Director of the Joint Institute for Aeronautics and Acoustics (JIAA) and Professor H. Levine for their support and invaluable advices. The first author wish also to extend his special thanks to the Tanzania Government, the Technical Assistance Bureau of the International Civil Aviation Organization (ICAO) and the Office of International Affairs Branch of the Federal Aviation Administration of the United States Government for a fellowship which made his studying in the country and this research work possible.



TABLE OF CONTENTS

	<u>Page</u>
ACKNOWLEDGEMENTS.....	i
LIST OF TABLES.....	iv
LIST OF ILLUSTRATIONS.....	v
ABSTRACT.....	viii

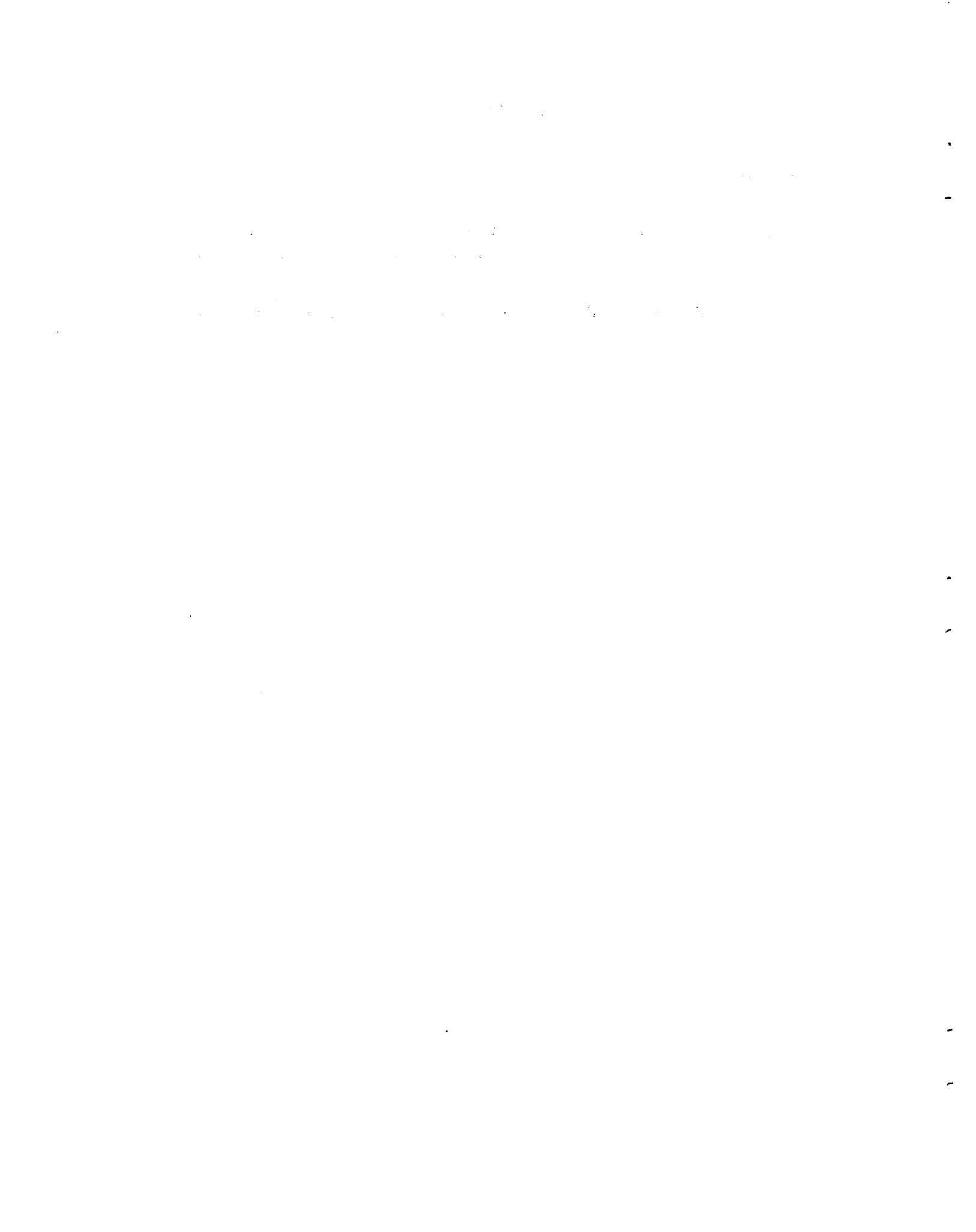
Chapter

I	INTRODUCTION.....	1
II	SLOTTED WING PROBLEM.....	18
	II-1 Background.....	18
	II-2 Mathematical model.....	19
	II-3 Field equations.....	22
	II-4 The first order outer solution.....	22
	II-5 The first order inner solution.....	27
	II-6 The second order outer solution.....	38
	II-7 Discussion and conclusions.....	41
III	GENERAL METHOD FOR HIGH FREQUENCY WAVES.....	45
	III-1 Background.....	45
	III-2 An illustrative problem of diffraction of sound from a three-dimensional source.....	47
	III-3 Solution by stationary phase method..	53
	III-4 Conclusions and discussions.....	69
	III-5 Applications and comparisons with known solutions.....	73

IV	TWO-STREAM-FLOW ACOUSTIC PROBLEM.....	79
IV-1	Nature of the problem.....	79
IV-2	Problem formulation.....	82
IV-3	(1) The dispersion relation of a plane wave in a uniform flow stream.....	84
	(2) Reflection and deflection at the interface of two uniform flows with different velocities U_1 and U_2	85
	(3) The transmission and reflection coefficients.....	87
IV-4	Solution of the two-stream problem....	90
IV-5	Field equations and solution procedure.	93
V	CONCLUSIONS.....	97
V-1	Shielding by a finite plate.....	97
V-2	Effect due to gaps, angular deflection and other geometrical variation of the wing surface.....	106
V-3	Effect due to source distribution on power radiation.....	107
V-4	The effect of uniform flow.....	114
	BIBLIOGRAPHY.....	126

LIST OF TABLES

Table		Page
I	Transition layer thickness as a function of the Mach number.....	124
II	Values of $\bar{\beta}$ when $kr_0 = 2500$ and $\theta_0 = \pi/4$	125



LIST OF ILLUSTRATIONS

Illustrations	Page
2-A Under-the-wing jet blowing.....	18
2-B Slotted wing and noise source in uniform subsonic flow.....	20
2-C Sound emission from a source in the presence of a semi-infinite plate.....	24
2-D Configuration of the slot region.....	27
2-E Geometry of the slot for large distance solution calculation.....	30
2-F The definition of the complex function $\sqrt{z, -l^2/4}$	31
2-G Uniform flow.....	32
2-H Flow past a slot.....	32
2-I Uniform and slot flow superposed.....	33
2-J Flow under the plate in the slot region.....	34
2-K Flow over the plate in the slot region.....	34
2-L Infinity point not in the cut.....	37
2-M Sound field generated by the slot.....	42
2-N Relative amplitude of the velocity potential $ \phi $	42
2-O Induced dipole is proportional to $1/\sqrt{r_0}$	43
2-P Direction of minimum radiation.....	44
3-A Three-dimensional source close to a semi-infinite plate.....	47
3-B Boundaries for the Kirchhoff's integral.....	49

3-C	Acoustic field from a point source with a boundary present.....	51
3-D	Half plane (η, ζ)	56
3-E	Line joining the points S and P passes through the stationary point.....	58
3-F	The range of the limit of integration for $\bar{\beta}$	65
3-G	Acoustic lengths on the projection of the plane (η, ξ)	66
3-H	Graphical sketch of acoustic length in relation to the stationary point....	68
3-I	Wave reception at P due to three-dimensional source in the presence of a semi-infinite plate.....	69
3-J	Variation of the diffraction factor $F(\bar{\beta})$	72
3-K	Two-dimensional problem sketch.....	74
3-L	Plane wave problem showing ranges of integration $(\bar{\beta})$	76
4-A	Over the wing external blowing.....	79
4-B	Two stream flow with plane wave and solid plate.....	80
4-C	An ellipse showing the locus of the incident wave number k_1	84
4-D	Superposed ellipses showing the two stream flow acoustic structure.....	85
4-E	Transition zones in ray acoustics.....	91
4-F	The geometry showing the transformation as in the solution in equation (4-25)..	96
5-A	Geometry defining the diffraction factor for the two-dimensional case.....	98
5-B	Far field approximation of wave reception at P.....	99

Illustration		Page
5-C	Incident wave field variation.....	101
5-D	Reflected wave field variation.....	101
5-E	Configuration of a finite plate and a simple source above it.....	102
5-F	Finite plate solution for $\lambda = 1$ with the source centrally located.....	103
5-G	Finite plate solution for $\lambda = 2$ with the source centrally located.....	104
5-H	Finite plate solution for $\lambda = 2$ with the source not centrally located.....	105
5-I	Spherical geometry for source distribution solution.....	108
5-J	Set up for power approximation for distributed sources.....	110
5-K	Power variation as a function of the wave number k and height h	112
5-L	A monopole in a uniform flow in the presence of a semi-infinite plate.....	114
5-M	Geometry to show the boundary according to ray acoustics.....	116
5-N	A monopole source field in two-dimensional geometry in the presence of a uniform flow.....	118
5-O	A plane wave field in two-dimensional geometry in the presence of a uniform flow.....	119
5-P	Transition zone layout.....	121
5-Q	Transition layer thickness.....	124

1. The first part of the document discusses the importance of maintaining accurate records of all transactions and activities. It emphasizes that this is crucial for ensuring transparency and accountability in the organization's operations.

2. The second part of the document outlines the various methods and tools used to collect and analyze data. It highlights the need for consistent data collection procedures and the use of advanced analytical techniques to derive meaningful insights from the data.

3. The third part of the document focuses on the role of technology in data management and analysis. It discusses how modern software solutions can streamline data collection, storage, and processing, thereby improving efficiency and accuracy.

4. The fourth part of the document addresses the challenges associated with data management, such as data quality, security, and privacy. It provides strategies to mitigate these risks and ensure that the data remains reliable and secure throughout its lifecycle.

5. The fifth part of the document concludes by summarizing the key findings and recommendations. It stresses the importance of ongoing monitoring and evaluation to ensure that the data management processes remain effective and aligned with the organization's goals.

ABSTRACT

In recent years the subject of suppressing aerodynamic noise by shielding has actively been pursued both analytically and experimentally. Although there is a reasonably good agreement between the experimental results obtained under laboratory conditions and analytical results, the comparison is far from being satisfactory under flight conditions where several physical factors come into play in this problem. In order to make a reasonable study of the problem, the whole range of the frequency spectrum has to be studied.

In the present study the frequency spectrum has conveniently been divided into two regimes: the low frequency and high frequency regimes. Two separate methods have been developed for application to each regime.

For the long wave length propagation, the acoustic field due to a point source near a solid obstacle may be treated in terms of an inner region where the fluid motion is essentially incompressible, and an outer region which is a

linear acoustic field generated by the hydrodynamic disturbances in the inner region. This method has been applied to a case of a finite slotted plate modelled to represent a wing extended flap for both stationary and uniformly moving medium.

In the case of short wave length propagation, a very effective approach utilizing a combination of the method of ray acoustics, the Kirchhoff's integral formulation and the stationary phase approximation has been developed. The examples studied using this method include many limiting cases. The solutions of these limiting cases agree with the known solutions. This method, too, has been applied to a new problem of physical interest. The problem consists of a semi-infinite plate in a uniform flow velocity with a point source above the plate and embedded in a different flow velocity to simulate an engine exhaust jet stream surrounding the source.

Chapter I

Introduction:

...."Nature operates by the simplest and most expeditious means"....

-Fermat-

The introduction of more powerful jet engines in civil air transportation in the 1950s drastically revolutionized the aircraft operational speeds and altitudes. The side effect of this advanced technological advance was the build up of noise on approach to land and take off paths on airports.

Although the later generation of engines (turbofans) are relatively quieter, the increased sizes and power delivery of such engines still caused unacceptably high sound pressure levels (generally of the order of 110 dB at 30.5 meters). With a desire to operate aircraft services close to the city centres and to use shorter runways, the Short Take Off and Landing (STOL) concept using enhanced lift produced from the interaction of the engine jet with

the wing and flaps has evolved. This arrangement is used now to shield engine noise from an observer. The concept has attracted a wide range of research activities both analytical and experimental.

The numerous studies on diffraction and noise reduction by barriers can be divided into three groups roughly: theoretical studies, experimental studies using scaled models and full scale experiments under normal environmental conditions.

Comparison of experimental (under laboratory conditions) and theoretical results shows some disagreement for the lower frequency although there is a good agreement for the high frequency end of the spectrum.

A full scale experimental study was extensively carried by Jeffrey and Holbeche (19) using a Delta wing aircraft. In the long wave length region, particularly, the results showed a marked departure from those obtained by scaled model experiments or the theoretical ones. Similar observation is seen in experiments by Conticelli, De Blasi

and O'Keefe (7). Hoch (16) used the Bertin Aerotrainer to study the forward flight effects on aircraft engine noise. The results are in agreement with other studies although, again, there is a disagreement for the low frequency spectrum. Fink (15) reports results that show similar phenomena.

There are many physical factors that exist in the real situation but are generally not included in the analytical studies. In the following discussion, a few of the more important ones are mentioned.

1. Sound Source: In the analytical studies, the source is, in general, simulated mathematically by acoustic poles which are also usually assumed concentrated at a point. In the real situation, the sound is generated aerodynamically over a certain region by the mixing of the high speed turbulent jet with the free stream. Internally, the rotating compressor and the turbine blades are also sources of noise which transmits outside the engine. The

mechanisms of generation and transmission in the source region are extremely complex and by and large of an unknown nature. The strength, frequency content and directivity of the generated sound are not possible to be determined analytically to any degree of accuracy by the present knowledge.

2. Transmission Path: Before reaching the atmosphere, the sound generated at the source region must transmit through the jet exhaust. Due to the temperature, density and velocity non-uniformity and the temporal variations of these quantities caused by turbulence, the transmission characteristics of noise in this "near field" region is not easy to determine theoretically.

3. Shrouding Effect: At the interface between the jet and the free stream, there are strong temperature and velocity gradients resulting in reflection and refraction of the sound waves and causing the intensity, directivity and frequency content to change in the far field from those predicted by any simple theory assuming a uniform atmospheric

condition.

4. Reflection and other Effects due to the Geometry

of the Wing and the Airframe: For the engine

under the wing configuration, for example, sound may be strongly reflected by the under surfaces of the wing and the flaps. This causes a large increase of the sound intensity received on the ground. For the engine over the wing configuration, on the other hand, noise is greatly reduced. During landing, the gap between the main airfoil and the extended flap may cause "leakage" of sound from the upper side of the wing to the under side of the wing and thereby reducing the effectiveness of wing shielding.

5. Frequency on Diffraction: The aircraft noise

spectrum extends from very high frequency sounds to very low frequency ones. The low frequency sounds are not very effectively shielded by the wing because of the strong diffraction of waves of long wave length.

6. Forward Flight Effect: To compare laboratory and

in-flight data, it is important to know how the motion of

the aircraft affects the predicted or measured results.

7. Effect of Shed Vortex: Earlier investigations on wave-barrier interaction did not make any note of the sound that can be generated by shed vortex for finite or semi-infinite surfaces. This issue has occupied several researchers in the last twenty years: Orzag et al (35); Jones (20); Davis (11); Jeffery et al (18); and Broadbent (2), among others.

These studies have indicated that the trailing edge shed vortex has three roles:

- (i) It acts as a shield to sound from one region of such a vortex to the shadow.
- (ii) Such vortex is itself a source of sound.
- (iii) The vortex does refract sound if the source of sound is close to the vortex, but it has less refractive effect if the source is far enough, Cooke (8).

8. Effect of Viscous Boundary Layer: Powell (36)

studied the problem of sound caused by boundary layer on the solid surface. This is what many experimental investigators have referred to as scrubbing noise. In this case the dipole source noise as well as the quadrupole sources are present.

Many of the above phenomena are studied in classical theories in the propagation of light waves. The study of light refraction, reflection and diffraction has a long history. In the field of optics, the basic principles enunciated by Fermat, Huygens and Fresnel have been formulated into a general integral theorem by Kirchhoff. These basic principles, borrowed from the field of optics and later generalized in the general electromagnetic wave propagation after the Maxwell's development of the field equations, have been found applicable in the study of short wave length sound propagation. A combination of these principles has been employed in formulating a method applicable for short wave length acoustic propagation in the present study.

In recent times, with the rapid expansion of the air transportation, the subject of acoustic wave interaction with a barrier has attracted a considerable amount of research. Various theories have been explored in the ensuing search for various solutions to the problem.

The various published theories differ mainly in the way in which the fluctuating flow is assumed to interact with a barrier (with an edge of a plate in particular) to produce sound and fall roughly into the following four categories:

- (i) General theories based on aerodynamic noise based on the Lighthill (1952) acoustic analogy. These have been developed by Curle (10); Ffowcs-Williams and Hawkings (14); Howe (17); Jones (20); Powell (36); Ribner (39) among others.
- (ii) Theories based on the solution of special problems have been tackled by: Broadbent (2,4); Cooke (9); MacDonald (31); Orzag and Crow (35).

- (iii) Theories based on ad hoc models involve postulation of source distribution whose strengths and multipole types are generally determined empirically. This group would include: Clapper et al (6); Lan et al (22); Larson et al (23) and Maekawa (32) among others.
- (iv) The experimental work that generally may include analytical background material may be found in the work of Conticelli et al (7); Fink (15); Hoch (16); Jeffrey et al (18); Lush (30); Reshotko et al (38) and Strout and Atencio (40).

The above list is no way exhaustive but it is representative of the work that has been performed in different approaches. In all cases, however, the main concentration has been the study of short wave phenomena. The present study, presented in chapter II takes the long wave length into account to bridge the apparent gap in the literature.

In the chapters to follow, the wing shielding problem

will be treated in two aspects: One aspect involves sound of long wave length and the second aspects deals with sound of short wave length.

The main purpose of the analysis is to develop mathematical methods and to find physical solutions for the wave-barrier interaction problems typified by Sommerfeld's classical treatment of diffraction by a semi-infinite plate. The particular interest here is in examining the effectiveness of using the wing as a barrier to shield noise from the engine installed above the wing under flight conditions.

In chapter II, the shielding of a concentrated quadrupole sound source by a semi-infinite plate with a narrow slot is considered. This problem simulates the shielding by a wing with the flap in the extended position. The acoustic field as affected by the slot is determined by the method of matched asymptotic expansions, under the assumption of long wave length approximation.

In the outer region, far away from the slot, the presence of the slot can be neglected for a first

approximation. In such a case the solution is easily obtained from the principle of ray acoustics. Such a solution, however, would not be satisfactory in the region close to the slot.

The solution close to the slot is calculated by close examination of the inner flow. The long wave approximation together with the Prandtl-Glauert transformation enables one to derive the inner solution from the Laplace's equation. It is found that the inner solution contains a second order term which is a dipole singularity. In order to match the inner solution to the outer one, it is necessary to calculate the second order terms for the outer expansion. The dipole source term in the inner region becomes the generator of the secondary acoustic disturbances in the far region. It is observed, in conclusion, that the location of the engine noise source in relation to the slot is crucial in the shielding effect of the noise by the wing with a flap.

A method, suitable for deriving solutions for cases of

short wave length, is developed in chapter III. The method combines the basic techniques of ray acoustics, the Kirchhoff's integral and the stationary phase approximation. The basic principle of the method is based on the problem of a semi-infinite plate with a sinusoidal monopole source located above it. In the limit of very large wave number k , the approximate solution can be divided into three regions with sharp discontinuities. The solution is reasonably accurate and the order of the neglected term is $O(\frac{1}{k})$. This solution is not accurate at the boundaries separating the three regions where a transition layer with contributions to the solution to the order of $O(\frac{1}{\sqrt{k}})$ are present.

The method proposed for use is, therefore, to use the Kirchhoff's integral with a surface of integration lying outside the transition layers. One can then use the solution obtained by ray acoustics for ϕ and $\frac{\partial \phi}{\partial n}$ in the Kirchhoff's integral to determine the function ϕ at any point P , including that within the transition layer. The integral

generates the second order correction term which is of order $O\left(\frac{1}{\sqrt{k}}\right)$. The method of stationary phase is used to determine the second order approximation directly from the Kirchhoff's integral. In a sense, the method is to treat the Kirchhoff's integral as an integral equation and then solve it by the iteration procedure, using the ray acoustics as a starting first order approximation.

It is found that the stationary point "window" is of the order of $O\left(\frac{1}{\sqrt{k}}\right)$ where k is the wave number of the wave. The acoustic wave received at a point will depend on the proximity of the stationary point window to the trailing edge. It is then determined that the solution at a point P (observer position) is basically that due to the ray acoustics modified by the shielding factor $F(\bar{\beta})$. The shielding factor is a Fresnel integral form and cuts down the amount of the intensity of the wave as the stationary point window moves close to the edge, so that in the limit, the edge blocks the stationary point window leading to the total zone of silence (shadow).

The method is tested by solving two classical problems of wave diffraction. The first one is the interaction of the sound wave from a three dimensional point source with a semi-infinite plate first studied by MacDonald (31) and later extended by Cooke (9) under the condition of large k , which is the same as the condition of large distance used in the present study. The result obtained is in complete agreement with equation 13 on page 9 of Cooke (9). The second problem is the interaction of a plane wave with a semi-infinite plate. The far field solution obtained by the present method is in agreement with equation 2.86 on page 73 in the book by Noble (34) and with the result obtained more recently by Candel (5).

The method developed in chapter III has been applied to solve a problem of practical interest in chapters IV. The problem involves two flows with a semi-infinite plate separating the two uniform flows of different velocities. A source is assumed imbedded in the flow over the upper

surface of the plate. This is intended to simulate the problem of an engine situated above the wing. The acoustic field in the region below the wing, caused by the transmission and diffracted fields is to be determined. The boundary conditions on the free interface regarding the continuity of pressure and particle displacements determine the reflection and transmission coefficients of the wave at the interface. Using the Kirchhoff's integral for the semi-circular boundary and the theory developed in chapter III, the solution is derived without much difficulty. It is found that, in addition to the shielding factor $F(\bar{\beta})$ dependence, such a solution is dependent on the reflection and refraction of the incident ray at the interface. The Mach number has the effect of changing the boundaries and the thickness of the transition zone.

The main conclusions and applications of the developed principles are outlined in chapter V. From the results obtained in the problem of a semi-infinite plate, results for a finite plate as a model for an aircraft wing are

derived and numerical results presented.

The effect of the gaps, angular deflection and other geometrical variations of the wing surface, which represents the real physical situations has been studied and it is observed that the effects of gaps on the far field is equivalent to that produced by localized acoustic poles induced at the position of the slot.

Another major interesting factor regarding the effects of source distribution which has been studied by Thiessen (41); Levine (27); and Embleton (12) is re-examined for the geometry of the semi-infinite plane. The appropriate power radiation in the different regions determined by ray acoustics is presented in integral form.

Finally, the question of how the flow velocity affects the shielding of a semi-infinite plate in a subsonic flow is briefly studied. It is found that the fluid motion causes two important effects:

- (i) The boundary of the shadowed region depends only on the location of the source relative to the plate

trailing edge.

- (ii) The angular thickness of the transition zone is affected by the fluid motion. The quantitative values of these effects can be numerically evaluated as a function of the Mach number, as shown by a numerical example.

Chapter IITHE SLOTTED WING PROBLEM:II-1 Background:

In recent years the concept of the Short Take Off and Landing (STOL) has evolved a principle of externally blown flap to generate the additional high lift necessary for such operations. In the approach or take off phase, the jet from the engine interacts with the extended flaps. The slots between the main wing and the flaps become sources of noise as shown in figure (2-A). The engine may be situated above or below the wing. Figure (2-A) shows the case of an engine below the wing but the principle applies for the over-the-wing external blowing as well.

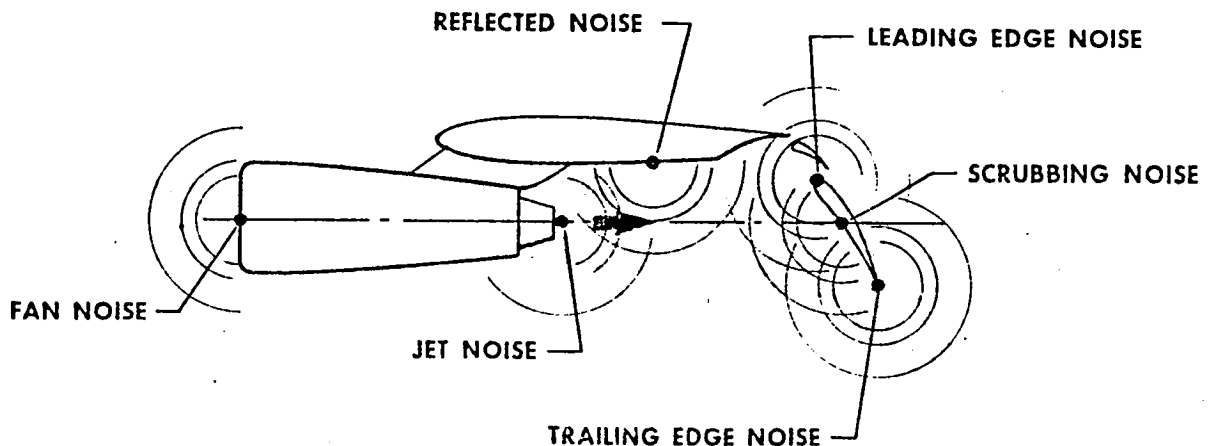


Figure (2-A): Under-the-wing jet blowing.

Although a substantial amount of effort has been made experimentally to determine the noise emitted from the engine jet and the wing/flap interactions (see Lasagna et al (24) and Falarski et al (13)) where it has been observed that the deflection of the flap generates a greater amount of sound intensity, there has been a limited analytical investigation of the problem. Ting (42) and Leppington (25) have investigated curvature effects of barriers on wave diffraction but such work did not involve gaps (slot) effects which is the real situation in the take off and landing phase of aircraft operation. The mathematical model, and method used in the study of this problem is presented in section II-2 below.

II-2 Mathematical Model:

In order to analyse the problem described in section II-1, a model is constructed as in figure (2-B) next page to represent a slotted semi-infinite plate and a quadrupole source S . A uniform flow with Mach number $M < 1$ is assumed. The source S is monochromatic with frequency $f = a_0/\lambda$,

where λ is the wave length and a_0 is the speed of the wave. The dimensions h , b , and L are assumed much larger than the wave length of the propagating wave λ . The plate is assumed to be of zero thickness and zero angle of attack.

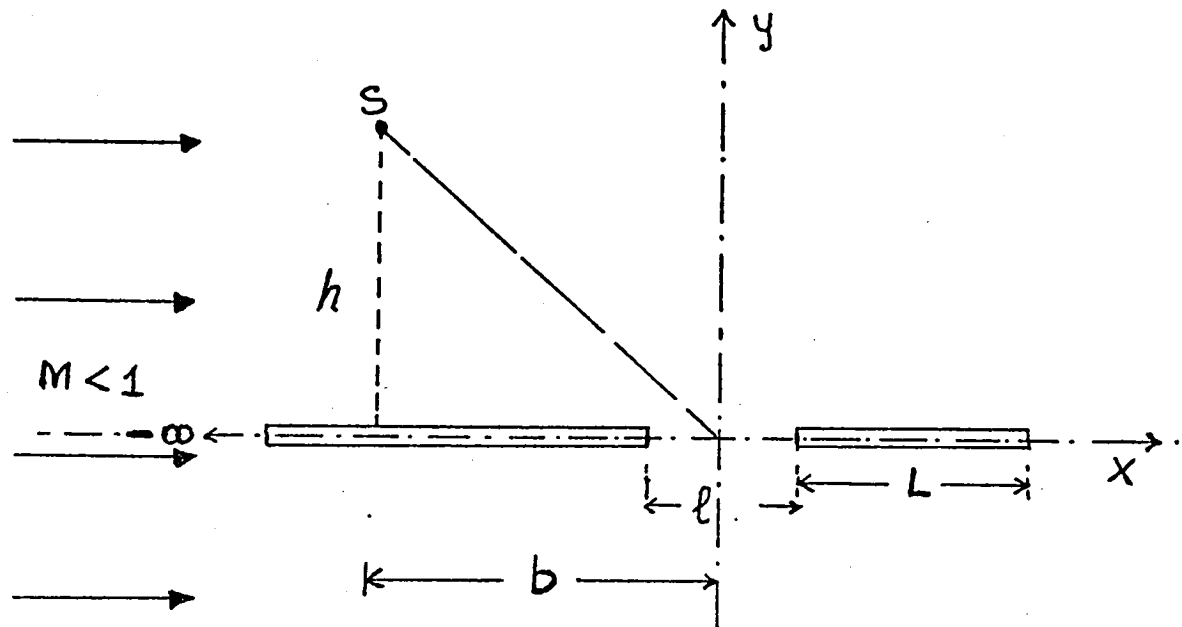


Figure (2-B): Slotted wing and noise source in uniform subsonic flow.

A method of matched asymptotic expansions using $k\ell = \epsilon$ as the small parameter will be applied in the solution of this problem. In the region far from the slot ($r \gg \ell$), the presence of the slot may be neglected in the first approximation. The solution for this region is referred to

as the outer solution. For convenience, the outer solution is constructed by the ray acoustics on the account that by assumption $\lambda \ll h, b, \text{ and } L$. As a result, the solution for the outer region has discontinuities at the boundary of the regions according to ray acoustics and it is necessary therefore to relax condition (ii) in section II-3 to allow such discontinuities. In the small neighbourhood surrounding the slot, the time variation of the fluid motion is nearly simultaneous and therefore a quasi-steady approximation may be applied to the wave equation. The resulting equation is the steady compressible flow equation which can be reduced to the form of the Laplace equation by the Prandtl-Glauert transformation. In solving for the inner solution near the slot, the exact boundary condition of the slot must be used. however.

In the following analysis the total velocity potential Φ will be written as the superposition of the uniform flow potential Ux and a perturbation potential ϕ , so that:

$$\Phi = Ux + \phi \quad (2-1)$$

where ϕ is the potential due to the presence of the source and the slotted plate. The solution of ϕ is sought in the analysis that follows.

II-3 Field Equations:

The governing equation is the convected wave equation:

$$(1-M^2) \frac{\partial^2 \phi}{\partial x^2} + \frac{\partial^2 \phi}{\partial y^2} - 2ikM \frac{\partial \phi}{\partial x} + k^2 \phi = \frac{\partial^2}{\partial x_i \partial x_j} \left[T_{ij} \delta(x+b) \delta(y-h) \right] \quad (2-2)$$

where ϕ is the velocity potential defined in equation (2-1)

with $\frac{\partial^2}{\partial x_i \partial x_j} = \left(\frac{\partial^2}{\partial x^2}, \frac{\partial^2}{\partial x \partial y}, \frac{\partial^2}{\partial y^2} \right)$ and T_{ij} is the amplitude of the source strength in tensor notation. The boundary

conditions for this problem are:

- (i) $\frac{\partial \phi}{\partial y} = 0$ on $y = 0$; $-\infty < x \leq -l/2$ and $l/2 \leq x \leq (L + l/2)$.
- (ii) ϕ , $\frac{\partial \phi}{\partial x}$, $\frac{\partial \phi}{\partial y}$ are continuous everywhere except on the plate surface.
- (iii) The Sommerfeld radiation condition requiring outgoing wave at infinity must be satisfied.

II-4 The first order outer solution.

The first order outer solution will be derived by the

use of ray acoustics approximation. (This is not a necessary assumption, but it will serve to give an explicit solution to illustrate the procedure better). The outer region is, by definition, one which is far from the slot. In this region, one may assume an outer expansion of the form:

$$\phi = \tilde{\phi}_0 + \epsilon \tilde{\phi}_1 + \epsilon^2 \tilde{\phi}_2 + \dots \quad (2-3)$$

The first order solution for $\tilde{\phi}_0$ corresponds to the case when $\epsilon = 0$; that is, $\tilde{\phi}_0$ can be obtained from equation (2-2) with the approximation that the slot does not exist.

The solution for $\tilde{\phi}_0$ for a semi-infinite plate and a quadrupole source above it is derived by the method of ray acoustics. The acoustic field due to the source, according to this method, can be divided into three regions: a region where both the incident and reflected waves are present; another region where only the incident wave prevails and finally one finds a region (below the plate) which is in a complete shadow, figure (2-C) next page.

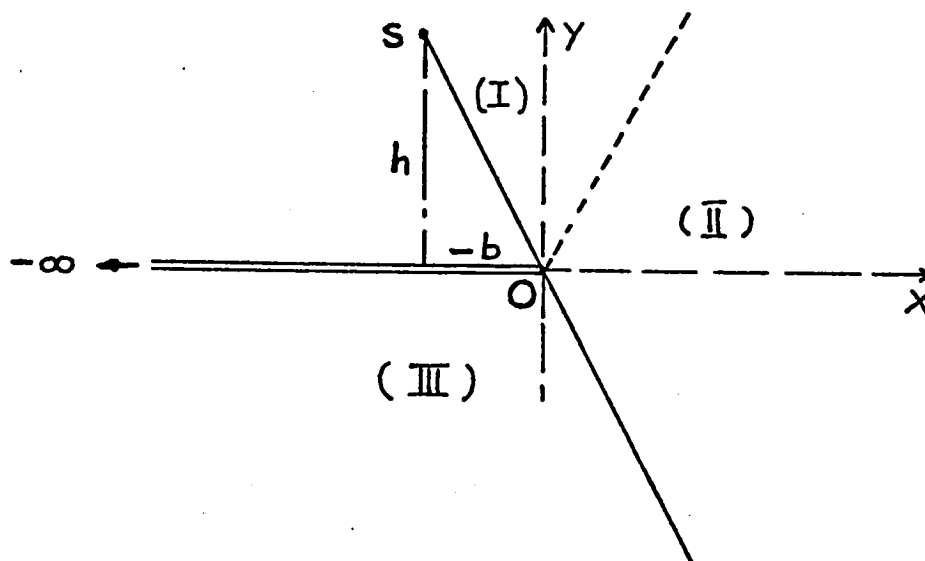


Figure (2-C): Sound emission from a source in the presence of a semi-infinite plate.

The solution for a monopole source at position $(-b, h)$ in uniform flow is known in the literature (ref. 37), and is given as:

$$\phi = e^{\frac{ikMX}{1-M^2}} \left[H_0^{(1)} \left(\frac{kr}{1-M^2} \right) \right] \quad (2-4)$$

where $r = \left[(x+b)^2 + (1-M^2)(y-h)^2 \right]^{1/2}$ and $H_0^{(1)} \left(\frac{kr}{1-M^2} \right)$

being the Hankel functions of the first kind and zeroth order.

The solution for a quadrupole can be constructed using equation (2-4). For the present purpose, only solutions of

$\tilde{\phi}_0$ in regions I and III are needed. In region I above the plate, $\tilde{\phi}_0$ is given by:

$$\tilde{\phi}_0 = \frac{\partial^2}{\partial x_i \partial x_j} \left[\pi_{ij} e^{\frac{ikM(x+b)}{1-M^2}} \left\{ H_0^{(1)}\left(\frac{kr}{1-M^2}\right) \mp H_0^{(1)}\left(\frac{k\bar{r}}{1-M^2}\right) \right\} \right] \quad (2-5)$$

$$\text{where } \bar{r} = \left[(x+b)^2 + (1-M^2)(y+h)^2 \right]^{1/2}$$

In equation (2-5) above, the term involving $H_0^{(1)}\left(\frac{kr}{1-M^2}\right)$ gives the potential due to the quadrupole in the absence of the plate; while the second term involving $H_0^{(1)}\left(\frac{k\bar{r}}{1-M^2}\right)$ is introduced to satisfy the solid boundary condition on the plate surface.

The appropriate sign in equation (2-5) is chosen in such a way that for quadrupoles whose directional derivatives involving $\frac{\partial^2}{\partial x^2}$ or $\frac{\partial^2}{\partial y^2}$ terms, a plus sign is selected between the two terms; while a minus sign is used for quadrupoles whose directional derivatives involve terms of the form $\frac{\partial^2}{\partial x \partial y}$.

According to ray acoustics, however, there is no acoustic perturbation in region III under the plate; so that:

$$\tilde{\phi}_o = 0 \quad (2-6)$$

From the first order solutions equations (2-5) and (2-6) for the acoustic perturbation, the velocity field can be determined. The perturbed velocities for the upper and lower surfaces of the plate are given by:

$$\left. \begin{array}{l} \text{over the plate } \tilde{u}_o = \left(\frac{\partial \tilde{\phi}_o}{\partial x} \right)_{y=0}, \quad \tilde{v}_o = 0 \\ \text{below the plate } \tilde{u}_o = 0, \quad \tilde{v}_o = 0 \end{array} \right\} \quad (2-7)$$

The velocity is, therefore, tangential to the plate and discontinuous across the plate. Such a discontinuity is acceptable across the plate but is not acceptable across the slot. Near the slot, a region referred here as the inner region (see figure 2-D), an inner solution must be constructed.

The velocity component at the slot is denoted as:

$$\tilde{U} = \left(\frac{\partial \tilde{\phi}_o}{\partial x} \right)_{\substack{x=0 \\ y=0}} \quad (2-8)$$

where $x = 0$ and $y = 0$ is the location of the centre of the slot. \tilde{U} is an implicit function of the location, strength and direction of the quadrupole source. The velocity field in the inner region should approach \tilde{U} on the upper side of the plate, but will go to zero in the lower part of the plate.

II-5 The first order inner solution.

The inner region is a region of the dimension $O(\ell)$ containing the slot figure (2-D). Since the wave length is much larger than the width of the slot ($\lambda \gg \ell$), the time variation is nearly simultaneous for all points inside this region; so that the differential equation to the first order approximation is a steady flow equation.

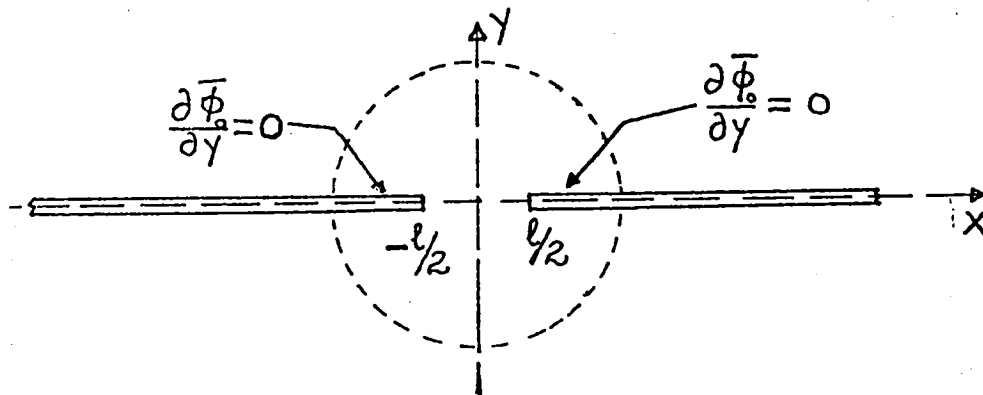


Figure (2-D): Configuration of the slot region.

More precisely, one may write the potential ϕ in terms of the following inner expansion:

$$\phi \simeq \bar{\phi}_0 + \varepsilon \bar{\phi}_1 + \dots \quad (2-9)$$

Substituting such an expansion into the governing equation (2-2); and after the quasi-steady state approximation is applied; the first order inner solution $\bar{\phi}_0$ satisfies the following Prandtl-Glauert equation:

$$\left(1 - M^2\right) \frac{\partial^2 \bar{\phi}_0}{\partial x^2} + \frac{\partial^2 \bar{\phi}_0}{\partial y^2} = 0 \quad (2-10)$$

For the potential $\bar{\phi}_0$, the exact boundary conditions at the slot will be used. However, since the slot is narrow, the plate may be treated as infinite in both directions. In addition, $\bar{\phi}_0$ must match the outer solution at large distances; so that the boundary conditions may be stated as follows:

$$(i) \quad \frac{\partial \bar{\phi}_0}{\partial y} = 0 \quad \text{on } y = 0, \quad -\infty < x < l/2 \quad \text{and} \quad l/2 < x < \infty$$

$$(ii) \quad \bar{\phi}_0, \quad \frac{\partial \bar{\phi}_0}{\partial x}, \quad \frac{\partial \bar{\phi}_0}{\partial y} \quad \text{must be continuous in the flow region.}$$

$$(iii) \quad \bar{\phi}_0 \quad \text{is to match the outer solution.}$$

This last condition requires that the velocity field obtained from $\bar{\phi}_0$ must match with the outer velocity field,

thus:

$$\frac{\partial \bar{\phi}_0}{\partial x} = \tilde{U} \quad \text{as } y \rightarrow +\infty$$

and $\frac{\partial \bar{\phi}_0}{\partial x} = 0 \quad \text{as } y \rightarrow -\infty$

The above boundary value problem may be solved by introducing the complex potential $F_0 (z_1)$ given by:

$$F_0 (z_1) = \phi (z_1) + i \psi (z_1)$$

where $\phi (z_1)$ and $\psi (z_1)$ are the velocity potential and stream functions respectively. The solution $\bar{F}_0 (z_1)$ adapted from ref. 33 is given by:

$$\bar{F}_0 (z_1) = \tilde{U}/2 \left[z_1 + \sqrt{z_1^2 - l^2/4} \right] \quad (2-11)$$

where $z_1 = x_1 + i y_1$; $x_1 = x$, $y_1 = y \sqrt{1-M^2}$, $i = \sqrt{-1}$

The function $\sqrt{z_1^2 - l^2/4}$ is defined as

$$\sqrt{z_1^2 - l^2/4} = \sqrt{r_+ r_-} e^{i \frac{\theta_+ + \theta_-}{2}} \equiv a + ib$$

where r_+ , r_- , θ_+ , and θ_- are as shown in the figure (2-E)

below. The functions $\bar{\phi}_0$ and $\bar{\psi}_0$ can now be written as:

$$\bar{\phi}_0(P) = \tilde{U}/2 \left[x_1 + \sqrt{r_+ r_-} \cos \frac{\theta_+ + \theta_-}{2} \right]$$

$$\bar{\psi}_0(P) = \tilde{U}/2 \left[y_1 + \sqrt{r_+ r_-} \sin \frac{\theta_+ + \theta_-}{2} \right]$$

where θ_+ and θ_- are such that the point P should not move across the cut in figure (2-F) next page.

In terms of $\bar{\phi}_0$, the analysis above gives; at large distance from the slot:

$$\bar{\phi}_0 \approx \tilde{U}_x - \frac{l^2 \tilde{U}_x}{16 [x^2 + (1-M^2) y^2]} + \dots \quad y > 0; \quad (2-12) \quad (a)$$

$$\bar{\phi}_0 \approx + \frac{l^2 \tilde{U}_x}{16 [x^2 + (1-M^2) y^2]} + \dots \quad y < 0; \quad (2-12) \quad (b)$$

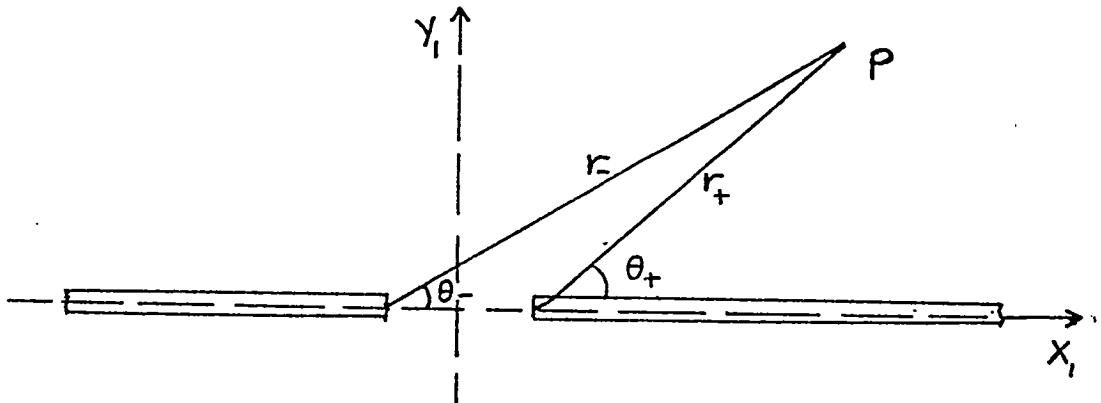


Figure (2-E): Geometry of the slot for large distance solution calculation.

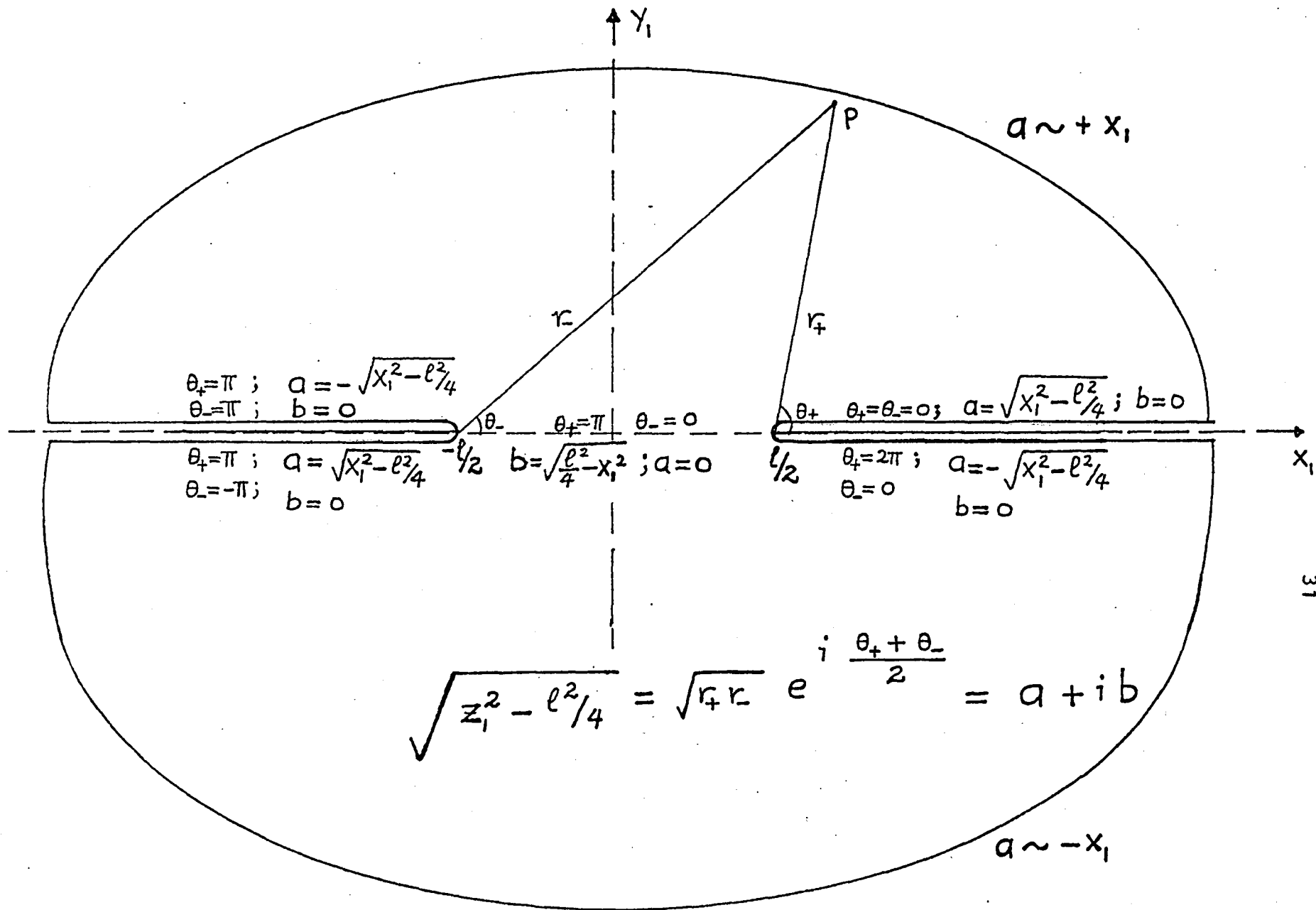


Figure (2-F): The definition of the complex function $\sqrt{z^2 - l^2/4}$

The first term of the solution given by equations (2-12) matches with the velocity of the first order outer flow field $\tilde{\phi}$; while the second term has a form of a dipole and represents the effect of the slot.

The inner solution has some rather interesting features. In equation (2-11), the first term $\tilde{U}z_1/2$ represents a uniform flow of velocity $\tilde{U}/2$ along the direction of the positive X-axis, figure (2-G). The second term $\tilde{U}/2 \sqrt{z_1^2 - l^2/4}$ represents a flow past a slot as shown by figure (2-H) below.

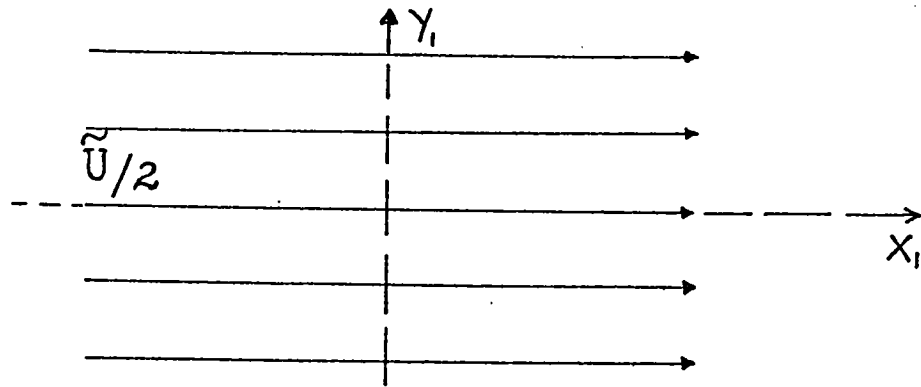


Figure (2-G): Uniform flow.

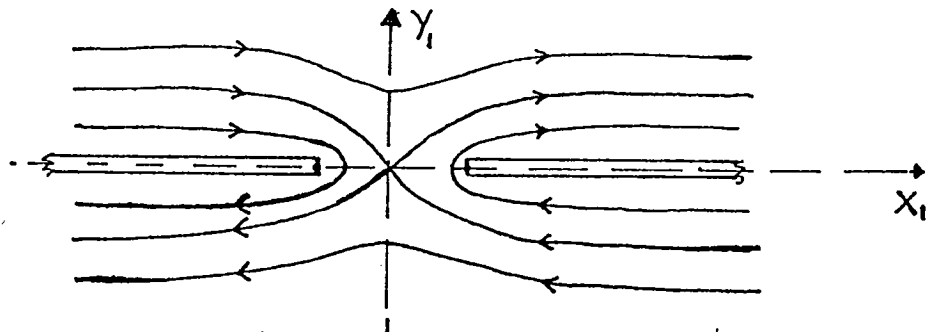


Figure (2-H): Flow past a slot.

The streamlines are adapted from (Ref. 33) with a change in the branch cut. When the uniform flow represented in figure (2-G) is superposed to figure (2-H), the flow velocity in the upper plane approaches the uniform velocity \tilde{U} at large distances; while in the lower region, the flows in the two figures are in opposite direction and tend to cancel out, so that only the flow velocities of lower order are present. The resulting flow pattern is shown in figure (2-I) below. Attention is called to the fact that the flow depicted here represents the perturbation potential ϕ of equation (2-1).

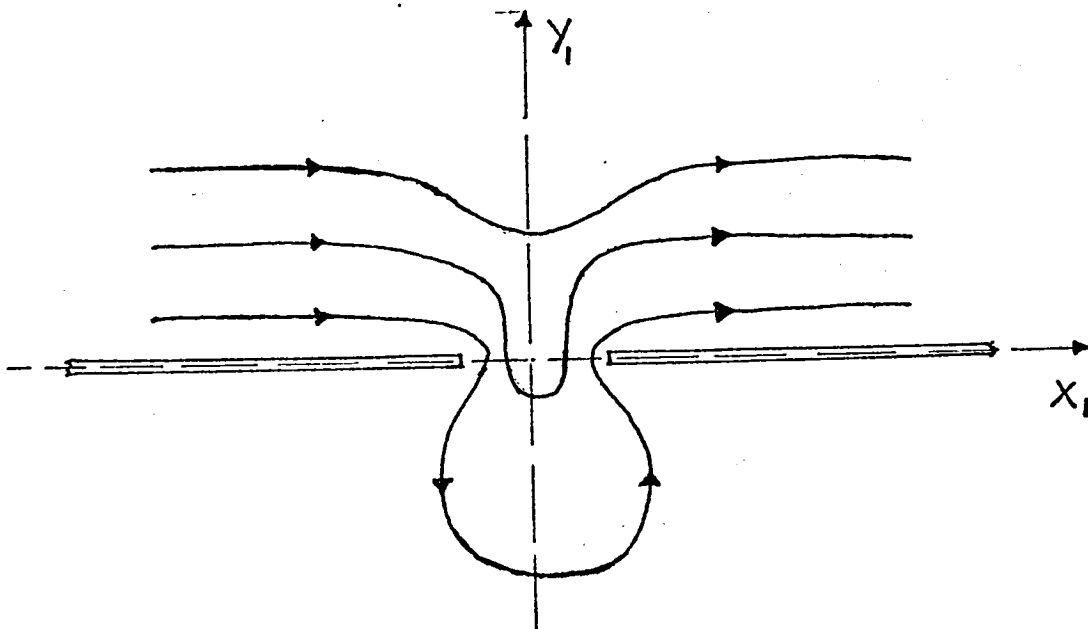


Figure (2-I): Uniform and slot flow superposed..

It is noted that at large distances, the flow field under the plate looks like that of a dipole with a source at $(-\ell/2, 0)$ and a sink at $(\ell/2, 0)$ figure (2-J) below. This flow is represented by the first term in the asymptotic expansion in equation (2-12) (b). In the upper half plane, the streamlines bend downward toward the plate on the left side of the slot and turn away from the plate on the right side of the slot. At large distances, the flow pattern is equivalent to the superposition of a uniform flow of velocity \tilde{U} and a dipole with a sink located on the left edge $(-\ell/2, 0)$ of the slot, figure (2-K).

Figure (2-J): Flow under the plate in the slot region.

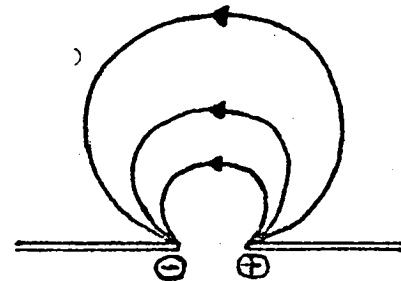
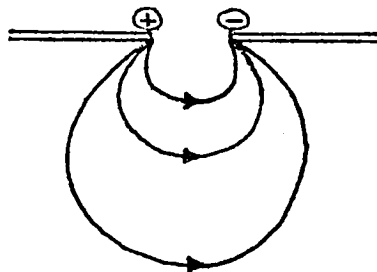


Figure (2-K):

Flow over the plate in the slot region

Thus the far field generated by the slot in a basic flow of velocity \tilde{U} for $y_1 > 0$; and zero velocity for $y_1 < 0$ is of a rather peculiar nature, namely, the perturbation at large distances are the perturbation given by dipoles of different signs. Note also that at both edges of the gap ($x_1 = \pm \ell/2, 0$) the x - velocity component has a well known square-root singularities which arise due to the assumption of the plate being of zero thickness.

On the line $y_1 = 0$, downstream of the plate, the velocity fields generated by the two dipoles of opposite signs are discontinuous. The velocity components given by the two dipoles are both zero at $y_1 = 0$ and hence are continuous, but the u - components are non-zero and of opposite signs and hence discontinuous. Since $y_1 = 0$ is the boundary between the acoustic field generated by the two dipoles (one on the upper surface and one on the lower surface of the plate) this discontinuity is acceptable according to ray acoustics.

There are three important observations to be made about

the inner solution.

- (i) The slot acts like a dipole.
- (ii) The axis of the dipole is along the surface of the plate (X_1 -axis).
- (iii) The signs of the dipole are different for the region $y_1 > 0$ and $y_1 < 0$.

A simple explanation of these features is given as follows:

(a) Due to the long wave length assumption ($l/\lambda \ll 1$), the effect of the slot is mathematically equivalent to the scattering of a plane wave by the incompressible flow region surrounding a small particle (Rayleigh scattering of scalar waves). The inner solution surrounding the slot, therefore, acts like a dipole to the outer acoustic field.

(b) By the assumption of a thin plate lying on the X_1 -axis, the dipole must lie on the X_1 -axis ($y_1 = 0$) with an axis directly along the plate. A vertical dipole would generate a vertical velocity component at $y_1 = 0$ and this cannot satisfy the boundary conditions imposed on $y_1 = 0$.

(c) The reason that the dipole has a different sign is mathematically due to the choice of the branch cut for the function $\sqrt{z_1^2 - \ell^2/4}$ as shown on page 31.

In the branch cut as in figure (2-L) below, the infinity point will not be contained in the cut. In such a case, the real part of $\sqrt{z_1^2 - \ell^2/4}$ denoted by \mathcal{Q} will approach the same value x_1 both for $y_1 \rightarrow \infty$ and $y_1 \rightarrow -\infty$.

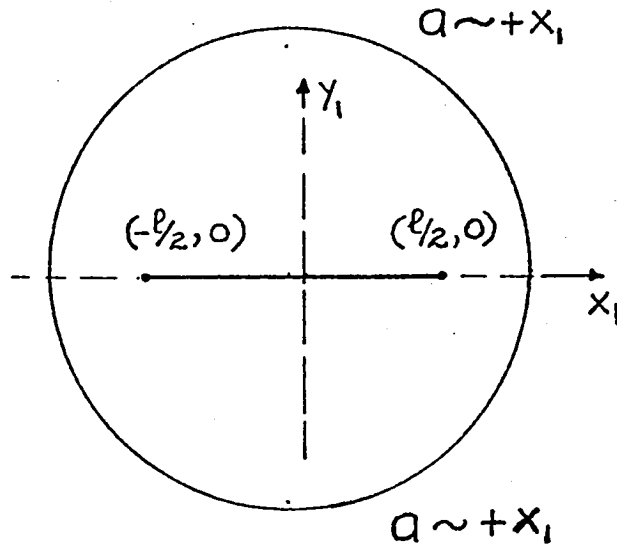


Figure (2-L): Infinity point not in the cut.

In the present problem, however, the matching condition imposed by the outer solution requires that $\mathcal{Q} \rightarrow x_1$ as $y_1 \rightarrow \infty$ and $\mathcal{Q} \rightarrow -x_1$ as $y_1 \rightarrow -\infty$. In order to obtain this result it is

necessary to draw the branch cut from $x_1 = -\ell/2$ to $-\infty$ and from $x_1 = \ell/2$ to $+\infty$. In this way, the infinity points of the two upper and lower planes, in figure (2-F) are on two different Riemann sheets in figure (2-L) so that the behaviour of the function and hence the dipoles have different sign for $y_1 > 0$ and $y_1 < 0$. Physically, the reason that the matching conditions require the real part of $\sqrt{z_1^2 - \ell^2/4}$ to behave like x_1 for $y_1 > 0$ and $-x_1$ for $y_1 < 0$ is that the outer solution for the upper and lower regions are obtained by ray acoustics, and there are strong discontinuities at the interfaces of the different regions.

II-6 The Second Order Outer Solution:

The differential equation for the second order outer solution is:

$$(1-M^2) \frac{\partial^2 \tilde{\phi}_1}{\partial x^2} + \frac{\partial^2 \tilde{\phi}_1}{\partial y^2} - 2ikM \frac{\partial \phi_1}{\partial x} + k^2 \phi_1 = 0 \quad (2-13)$$

The appropriate boundary conditions are:

(i) $\tilde{\phi}_1$; $\frac{\partial \tilde{\phi}_1}{\partial x}$; $\frac{\partial \tilde{\phi}_1}{\partial y}$ must be continuous except

at the plate and at the boundaries according to ray acoustics.

(ii) Radiation at infinity must be satisfied.

(iii) $\tilde{\phi}_1$ must match with the inner solution.

This means that as x and y approach the position of the slot ($x = y = 0$); $\tilde{\phi}_1$ takes the asymptotic values below. One must note that the discontinuity of the solution on $y = 0$ for $x > \ell/2$ must be admitted just like the discontinuities on ray acoustics boundaries.

$$\left. \begin{array}{l} \text{over the plate } \tilde{\phi}_1 \approx - \frac{\ell^2 U_x}{16(x^2 + (1-M^2)y^2)} \\ \text{below the plate } \tilde{\phi}_1 \approx + \frac{\ell^2 U_x}{16(x^2 + (1-M^2)y^2)} \end{array} \right\} \quad (2-14)$$

The solution for $\tilde{\phi}_1$ may be obtained by direct observation as follows:

Considering $\tilde{\phi}_1$ in region I above the plate, one may write:

$$\tilde{\phi}_1 = \frac{\partial}{\partial x} \left[A e^{\frac{ikMx}{1-M^2}} H_0^{(1)} \left(\frac{k}{1-M^2} \sqrt{x^2 + (1-M^2)y^2} \right) \right] \quad (2-15)$$

Where A is a constant to be determined. The above expression for $\tilde{\phi}_1$ represents a two-dimensional acoustic dipole in a uniform flow, and is obviously a solution of the governing equation (2-13). Such a solution also satisfies the radiation condition at infinity since it represents an outgoing wave. To determine the constant A by the marching condition one must expand the expression for small values of x and y to obtain:

$$\begin{aligned} \epsilon \tilde{\phi}_1 &= \epsilon \frac{\partial}{\partial x} \left[\frac{2Ai}{\pi} \ln \left(\sqrt{x^2 + (1-M^2)y^2} \right) \right] & (2-16) \\ &= \frac{klAi}{\pi} \frac{\partial}{\partial x} \left[\ln \left(x^2 + (1-M^2)y^2 \right) \right] \\ &= \frac{2klAi}{\pi} \frac{x}{\left[x^2 + (1-M^2)y^2 \right]} \end{aligned}$$

Comparing expression (2-16) above with the inner solution as presented in equation (2-12) one obtains:

$$\frac{2klAi}{\pi} = \frac{\tilde{U} l^2}{16}$$

so that
$$A = - \frac{\pi \tilde{U} l i}{32k} \quad (2-17)$$

Hence

$$\tilde{\phi}_1 = -\frac{\pi \ell^2 \tilde{U} i}{3z} \frac{\partial}{\partial x} \left[e^{\frac{ikMx}{1-M^2}} H_0^{(1)} \left(\frac{k}{1-M^2} \sqrt{x^2 + (1-M^2)y^2} \right) \right] \quad (2-18) \text{ (a)}$$

$y > 0$

Similarly, one finds that in region III below the plate:

$$\tilde{\phi}_1 = +\frac{\pi \ell^2 \tilde{U} i}{3z} \frac{\partial}{\partial x} \left[e^{\frac{ikMx}{1-M^2}} H_0^{(1)} \left(\frac{k}{1-M^2} \sqrt{x^2 + (1-M^2)y^2} \right) \right] \quad (2-18) \text{ (b)}$$

$y < 0$

II-7 Discussion and Conclusions:

(1) From the equations (2-18), one observes that the effect of the slot is equivalent to a dipole situated at the position of the slot. The strength of the dipole is directly proportional to \tilde{U} which is the velocity at the surface location of the slot due to the quadrupole. \tilde{U} is a scalar function of the strength, directivity and location of the quadrupole T_{ij} , and may be determined by the use of equations (2-5) and (2-8), when the value of T_{ij} is explicitly given. Note that the dipole is of opposite sign on the two sides of the slot figure (2-1).

(2) The sound field pattern generated by the slot in the

uniform moving medium is sketched in figure (2-M) below and the relative amplitude pattern for the velocity potential is in figure (2-N) below.

(3) The strength of the induced dipole is proportional to (l^2) , so that if the slot width l is reduced by half (say), the strength of the dipole is reduced four times.

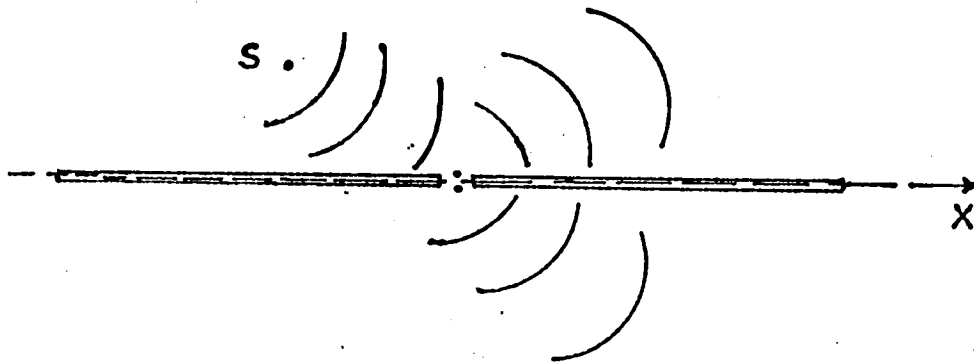


Figure (2-M): Sound field generated by the slot.

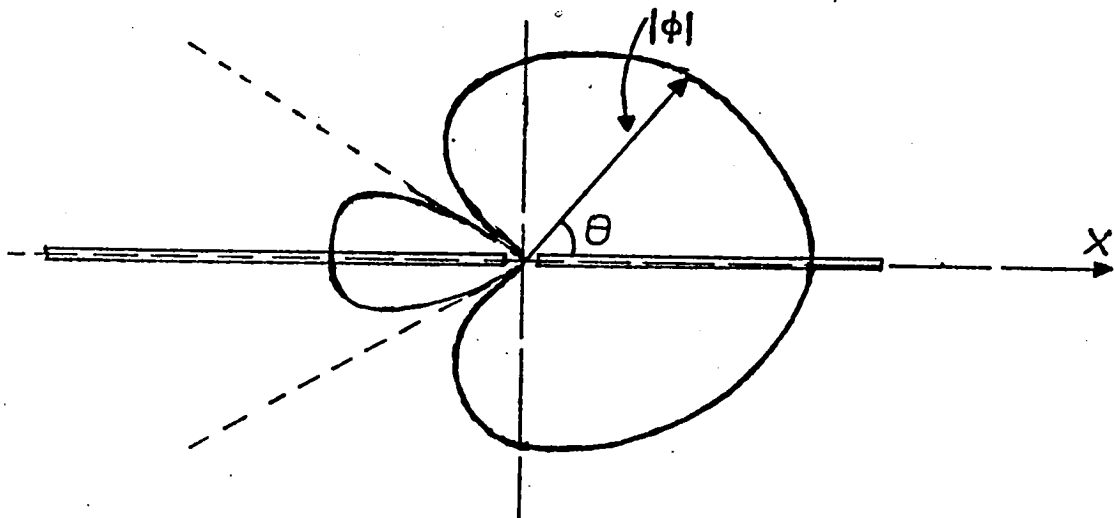


Figure (2-N): Relative amplitude of the velocity potential $|\phi|$.

(4) The asymptotic behaviour of the Hankel function of argument α is:

$$H_0^{(1)}(\alpha) \approx \frac{e^{i\alpha}}{\sqrt{\alpha}} \quad \text{as } \alpha \rightarrow \infty$$

Hence the strength of the induced dipole is proportional to $\frac{1}{\sqrt{r_0}}$ when $r_0 \gg \ell$ and $r_0 = \sqrt{b^2 + (1-M^2)h^2}$ as shown in figure (2-0) below. This means that when M is not too small, b has a greater weighting in the determination of the value of r_0 , so that an increase in the horizontal distance is more effective in reducing the strength than the increase in vertical distance from the plate to the source.

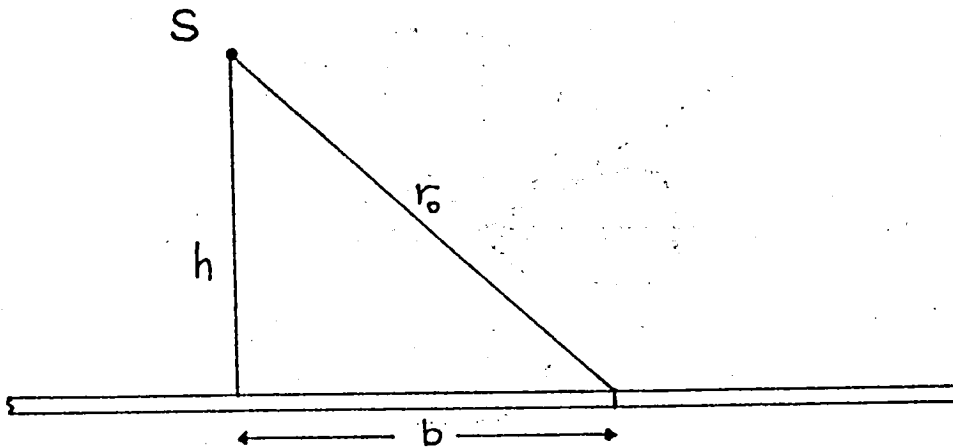


Figure (2-0): Induced dipole is proportional to $\frac{1}{\sqrt{r_0}}$.

(5) When the original sound source has a directivity (such as a quadrupole), it is advisable to locate the slot in the direction of minimum radiation (see figure (2-P) below.

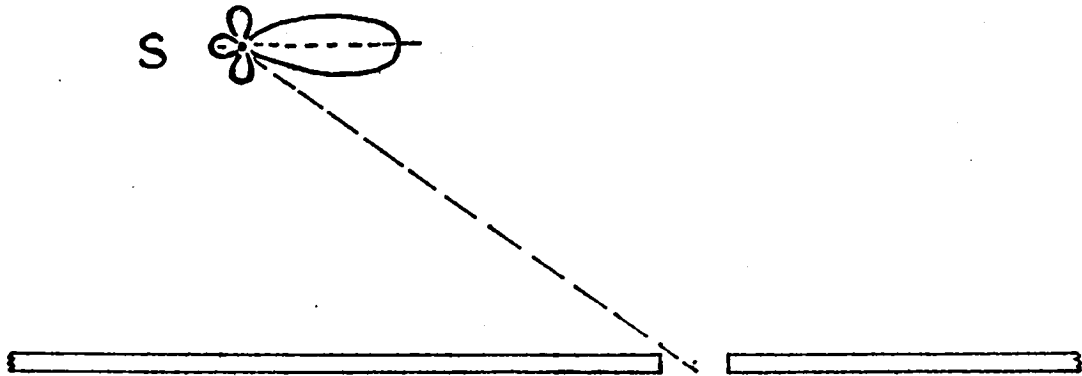


Figure (2-P): Direction of minimum radiation.

1. The first part of the document discusses the importance of maintaining accurate records of all transactions and activities. It emphasizes that this is crucial for ensuring transparency and accountability in the organization's operations.

2. The second part of the document outlines the various methods and tools used to collect and analyze data. It highlights the need for consistent and reliable data collection processes to support informed decision-making.



3. The third part of the document provides a detailed overview of the organization's current status and performance. It includes key metrics and indicators that demonstrate the progress made towards the organization's strategic goals.

4. The final part of the document discusses the future outlook and the strategies being implemented to address the challenges and opportunities ahead. It outlines the organization's commitment to continuous improvement and innovation.

Chapter III:GENERAL METHOD FOR HIGH FREQUENCY WAVES:III-1 Background:

The development given below indicates a general method that will be used in solving problems of acoustic wave propagation in the high frequency end of the wave spectrum. The method is developed out of a combination of the ray acoustics, Kirchhoff's integral and the stationary phase method and applied to the problem of a semi-infinite solid plate.

The basic principle can be outlined as follows. Consider a sinusoidal monopole source located above the semi-infinite plate. In the limit of very large wave number k , the approximate solution can be constructed by means of ray acoustics. The solutions are defined in three regions with sharp discontinuities. The solution is reasonably accurate and the order neglected is $O\left(\frac{1}{k}\right)$. This solution is not accurate at the boundaries separating the three regions where a transition layer with contributions to the solution

of $O\left(\frac{1}{\sqrt{k}}\right)$ are present. The proposed method uses the Kirchhoff's integral with a surface lying outside the transition layers. The solution obtained by ray acoustics defines the first approximate solution for ϕ and $\frac{\partial \phi}{\partial n}$ that are contained in the Kirchhoff's integral. It is then possible to determine the function ϕ at any point P including that within the transition layer. This integral generates the second order correction which is of order $O\left(\frac{1}{\sqrt{k}}\right)$. The method of stationary phase is used to determine the second order approximation directly by applying the stationary phase method to the integral.

In a sense, the method is to treat the Kirchhoff's integral as an integral equation which is solved by an iterative procedure using the ray acoustics solution as a first approximation.

In order to demonstrate the development and application of the method, a three-dimensional problem is solved as in Section III-2 which follows, From the solution derived for the three-dimensional problem, the solution for a two

dimensional case is deduced and compared to already known solutions. Such a comparison shows a good agreement for the present solution with known solutions obtained by more elaborate mathematical procedures.

III-2 An Illustrative Problem of Diffraction of Sound from a Three-Dimensional Source.

A three-dimensional source S is situated above a semi-infinite plate as shown in figure (3-A) below.

Problem Statement: The acoustic field due to a sinusoidal monopole source located above a semi-infinite plate in a stationary medium is to be determined.

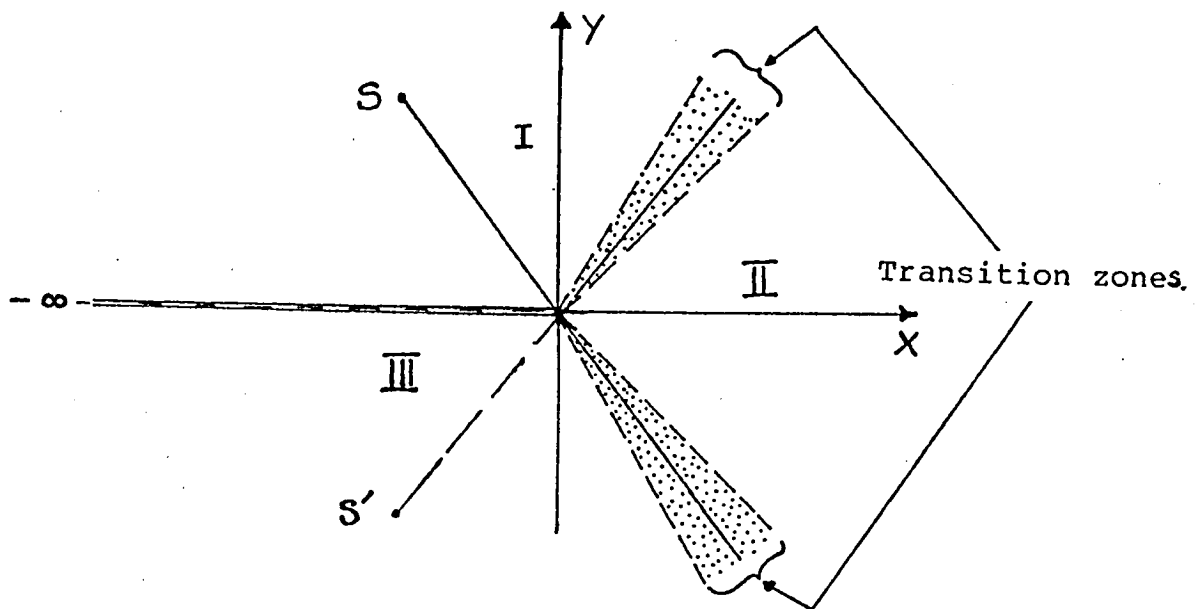


Figure (3-A): Three-dimensional source close to a semi-infinite plate.

Assumptions: (i) A simple (three-dimensional) source whose wavelength is short is used.

(ii) A semi-infinite plane extends along the $-\infty < x \leq 0$ region.

(iii) The surface of the plane is rigid so that the normal velocity vanishes there.

(iv) A stationary medium surrounding the source and the semi-infinite plane.

Method of solution: With this arrangement, the first order solution can be obtained by use of the ray acoustics. Such a first approximation would provide solutions for regions I, II and III indicated in figure (3-A) as follows:

$$\begin{array}{l}
 \text{Region I:} \quad \phi_{\text{I}} = -\frac{e^{ikR}}{4\pi R} - \frac{e^{ik\bar{R}}}{4\pi\bar{R}} \\
 \text{Region II:} \quad \phi_{\text{II}} = -\frac{e^{ikR}}{4\pi R} \\
 \text{Region III:} \quad \phi_{\text{III}} = 0
 \end{array} \quad \left. \vphantom{\begin{array}{l} \text{Region I:} \\ \text{Region II:} \\ \text{Region III:} \end{array}} \right\} \quad (3-1)$$

where R and \bar{R} are the distances from the source and from the image to the observer at P respectively.

This approximation is reasonably accurate as a first

solution approximation of the problem, but will not be sufficiently accurate in the thin shaded zones marking transitions from the source reflection reception to the source affected zone only; and that from the source affected zone to the shadow zone.

The method now formulated will avoid these difficulties and hence provide a solution that can be applied at any point including the shaded (transition) zone. To do this, use is made of the Kirchhoff's integral as outlined below. Let G and ϕ be defined inside a closed surface S as in figure (3-B) below.

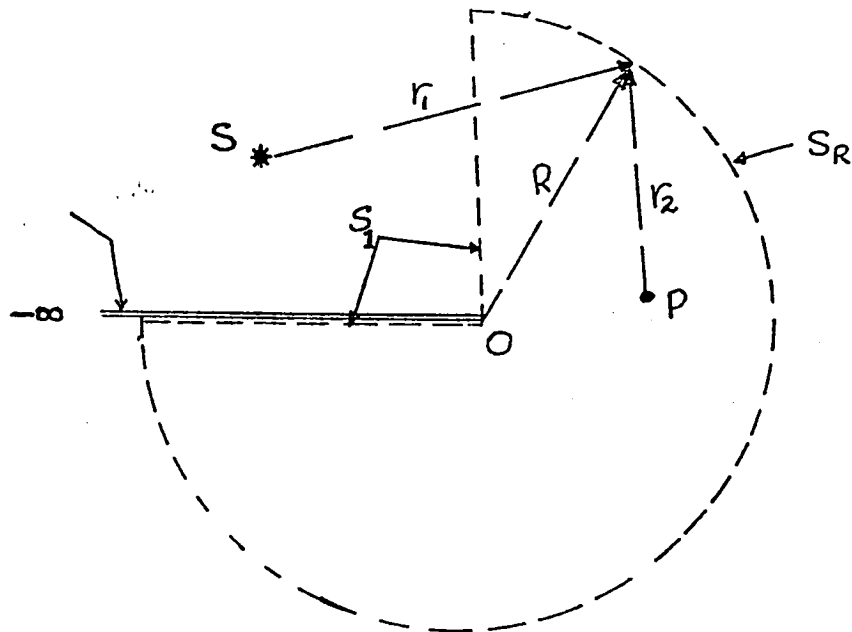


Figure (3-B): Boundaries for the Kirchhoff's integral.

The following equations can be written thus:

$$\nabla^2 G + k^2 G = \delta(\vec{y} - \vec{x}) \quad (3-2)$$

$$\nabla^2 \phi + k^2 \phi = 0 \quad (3-3)$$

From equations (3-2) and (3-3) one obtains, by the standard procedure:

$$\phi \nabla^2 G - G \nabla^2 \phi = \phi \delta(\vec{y} - \vec{x}) \quad (3-4)$$

Hence

$$\phi(\vec{x}) = \iiint_S [\phi \nabla^2 G - G \nabla^2 \phi] \cdot \hat{n} dS \quad (3-5)$$

If the source considered is a point source, and the acoustic field is three-dimensional, then

$$\phi_s = -\frac{A_0 e^{-ikr_1}}{4\pi r_1} \quad ; \quad G = -\frac{e^{-ikr_2}}{4\pi r_2} \quad (3-6)$$

where $r_1 = |\mathbf{x} - \mathbf{x}_s|$ and $r_2 = |\mathbf{x}_p - \mathbf{x}|$ as shown in the

figure (3-C) next page.

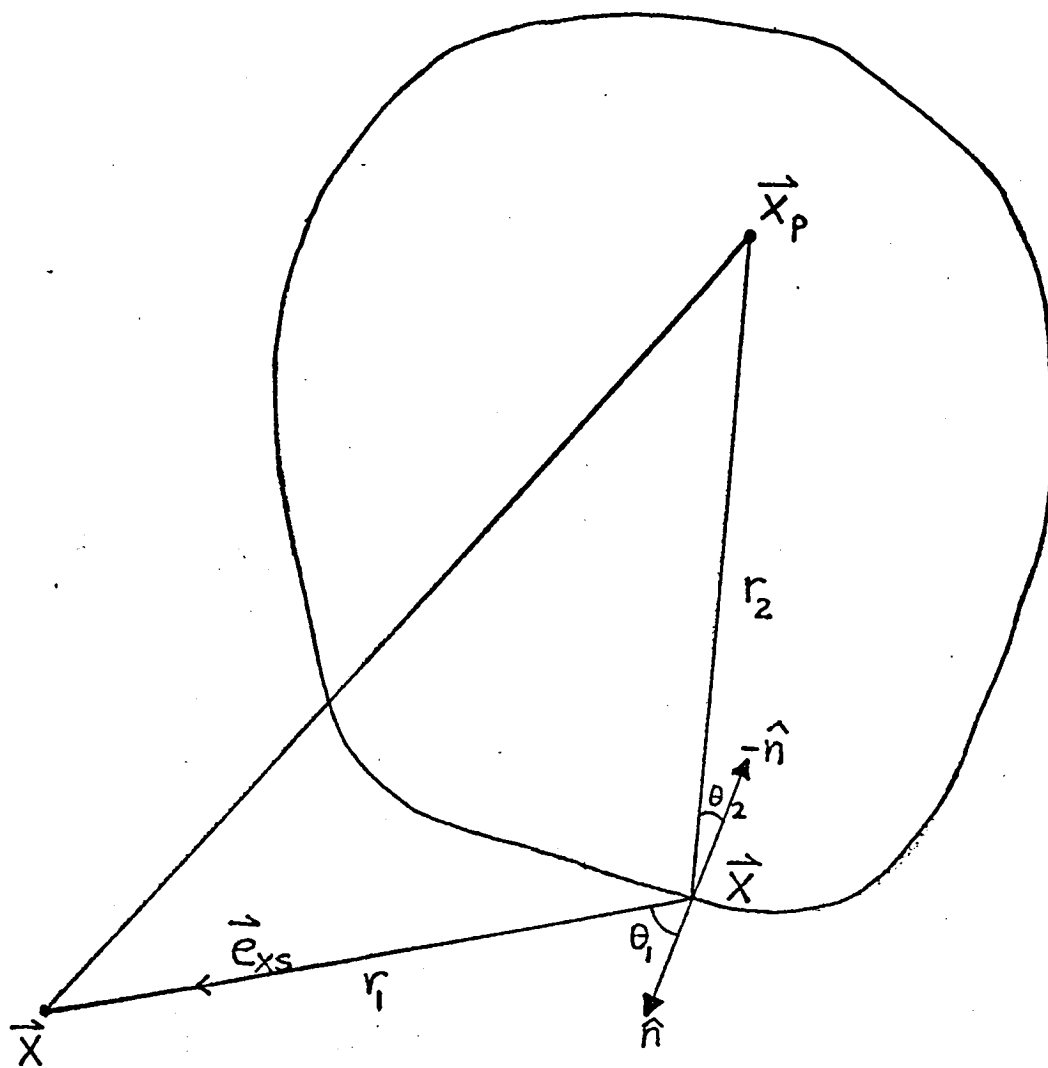


Figure (3-C): Acoustic field from a point source with a boundary present.

$$\nabla \phi = \frac{A_0}{4\pi} \left[\frac{ik}{r_1} + \frac{1}{r_1^2} \right] e^{-ikr_1} \nabla r_1$$

When k is large, and r_1 not too small, the second term is $O(\frac{1}{k})$ as compared with the first term, and can be neglected.

This gives:

$$\nabla \phi \sim \frac{A_0 ik}{4\pi r_1} e^{-ikr_1} \nabla r_1$$

$$\nabla r_1 = \frac{\vec{x} - \vec{x}_s}{|\vec{x} - \vec{x}_s|} = -\frac{\vec{x}_s - \vec{x}}{|\vec{x} - \vec{x}_s|} = -\vec{e}_{xs}$$

where \vec{e}_{xs} is a unit vector from \vec{x} to \vec{x}_s ; so that:

$$\cos \theta_1 = \vec{e}_{xs} \cdot \hat{n} = -\nabla r_1 \cdot \hat{n}$$

and thus:

$$\hat{n} \cdot \nabla \phi \simeq -\frac{A_0 ik}{4\pi r_1} e^{-ikr_1} \cos \theta_1$$

A similar evaluation can be done for the function G ; but

in this case the normal vector \hat{n} is negative and this gives:

$$\hat{n} \cdot \nabla G = \frac{ik}{4\pi r_2} e^{-ikr_2} \cos \theta_2$$

The Kirchhoff's integral equation (3-5) now becomes, on substitution of the above:

$$\phi(\vec{x}) = \iint_S -\frac{A_{jk}}{16\pi^2} \frac{e^{-ik(r_1+r_2)}}{r_1 r_2} (\cos \theta_1 + \cos \theta_2) dS \quad (3-7)$$

With the assumptions of short wave length and hence k is large, use can be made of the stationary phase approximation in evaluating the integral appearing in equation (3-7) as shown below.

III-3 Solution by Stationary Phase Method:

The stationary phase method was developed by Lord Kelvin (21) toward the end of the last century and is based on the idea that the value of an integral containing a fast oscillating integral is essentially given by integrating over that part of the path where the phase change of the integrand is the slowest. The contribution from other parts of the integration parts will become very small due to strong cancellations. This method will be applied to the Kirchhoff's integral:

$$\phi(P) = \iint_{S_1 S_R} \left[\phi \frac{\partial G}{\partial n} - G \frac{\partial \phi}{\partial n} \right] dS \quad (3-8)$$

The surface of integration is shown in figure (3-B). It consists of two surfaces bounding the left upper quadrant (surface S_1), and a spherical surface (surface S_R) thus completing the boundary.

In equation (3-8) one may use the ray acoustic solution for ϕ , and $\frac{\partial \phi}{\partial n}$. Those solutions are accurate to the order of $(\frac{1}{k})$, except in the transition zone. The boundary shown in figure (3-B) is chosen to be outside the transition zone.

Since ϕ and $\frac{\partial \phi}{\partial n}$ are known the integral could, in principle, be integrated directly. Based on the assumptions stated previously, however, the mathematical procedure can be reduced immensely by the present method.

The expressions for ϕ_s and G are, respectively:

$$\phi_s = - \frac{e^{ikr_1}}{4\pi r_1} \quad ; \quad G = - \frac{e^{ikr_2}}{4\pi r_2} \quad (3-9)$$

For large k , the integral shown in equation (3-8) is approximately given by:

$$\phi(P) \simeq \frac{ik}{16\pi^2} \iint_{S_1, S_R} \left[\frac{\partial r_2}{\partial n} - \frac{\partial r_1}{\partial n} \right] \frac{e^{ik(r_1+r_2)}}{r_1 r_2} ds \quad (3-10)$$

It will first be shown in the following discussion that for any given wave number k , the contribution to the integral from the spherical surface S_R tends to zero as the sphere radius R tends to infinity. This result is obvious due to the fact that the distance from a point of integration on a spherical surface to the source S and the observation point P approach the same value as R becomes very large; so that the difference of the two terms $(\frac{\partial r_1}{\partial n} - \frac{\partial r_2}{\partial n}) \rightarrow 0$ as $R \rightarrow \infty$

Hence

$$\int_{S_R} \left[\frac{\partial r_2}{\partial n} - \frac{\partial r_1}{\partial n} \right] \frac{e^{ik(r_1+r_2)}}{r_1 r_2} dS = o(1) \cdot O\left(\frac{1}{R^2}\right) \cdot O(R^2) = o(1): (3-11)$$

$$\rightarrow 0 \quad \text{as } R \rightarrow \infty$$

From the ray acoustics solutions, it is observed that the integral that extends over the under surface of the plate is zero because this boundary is in the shadow region where the value of the velocity potential is identically zero.

Equation (3-8) then reduces to the form:

$$\phi(P) \approx \frac{ik}{16\pi^2} \int_{S_1} \int_{S_R} \left[\frac{\partial r_2}{\partial \xi} - \frac{\partial r_1}{\partial \xi} \right] \frac{e^{ik(r_1+r_2)}}{r_1 r_2} dS \quad (3-12)$$

where S_R denotes the half plane $\eta-\zeta$ as shown in figure (3-D).

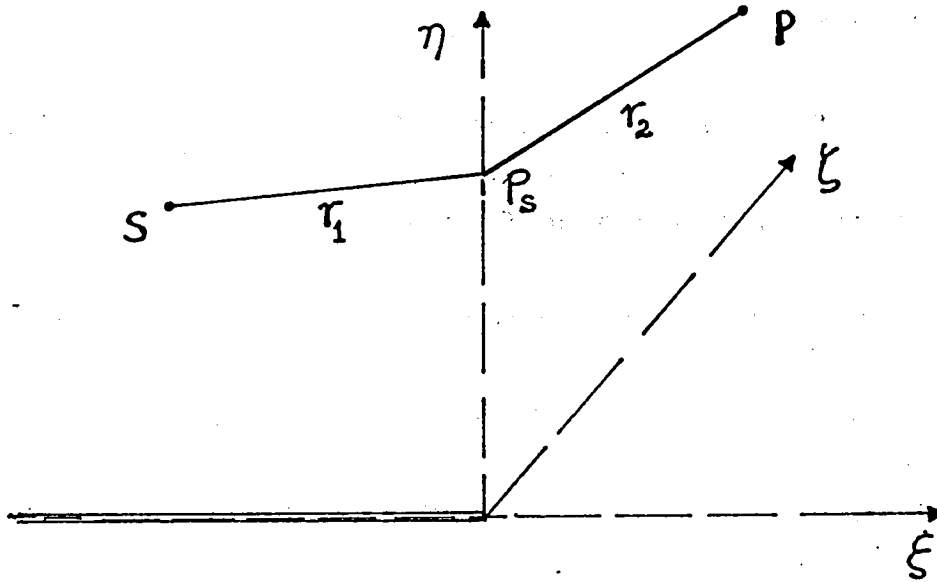


Figure (3-D): Half plane (η, ζ) .

Let (X_s, Y_s, Z_s) denote the position of the source and (X_p, Y_p, Z_p) the position of the observer and (ξ, η, ζ) the point of integration. The expression for r_1 and r_2 appearing in equation (3-10) are defined by:

$$\left. \begin{aligned} r_1 &= \sqrt{(\xi - X_s)^2 + (\eta - Y_s)^2 + (\zeta - Z_s)^2} \\ r_2 &= \sqrt{(X_p - \xi)^2 + (Y_p - \eta)^2 + (Z_p - \zeta)^2} \end{aligned} \right\} \quad (3-13) \quad (a, b)$$

The method of stationary phase can now be applied if it is assumed $k \gg 1$. For convenience, equation (3-10) is expressed in the form:

$$\phi(P) = ik \int_0^{\infty} d\eta \left[\int_{-\infty}^{\infty} F(\eta, \xi) e^{ikf(\eta, \xi)} d\xi \right] \quad (3-14)$$

where

$$F(\eta, \xi) = \frac{1}{16\pi^2} \left[\frac{\partial r_2}{\partial \xi} - \frac{\partial r_1}{\partial \xi} \right] \frac{1}{r_1 r_2} \quad (3-15) \text{ (a)}$$

and $f(\eta, \xi) = r_1 + r_2 \quad (3-15) \text{ (b)}$

The function $f = r_1 + r_2$ has a simple physical meaning. It represents the total distance an acoustic ray travels from the source point S to the observer point P through the point P_0 on the integration path. As the integration point P_0 moves on the $(\eta - \xi)$ plane, the phase angle $k(r_1 + r_2)$ of the exponential function in equation (3-10) varies; resulting in strong cancellations of the wave for large values of k .

The attention will now be directed to the main

contribution of the integral in the neighbourhood of the stationary phase point (η_0, ζ_0) defined by:

$$\frac{\partial}{\partial \eta} (r_1 + r_2) = 0 \quad ; \quad \frac{\partial}{\partial \zeta} (r_1 + r_2) = 0 \quad (3-16)$$

Obviously, (η_0, ζ_0) is the point that lies on the straight line joining the points S and P, as shown in figure (3-E) below.

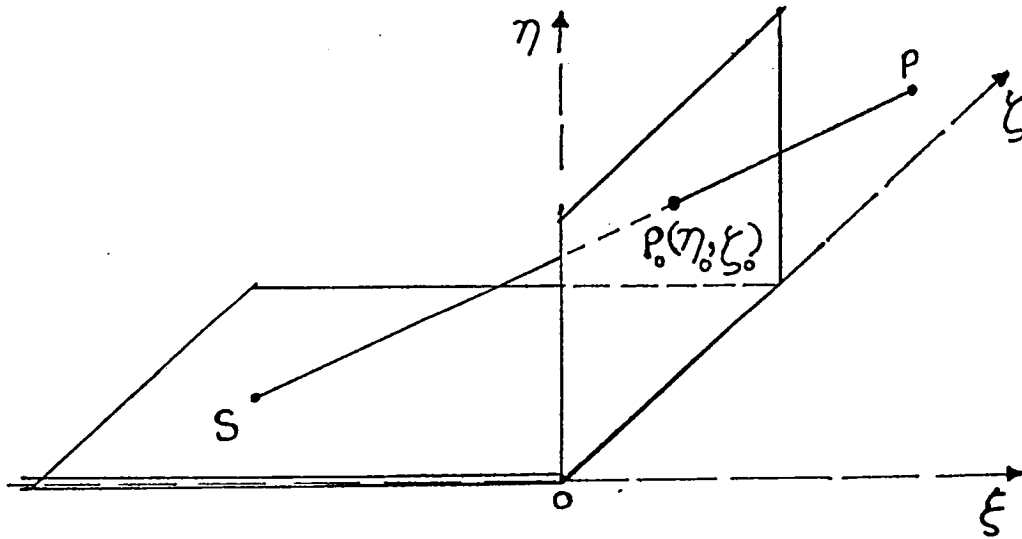


Figure (3-E): Line joining the points S and P passes through the stationary point.

To apply the stationary point method, the function

$f(\eta, \zeta)$ is expanded into a double Taylor series around

the point (η_0, ζ_0) thus:

$$f(\eta, \zeta) = f(\eta_0, \zeta_0) + \frac{1}{2} \left[A(\eta - \eta_0)^2 + 2B(\eta - \eta_0)(\zeta - \zeta_0) + C(\zeta - \zeta_0)^2 \right] + \dots \quad (3-17)$$

where $\frac{\partial f}{\partial \eta} = \frac{\partial f}{\partial \zeta}$ at (η_0, ζ_0)

From equations (3-13) it is found that:

$$\left. \begin{aligned} \frac{\partial}{\partial \eta}(r_1+r_2) &= \frac{\eta-\gamma_s}{r_1} - \frac{\gamma_p-\eta}{r_2} \\ \frac{\partial}{\partial \zeta}(r_1+r_2) &= \frac{\zeta-z_s}{r_1} - \frac{z_p-\zeta}{r_2} \end{aligned} \right\} \quad (3-18) \quad (a, b)$$

and

$$\left. \begin{aligned} \frac{\partial^2}{\partial \eta^2}(r_1+r_2) &= \left(\frac{1}{r_1} + \frac{1}{r_2}\right) - \left[\frac{(\eta-\gamma_s)^2}{r_1^3} + \frac{(\gamma_p-\eta)^2}{r_2^3} \right] \\ \frac{\partial^2}{\partial \eta \partial \zeta}(r_1+r_2) &= - \left[\frac{(\zeta-z_s)(\eta-\gamma_s)}{r_1^3} + \frac{(z_p-\zeta)(\gamma_p-\eta)}{r_2^3} \right] \\ \frac{\partial^2}{\partial \zeta^2}(r_1+r_2) &= \left(\frac{1}{r_1} + \frac{1}{r_2}\right) - \left[\frac{(\zeta-z_s)^2}{r_1^3} + \frac{(z_p-\zeta)^2}{r_2^3} \right] \end{aligned} \right\} \quad (3-19) \quad (a, b, c)$$

At the stationary phase point $\eta = \eta_0$; $\zeta = \zeta_0$, so that

$$\left. \begin{aligned} \frac{\partial}{\partial \eta}(r_1+r_2) &= \frac{\eta-\gamma_s}{r_1} - \frac{\gamma_p-\eta}{r_2} = 0 \\ \frac{\partial}{\partial \zeta}(r_1+r_2) &= \frac{\zeta-z_s}{r_1} - \frac{z_p-\zeta}{r_2} = 0 \end{aligned} \right\} \quad (3-20) \quad (a, b)$$

It follows from equations (3-13 a,b) that at (η_0, ζ_0)

$$\begin{aligned} \frac{\xi - X_s}{r_1} &= \sqrt{1 - \frac{(\eta - Y_s)^2}{r_2^2} - \frac{(\zeta - Z_s)^2}{r_1^2}} = \sqrt{1 - \frac{(Y_p - \eta)^2}{r_2^2} - \frac{(Z_p - \zeta)^2}{r_1^2}} \\ &= \frac{X_p - \xi}{r_2} \end{aligned} \quad (3-21)$$

thus,

$$\frac{\xi_0 - X_s}{X_p - \xi_0} = \frac{\eta_0 - Y_s}{Y_p - \eta_0} = \frac{\zeta_0 - Z_s}{X_p - \zeta_0} \quad (3-22)$$

That is, the three points (X_s, Y_s, Z_s) , (ξ_0, η_0, ζ_0)

and (X_p, Y_p, Z_p) all lie on the same straight line. Using

equations (3-13 a, b), the expressions for $\frac{\partial^2}{\partial \eta^2}(r_1 + r_2)$,

$\frac{\partial^2}{\partial \eta \partial \zeta}(r_1 + r_2)$, and $\frac{\partial^2}{\partial \zeta^2}(r_1 + r_2)$ may be written as:

$$\begin{aligned} A &\equiv \left[\frac{\partial^2}{\partial \zeta^2}(r_1 + r_2) \right]_0 = \frac{r}{(r_1 r_2)_0} \left[1 - \frac{(Z_p - Z_s)^2}{r^2} \right] \\ B &\equiv \left[\frac{\partial^2}{\partial \eta \partial \zeta}(r_1 + r_2) \right]_0 = -\frac{r}{(r_1 r_2)_0} \frac{(Z_p - Z_s)(Y_p - Y_s)}{r^2} \\ C &\equiv \left[\frac{\partial^2}{\partial \eta^2}(r_1 + r_2) \right]_0 = \frac{r}{(r_1 r_2)_0} \left[1 - \frac{(Y_p - Y_s)^2}{r^2} \right] \end{aligned} \quad (3-23) \text{ (a, b, c)}$$

where $r = \sqrt{(X_p - X_s)^2 + (Y_p - Y_s)^2 + (Z_p - Z_s)^2}$ and the subscript 0

denotes evaluation at $\eta = \eta_0$ and $\zeta = \zeta_0$.

To carry out the integration separately with respect to η and ξ one can write equation (3-17) in the form:

$$k(r_1+r_2) = kr + \frac{k}{2} \left[\sqrt{A} (\xi - \xi_0) + \frac{B}{\sqrt{A}} (\eta - \eta_0) \right]^2 + \frac{k}{2} \left(c - \frac{B^2}{A} \right) (\eta - \eta_0)^2 \quad (3-24)(a)$$

$$= kr + \alpha_0^2 + \beta^2 \quad (3-24) (b)$$

where the new variables α_0 and β are defined by:

$$\left. \begin{aligned} \alpha_0^2 &= \frac{k}{2} \left[\sqrt{A} (\xi - \xi_0) + \frac{B}{\sqrt{A}} (\eta - \eta_0) \right]^2 \\ \beta^2 &= \frac{k}{2} \left[c - \frac{B^2}{A} \right] (\eta - \eta_0)^2 \end{aligned} \right\} \quad (3-35) (a, b)$$

then

$$d\alpha_0 = \sqrt{\frac{kA}{2}} d\xi \quad ; \quad d\beta = \sqrt{\frac{k}{2}} \sqrt{c - \frac{B^2}{A}} d\eta$$

By substituting the expressions for A, B, C, one finds that:

$$d\beta = \sqrt{\frac{k}{2}} \frac{1}{\sqrt{A}} \frac{(X_p - X_s)}{(r_1 r_2)_0} d\eta$$

and

$$d\alpha_0 d\beta = \frac{k}{2} \frac{(X_p - X_s)}{(r_1 r_2)_0} d\eta d\xi$$

The integral of ϕ then becomes:

$$\begin{aligned}
 \phi &= \frac{ik}{16\pi^2} \iint \frac{1}{r_1 r_2} \left[\frac{\xi - x_s}{r_1} + \frac{x_p - \xi}{r_2} \right] e^{ik(r_1 + r_2)} d\eta d\xi \\
 &= \frac{ik}{16\pi^2} \iint \frac{2}{(r_1 r_2)_0} \frac{x_p - x_s}{r} e^{ik(r_1 + r_2)} d\eta d\xi \\
 &= \frac{ie^{ikr}}{4\pi^2 r} \int_{\bar{\beta}}^{\infty} \left[\int_{-\infty}^{\infty} e^{i\alpha^2} d\alpha_0 \right] e^{i\beta^2} d\beta
 \end{aligned} \quad (3-26)$$

where the end point value $\bar{\beta}$ will be defined later. Note that

in obtaining equation (3-26) one has to use the relation that

at the point (η_0, ξ_0) ,

$$\frac{\xi - x_s}{r_1} = \frac{x_p - \xi}{r_2} = \frac{x_p - x_s}{r} \quad (3-27)$$

The definite integral in equation (3-26) can be readily

integrated, yielding:

$$\int_{-\infty}^{\infty} e^{i\alpha_1^2} d\alpha_0 = \frac{\pi}{2} (1+i) \quad (3-28)$$

For the integral involving β one may define a function $F(\bar{\beta})$

by:

$$F(\bar{\beta}) = \frac{1-i}{2} \sqrt{\frac{2}{\pi}} \int_{\bar{\beta}}^{\infty} e^{i\beta^2} d\beta \quad (3-29)$$

Upon substitution of equations (3-28) and (3-29) then

equation (3-26) becomes:

$$\phi = -\frac{e^{ikr}}{4\pi r^2} F(\bar{\beta}) \quad (3-30)$$

If the common forms of Fresnel integrals are used:

$$\left. \begin{aligned} C(z) &= \int_0^z \cos\left(\frac{\pi t^2}{2}\right) dt \\ S(z) &= \int_0^z \sin\left(\frac{\pi t^2}{2}\right) dt \end{aligned} \right\} \quad (3-31)$$

$F(\bar{\beta})$ may be written as:

$$F(\bar{\beta}) = \frac{1}{2} - \frac{1-i}{2} \left[C\left(\sqrt{\frac{2}{\pi}} \bar{\beta}\right) + S\left(\sqrt{\frac{2}{\pi}} \bar{\beta}\right) \right] \quad (3-32)$$

The asymptotic behaviour of $C(z)$ and $S(z)$ are given by the following equations.

$$C(z) \simeq \frac{1}{2} + \frac{\sin\left(\frac{\pi}{2} z^2\right)}{\pi z} + O\left(\frac{1}{z^3}\right) \quad (3-33) \text{ (a)}$$

$(z \rightarrow \infty, z > 0)$

$$S(z) \simeq \frac{1}{2} - \frac{\cos\left(\frac{\pi}{2} z^2\right)}{\pi z} + O\left(\frac{1}{z^3}\right) \quad (3-33) \text{ (b)}$$

It can then be easily seen that:

$$\left. \begin{aligned} F(\bar{\beta}) &\simeq 1 + \frac{1+i}{2} \frac{e^{i\bar{\beta}^2}}{\sqrt{2\pi} \bar{\beta}} + O\left(\frac{1}{\bar{\beta}^3}\right); (\bar{\beta} > 0) \\ F(\bar{\beta}) &\simeq 1 - \frac{1+i}{2} \frac{e^{i\bar{\beta}^2}}{\sqrt{2\pi} \bar{\beta}} + O\left(\frac{1}{\bar{\beta}^3}\right); (\bar{\beta} < 0) \end{aligned} \right\} (3-34) \text{ (a, b)}$$

In deriving the second expression in equation (3-34) (a) and

(b) above, use has been made of the relations $C(-z) = -C(z)$

and $S(-z) = -S(z)$.

The Lower Limit $\bar{\beta}$:

One recalls that the equation (3-26) is integrated using the new variables defined by:

$$\left. \begin{aligned} \alpha_0 &= \sqrt{\frac{k}{2}} \left[\sqrt{A} (\xi - \xi_0) + \frac{B}{\sqrt{A}} (\eta - \eta_0) \right] \\ \beta &= \sqrt{\frac{k}{2}} \sqrt{(c - \frac{B^2}{A})} (\eta - \eta_0) \end{aligned} \right\} (3-35) \text{ (a, b)}$$

The line $\alpha_0 = 0$ is the locus of point on which $\frac{\partial f}{\partial \zeta} = 0$.

This means that along such a line, the function f has stationary values with respect to the variable ζ . The range of the limit of integration for $\bar{\beta}$ is, therefore, from P^* to $\bar{\beta} = \infty$ as shown in figure (3-F) below.

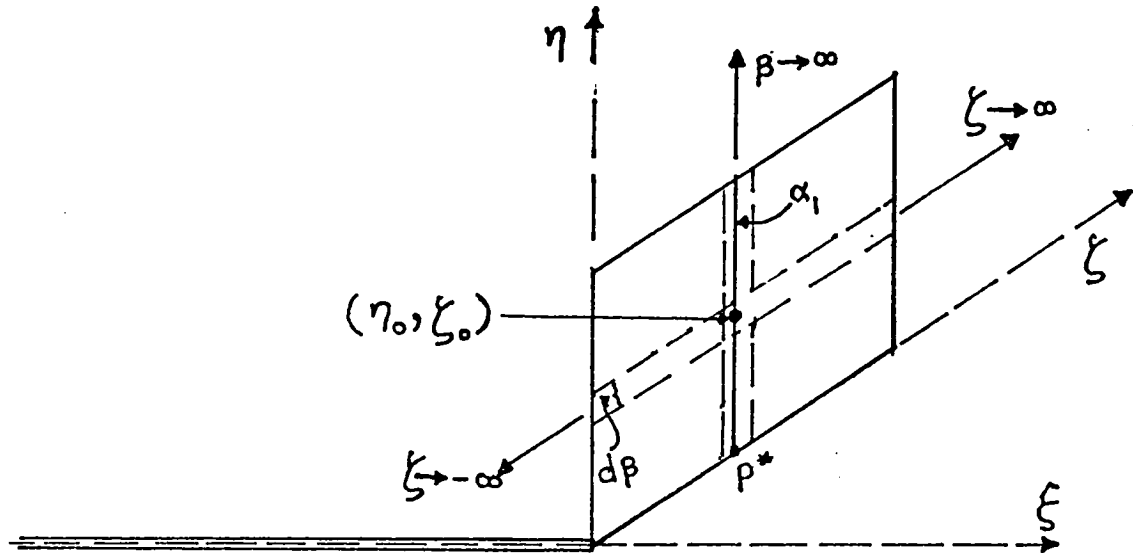


Figure (3-F): The range of the limit of integration for $\bar{\beta}$.

The point P^* lies on the trailing edge of the plate where

$\frac{\partial f}{\partial \zeta} = 0$. From equation (3-24) (b) it can be seen that

$$\bar{\beta}^2 = kr_0 - kr \quad (3-36)$$

where $r_0 = r_1 + r_2$ at the point P^* .

To derive the expression r_0 , one may write r_1 and r_2 in

the form:

$$r_1 = \sqrt{\rho_1^2 + (\zeta - z_s)^2} \quad (3-37) \text{ (a)}$$

$$r_2 = \sqrt{\rho_2^2 + (z_p - \zeta)^2} \quad (3-37) \text{ (b)}$$

where ρ_1 and ρ_2 are the projections of r_1 and r_2 on the (ξ, η) plane figure (3-G) below.

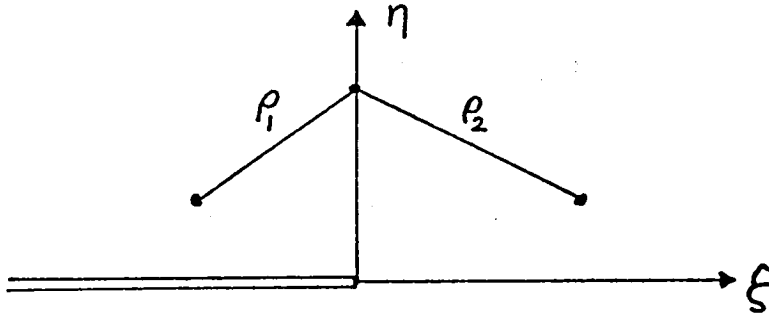


Figure (3-G): Acoustic lengths on the projection of the plane (η, ξ) .

At P^* , ζ satisfied the equation:
$$\frac{\partial f}{\partial \zeta} = \frac{\partial}{\partial \zeta} (r_1 + r_2) \quad (3-38)$$

Using equations (3-37) (a), (b), this becomes:

$$\frac{\zeta^* - z_s}{\sqrt{\rho_1^2 + (\zeta^* - z_s)^2}} - \frac{z_p - \zeta^*}{\sqrt{\rho_2^2 + (z_p - \zeta^*)^2}} = 0 \quad (3-39)$$

which can be written in the form:

$$\frac{\zeta^* - z_s}{\sqrt{\rho_1^2 + (\zeta^* - z_s)^2}} = \frac{z_p - \zeta^*}{\sqrt{\rho_2^2 + (z_p - \zeta^*)^2}} = \gamma \text{ (say)} \quad (3-40)$$

Hence

$$\left. \begin{aligned} \zeta^* - z_s &= \frac{\gamma}{\sqrt{1 - \gamma^2}} \rho_1 \\ z_p - \zeta^* &= \frac{\gamma}{\sqrt{1 - \gamma^2}} \rho_2 \\ z_p - z_s &= \frac{\gamma}{\sqrt{1 - \gamma^2}} (\rho_1 + \rho_2) \\ \gamma &= \frac{z_p - z_s}{\sqrt{(\rho_1 + \rho_2)^2 + (z_p - z_s)^2}} \end{aligned} \right\} (3-41) \text{ (a, b, c, d)}$$

At the point $\zeta = \zeta^*$ one has, therefore, the following relation:

$$\frac{\zeta - z_s}{\sqrt{\rho_1^2 + (\zeta - z_s)^2}} = \frac{z_p - \zeta}{\sqrt{\rho_2^2 + (z_p - \zeta)^2}} = \frac{z_p - z_s}{\sqrt{(\rho_1 + \rho_2)^2 + (z_p - z_s)^2}} \quad (3-42)$$

Equation (3-42) is presented graphically by figure (3-H).

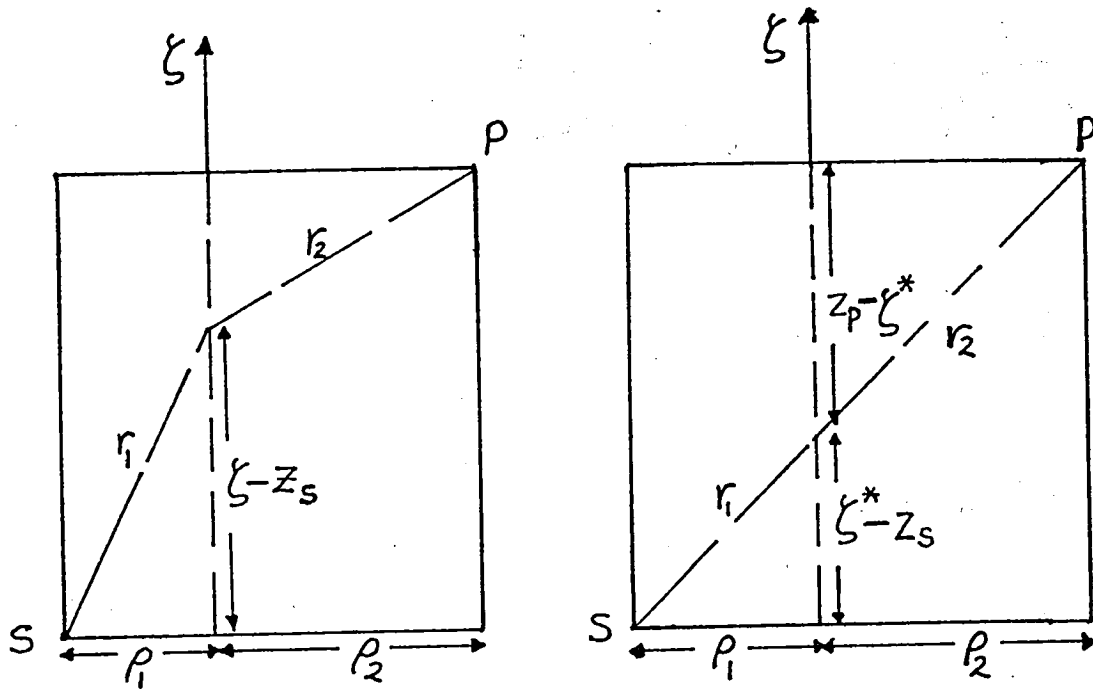


Figure (3-H): Graphical sketch of acoustic length in relation to the stationary point.

The distances r_1 and r_2 at P^* are seen to be:

$$r_0 = \sqrt{(\rho_s + \rho_p)^2 + (z_p - z_s)^2} \quad (3-43)$$

so that $\bar{\beta}^2$ can then be expressed as:

$$\bar{\beta}^2 = k \left[\sqrt{(\rho_s + \rho_p)^2 + (z_p - z_s)^2} - \sqrt{(x_p - x_s)^2 + (y_p - y_s)^2 + (z_p - z_s)^2} \right] \quad (3-44)$$

III-4 Conclusions and Discussions:

Based on the geometrical configuration shown in figure (3-I) the main results of the above analysis can be summarized.

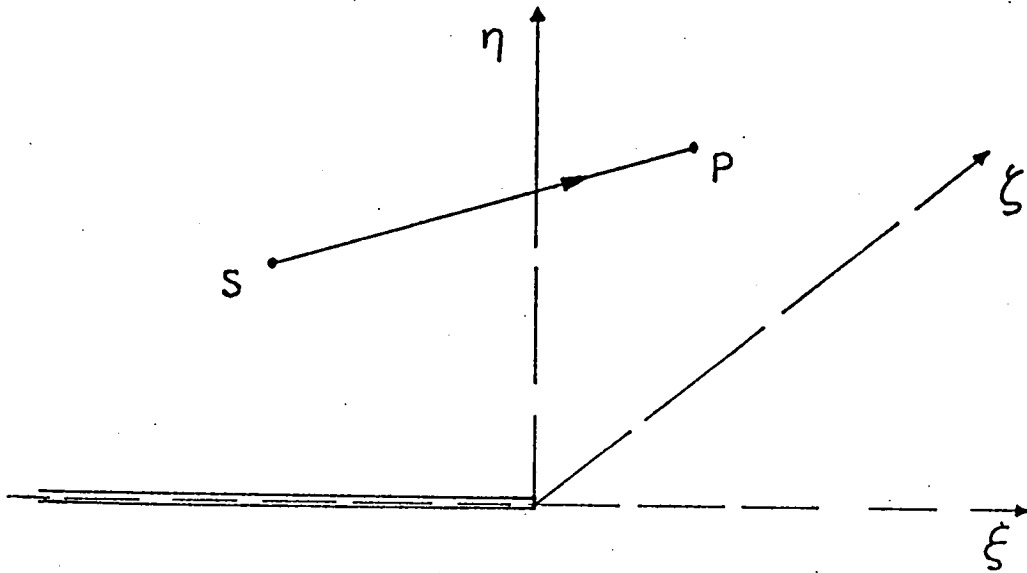


Figure (3-I): Wave reception at P due to three-dimensional source in the presence of a semi-infinite plate.

The formulae that have been developed in the analysis take into account only the radiation from the source **S**. To obtain the complete solution, the contribution from the reflected waves from the upper surface, which can be calculated by the same procedure, must be included.

The formulae for calculating the acoustic field by a

source at S are as follows:

Let $\phi_0(P)$ denoted the potential at the point P due to the source S in the absence of the plate.

$$\phi_0(P) = - \frac{e^{ikr}}{4\pi r} \quad (3-45)$$

The velocity potential $\phi(P)$ in the presence of the plate will be:

$$\phi(P) = \phi_0(P) F(\bar{\beta}) \quad (3-46)$$

where $F(\bar{\beta})$ is the diffraction factor. The function $F(\bar{\beta})$ is defined by the integral:

$$F(\bar{\beta}) = \frac{1-i}{2} \sqrt{\frac{2}{\pi}} \int_{\bar{\beta}}^{\infty} e^{i\beta^2} d\beta \quad (3-47) \text{ (a)}$$

$$= \frac{1}{2} - \frac{1-i}{2} \left[C\left(\sqrt{\frac{2}{\pi}} \bar{\beta}\right) + iS\left(\sqrt{\frac{2}{\pi}} \bar{\beta}\right) \right] \quad (3-47) \text{ (b)}$$

$$= \left\{ \begin{array}{ll} 0 & \bar{\beta} \rightarrow \infty \\ \frac{1}{2} & \bar{\beta} \rightarrow 0 \\ 1 & \bar{\beta} \rightarrow -\infty \end{array} \right\} \quad (3-47) \text{ (c)}$$

The following three cases for the values of $\bar{\beta}$ are considered.

Case 1 $\bar{\beta}=0$:

This corresponds to the case when the line drawn from

the observer point P to the source passes through the edge of the plate. In such a case,

$$F(\bar{\beta}) = 1/2 \text{ and therefore}$$

$$\phi = 1/2 \phi_0(P) \quad (3-48)$$

This means that half of the radiation emitted by the source is received by the observer.

Case 2 $\bar{\beta} < 0$:

In this case, the observer is on the upper side of the line $\bar{\beta} = 0$. The edge of the plate lies below the stationary phase point. The diffraction factor $F(\bar{\beta})$ is greater than half, and increases to unity, as the observation point moves further upwards. In the limit, $\phi(P)$ takes the value $\phi_0(P)$ so that the sound emitted is not obstructed.

Case 3 $\bar{\beta} > 0$:

This occurs when the observer is at the lower side of the $\bar{\beta} = 0$ line. The value of $\bar{\beta}$ is positive and continues to increase as the observation point P moves downward. The value $F(\bar{\beta})$ decreases as $\bar{\beta}$ increases, and in the limit ϕ

tends to zero, so that the observer is in the shadow region.

For any given value of $\bar{\beta}$, the variation of the diffraction factor $F(\bar{\beta})$ is shown in figure (3-J) below.

As the observer moves from P_+ in the transmission region to P_- in the shadow region, the sound varies from complete reception to zero. The transition of $F(\bar{\beta})$ from zero to unity occurs in the range of approximately (ref. 1)

$$-20 \leq \bar{\beta} \leq 20$$

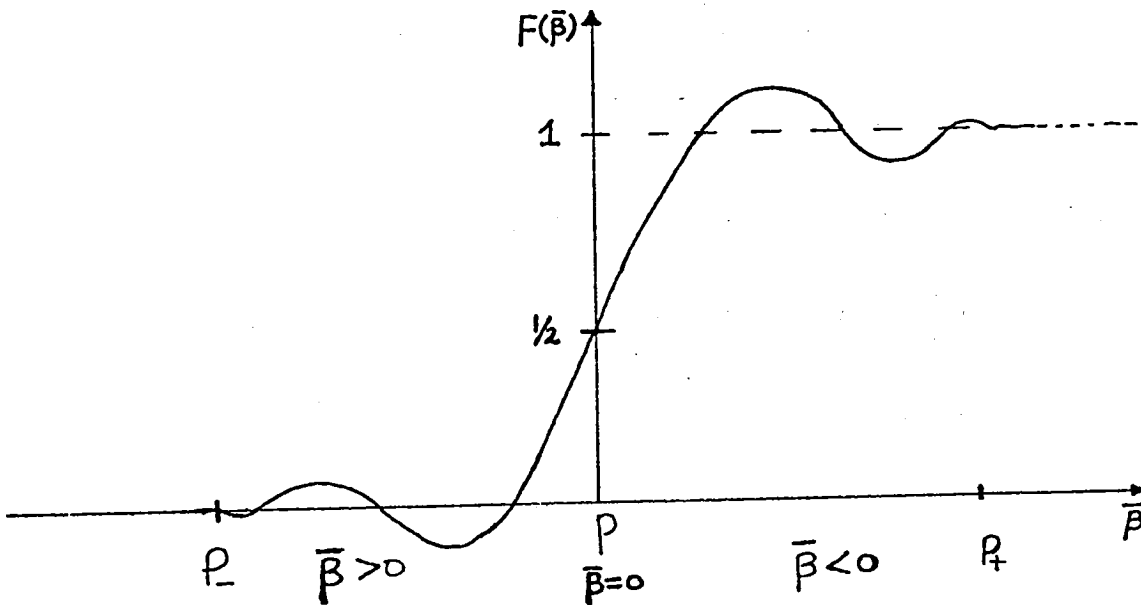


Figure (3-J): Variation of the diffraction factor $F(\bar{\beta})$.

One may note that for large values of k , the value of $\phi(P)$ depends on the integration over a small region around a stationary phase point. If the edge of the plate lies inside this region, it will make no effect on the transmission of sound from the source to the observer.

III-5 Applications and Comparisons with known Solutions:

Cooke (9) has derived an approximate expression for the far field due to a three-dimensional source over a semi-infinite plate. He gives the solution for ϕ for the direct radiation from the source as:

$$\phi(P) = \frac{e^{ikr}}{r} \left[\frac{1}{2} - \frac{1-i}{2} \left[C(\beta) + i S(\beta) \right] \right] \quad (3-49)$$

The solution derived in the present study is given by the multiplication of the results obtained in equations (3-46) and (3-47)(b), so that

$$\phi(P) = -\frac{e^{ikr}}{4\pi r} \left[\frac{1}{2} - \frac{1-i}{2} \left[C\left(\sqrt{\frac{2}{\pi}} \bar{\beta}\right) + i S\left(\sqrt{\frac{2}{\pi}} \bar{\beta}\right) \right] \right] \quad (3-50)$$

Apart from the difference in the factor $\left(-\frac{1}{4\pi}\right)$, the solution obtained in the present study agrees with that

obtained by Cooke.

The two-dimensional problem shown in figure (3-K) below may be considered as a special case of the above three-dimensional problem, and its solution may be obtained by letting $\mathbf{z} = \mathbf{z}_0 = \mathbf{0}$ and $\rho_s \rightarrow \infty$ in equations (3-44) and (3-46). In taking the limit, the equations

$$\phi(\rho) = \phi(\rho) F(\bar{\beta})$$

$$F(\bar{\beta}) = \frac{1-i}{2} \sqrt{\frac{2}{\pi}} \int_{\bar{\beta}}^{\infty} e^{i\beta^2} d\beta$$

remain unchanged. The two important quantities that need to be calculated when $\rho_s \rightarrow \infty$ are r , the distance from the point P to the source, and r_0 , the acoustic length given by equation (3-43).

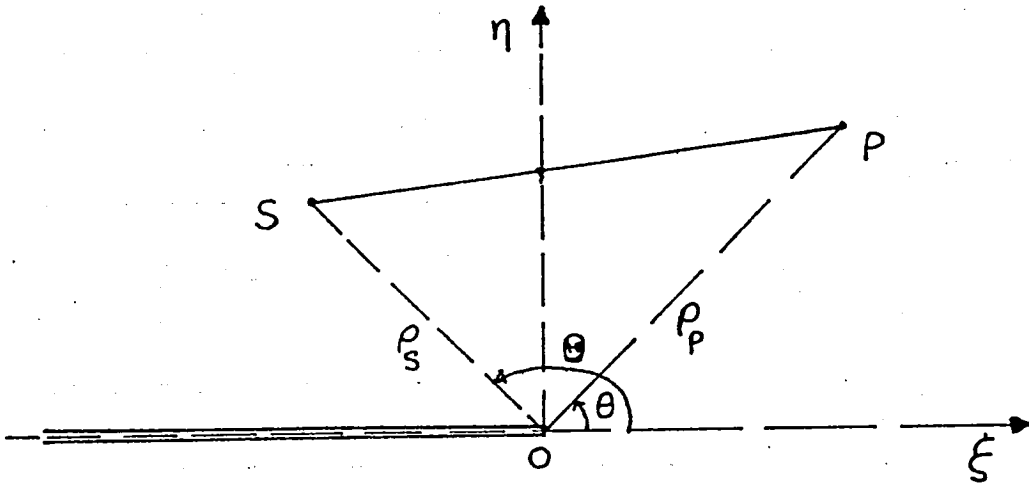


Figure (3-K): Two-dimensional problem sketch.

In terms of the notations used in figure (3-K), one finds:

$$r = \sqrt{\rho_s^2 + \rho_p^2 - 2\rho_s\rho_p \cos(\Theta - \theta)}$$

$$\simeq \rho_s - \rho_p \cos(\Theta - \theta) \quad \text{as } \rho_s \rightarrow \infty$$

$$\text{and } r_0 = \rho_s + \rho_p$$

Using these values, the expressions of $\phi(\rho)$ and $\bar{\beta}$ are

simplified to the forms:

$$\phi_0(\rho) = - \left. \begin{array}{l} \frac{e^{ik\rho_s} e^{-ik\rho \cos(\Theta - \theta)}}{4\pi\rho_s} \\ \simeq e^{-ik\rho \cos(\Theta - \theta)} \end{array} \right\} \quad (3-44)$$

(after removing the non-essential constant multiplier by

re-normalization) and:

$$\bar{\beta} = \sqrt{k(r_0 - r)} = \sqrt{k\rho(1 + \cos(\Theta - \theta))}$$

$$= \sqrt{2k\rho} \cos\left(\frac{\Theta - \theta}{2}\right)$$

Note that the sign of $\bar{\beta}$ is either negative or positive

depending on whether the plate tip ($\beta = \bar{\beta}$) is below or

above the stationary phase point $\beta = 0$, figure (3-L) shown

on the next page. For the incident wave, $\bar{\beta}$ is below the

point $\beta = 0$, so that it's value is negative and is given by:

$$\bar{\beta} = -\sqrt{2k\rho} \cos\left(\frac{\Theta - \theta}{2}\right)$$

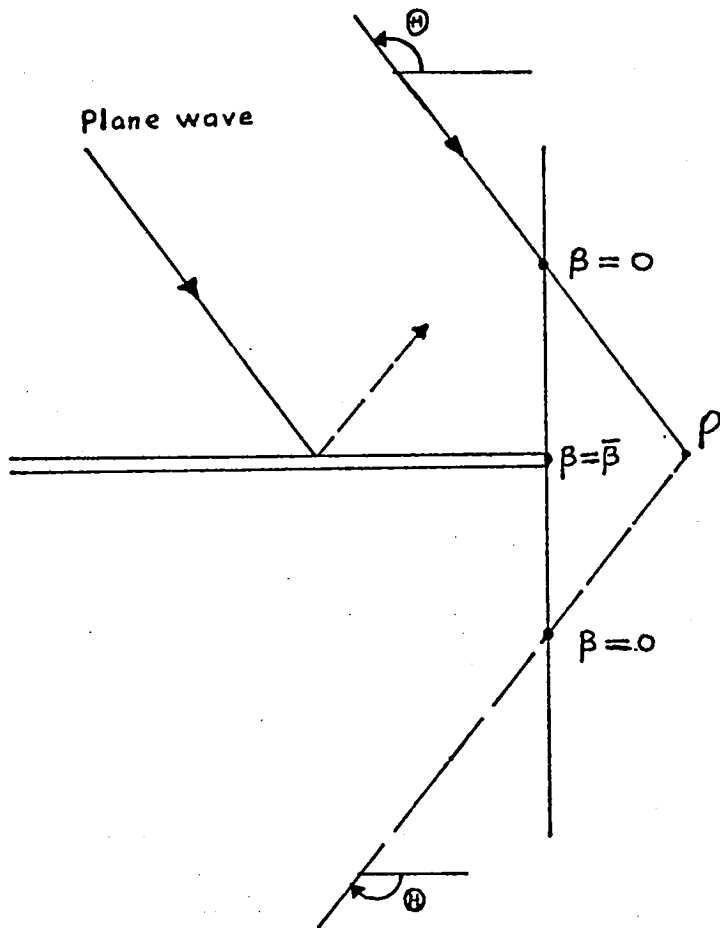


Figure (3-L): Plane wave problem showing ranges of integration ($\bar{\beta}$).

For the reflected waves, Θ must be changed to $-\Theta$ and the value of $\bar{\beta}$ is positive as given by:

$$\bar{\beta} = \sqrt{2k\rho} \cos\left(\frac{\Theta - \theta}{2}\right)$$

The total velocity potential due to both waves is then:

$$\begin{aligned} \phi_T(\rho) = & e^{-ik\rho \cos(\theta - \Theta)} F\left\{-\sqrt{2k\rho} \cos\left(\frac{\theta - \Theta}{2}\right)\right\} + \\ & e^{-ik\rho \cos\left(\frac{\theta + \Theta}{2}\right)} F\left\{\sqrt{2k\rho} \cos\left(\frac{\theta + \Theta}{2}\right)\right\} \end{aligned} \quad (3-45)$$

This result is identical to that given by equation (2.86) on page (73) of Noble*. When θ is sufficiently far from $\Theta - \pi$ and $\pi - \Theta$, the asymptotic expression for ϕ_T for large values of $k\rho$ may be obtained using the asymptotic expression of F given by equations (3-34) (a,b). With the aid of the

trigonometric identities: $2 \cos^2\left(\frac{\theta \pm \Theta}{2}\right) = 1 + \cos(\theta \pm \Theta)$

$$2 \cos\left(\frac{\theta + \Theta}{2}\right) \cos\left(\frac{\theta - \Theta}{2}\right) = \cos\theta + \cos\Theta$$

* Noble B., "Methods based on the Wiener-Hopf technique"

(1958); where ρ is denoted by r and $F(\nu)$ is replaced by

$$\frac{e^{-i\pi/4}}{\sqrt{\pi}} F(\nu) \text{ with } F(\nu) = \int_{\nu}^{\infty} e^{i\beta^2} d\beta$$

it is found that

$$\phi_T \simeq e^{-ik\rho \cos(\theta-\Theta)} + e^{-ik\rho \cos(\theta+\Theta)} + \phi_d$$

where

$$\phi_d \simeq (2\pi k\rho)^{-1/2} \frac{2 \sin \frac{\theta}{2} \sin \frac{\Theta}{2}}{\cos \theta + \cos \Theta} e^{-ik\rho + i\pi/4}$$

ϕ_d is the asymptotic expansion of the diffracted wave and is the same expression expressed by Candell (5) except for the sign in the complex exponent.

Chapter IVTWO-STREAM-FLOW ACOUSTIC PROBLEMIV-1 Nature of the Problem:

In conventional and short-take off and landing aircraft, the high velocity exhaust gas from the engine is usually the dominating noise source. The so-called "mixing noise", which is produced by the turbulent eddies in a region near the nozzle exit, together with the turbine and other engine noise is transmitted through a jet stream into the ambient atmosphere, which, in most cases, is in relative motion with respect to the aircraft. Figure (4-A) below shows the situation when the engine is installed over the wing.

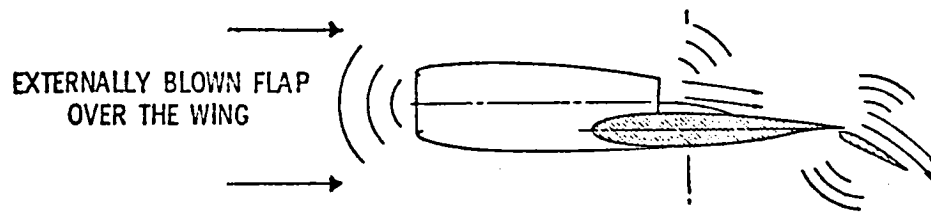


Figure (4-A): Over the wing external blowing.

Since the shielding of the wing is more effective on the high frequency end of the noise spectrum, the effect of shielding is studied based on the model problem shown in figure (4-B) below.

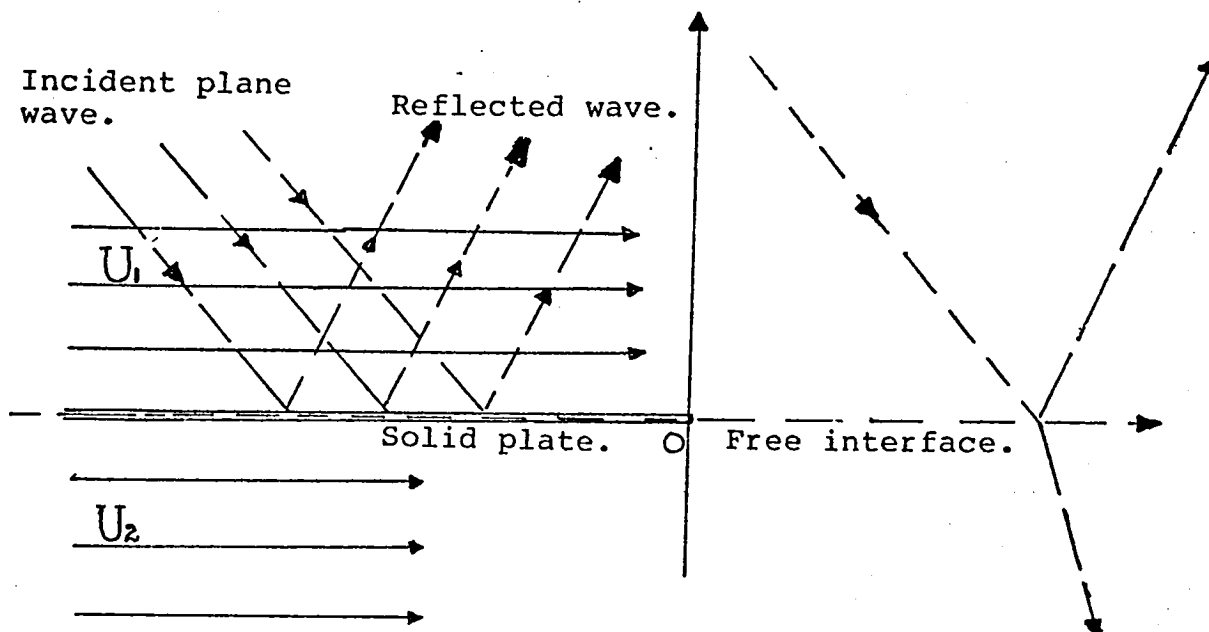


Figure (4-B): Two stream flow with plane wave and solid plate.

The problem consists of a wing surface which separates two of different velocities. In the region above the wing, the flow represents the exhaust of jet. The source of the noise is embedded in this flow at some distance from the surface. The flow below the surface represents the forward

motion of the aircraft, and the interest here is in studying the acoustic field below the wing.

The following assumptions will be used for the study of this problem.

- (i) The problem is treated as two dimensional.
- (ii) The wing surface is approximated by a semi-infinite thin plate lying along the negative X-axis.
- (iii) The dominant frequency of the source is high enough so that the short wave length approximation may be used.
- (iv) To simplify the mathematical treatment, the incoming sound wave is treated as a plane wave as an approximation to the case when the source is very far from the edge of the plate.
- (v) The jet stream is attached to the wing surface and extends over the entire half plane.

The method to be used in studying this problem is basically that discussed in chapter III. The first approximation of the problem is obtained by applying the

method of ray acoustics. The boundary surface consists of not only solid surface but also the interface between the two streams where transmission and reflection take place.

In solving this classical problem (transmission of sound through a shear layer), no consideration will be attempted in the stability of the problem. The study here will be confined to the study of the sound field below the plate, so that the boundary chosen for the Kirchhoff's integral consists of the half circle bounded by the flat plate and the free layer.

The solution for this problem is obtained for the case of a large wave number. Since the problem involves no characteristic length, this solution will be valid for any value of k at a large distance also. The effects of the free stream, the deflection and reflection at the interface are contained in the results obtained. However, no numerical calculations have been attempted.

IV-2 Problem Formulation:

The problem outlined in section IV-1 above is

represented in figure (4-B). The field equations are appropriately given as:

$$\frac{\partial^2 \phi_1}{\partial x^2} + \frac{\partial^2 \phi_1}{\partial y^2} + \frac{\partial^2 \phi_1}{\partial z^2} - \frac{1}{a_0} \left(\frac{\partial}{\partial t} + U_1 \frac{\partial}{\partial x} \right)^2 \phi_1 = 0 \quad (4-1)$$

$$\frac{\partial^2 \phi_2}{\partial x^2} + \frac{\partial^2 \phi_2}{\partial y^2} + \frac{\partial^2 \phi_2}{\partial z^2} - \frac{1}{a_0} \left(\frac{\partial}{\partial t} + U_2 \frac{\partial}{\partial x} \right)^2 \phi_2 = 0 \quad (4-2)$$

where ϕ_1 and ϕ_2 are velocity potentials above and below the $y = 0$ plane respectively. The boundary conditions are:

$$(i) \quad \frac{\partial \phi_1}{\partial y} = \frac{\partial \phi_2}{\partial y} = 0 \quad \text{on } y = 0; \quad -\infty < x < 0$$

$$(ii) \quad P_1 = P_2 \quad \text{and} \quad \eta_1 = \eta_2 \quad \text{on } y = 0; \quad 0 < x < \infty \quad \text{where } P_1$$

and P_2 are the pressures and η_1 and η_2 the particle displacements above and below the $y = 0, x > 0$ plane calculated from ϕ_1 and ϕ_2

(iii) The Sommerfeld radiation condition is to be satisfied.

The above problem will be solved by applying the Kirchhoff's integral over the lower half plane. To do this one has to find the boundary value of ϕ_2 at the interface by the analysis given in section IV-3.

IV-3 (1) The Dispersion Relation of a Plane wave in aUniform Stream:

The convected wave equation in a stream of velocity U

$$\text{is } \frac{\partial^2 \phi}{\partial x^2} + \frac{\partial^2 \phi}{\partial y^2} - \frac{1}{a_0} \left(\frac{\partial}{\partial t} + U \frac{\partial}{\partial x} \right) \phi = 0 \quad (4-3)$$

If $\phi = e^{i(k_1 x + k_2 y) - i\omega t}$ then equation (4-3) becomes,

with the definition of $k = \frac{\omega}{a_0}$; $M = \frac{U}{a_0}$

$$\left(k_1 + \frac{Mk}{1-M^2} \right)^2 + \frac{k_2^2}{1-M^2} = \frac{k^2}{(1-M^2)^2} \quad (4-4)$$

The locus of relation (4-4) is an ellipse as shown in figure

(4-C).

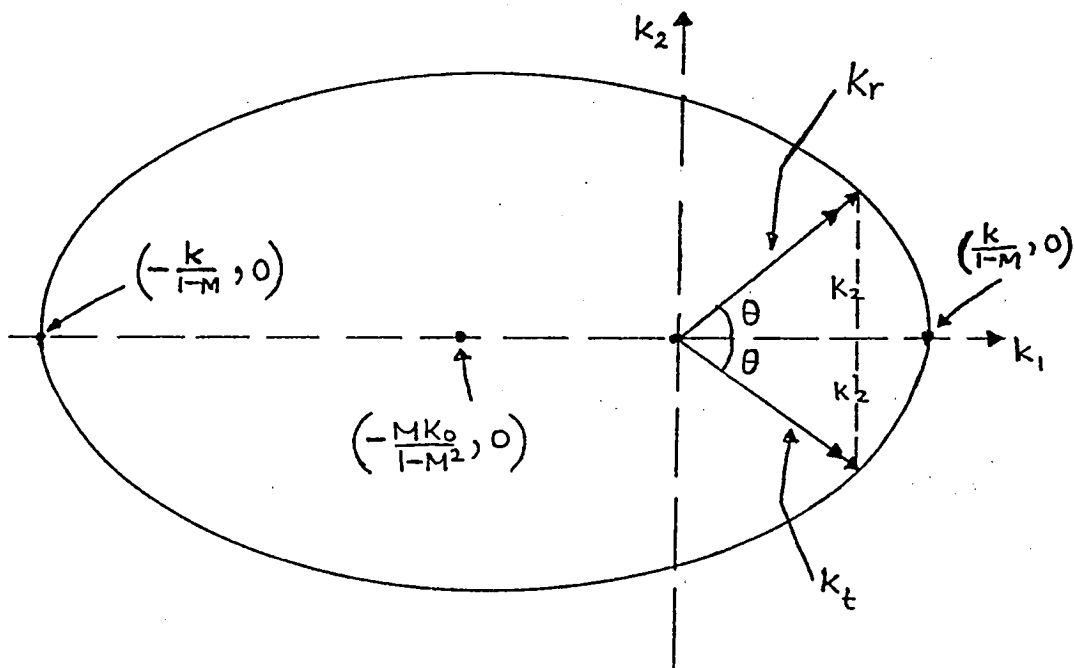


Figure (4-C): An ellipse showing the locus of the incident wave number k_1 .

It is to be noted that for any given value of K_1 , two solutions of K_2 are possible. The one denoted by \vec{K}_r has a positive K_2 and corresponds to a plane wave propagating upward away from the $y = 0$ plane; while the one denoted by \vec{K}_t has a negative value of K_2 and corresponds to a plane wave propagating downward into the half-plane.

(2) Reflection and deflection at the interface of two uniform flows with different velocities U_1 and U_2 :

If two flows are involved as in section IV-2, then there will be equations for the two conic sections (ellipses) determined in the manner outlined in the last section. The two ellipses which intersect one another are shown in figure (4-D) below.

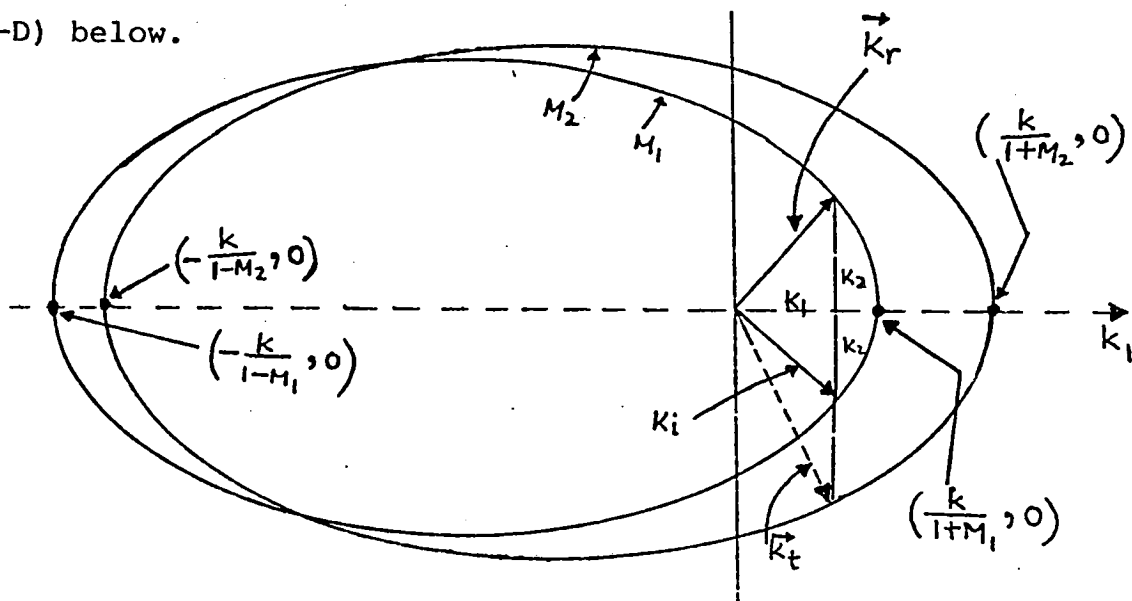


Figure (4-D): Superposed ellipses showing the two stream flow acoustic structure.

The equations are given below:

$$\left(k_1 + \frac{M_1 k}{1-M_1^2}\right)^2 + \frac{k_2^2}{1-M_1^2} = \frac{k^2}{(1-M_1^2)^2} ; \quad y > 0 \quad (4-5)$$

$$\left(k_1 + \frac{M_1 k}{1-M_1^2}\right)^2 + \frac{k_2^2}{1-M_2^2} = \frac{k^2}{(1-M_2^2)^2} ; \quad y < 0 \quad (4-6)$$

At the interface $y = 0$ separating the two streams U_1 and U_2 an incident wave will produce a transmitted wave as well as a reflected one. As will be shown in the next section, the K_1 component of these three waves must be equal. With a given incident wave K_i propagating towards the interface, the reflected wave K_r in the upper half plane $y > 0$ is determined from the ellipse $M = M_1$ which is the Mach number of the upper stream, and the transmitted wave \vec{K}_t in the lower half-plane $y < 0$ is determined from the other ellipse denoted by $M = M_2$ which is the Mach number of the lower stream. Thus, in the case $M_1 > M_2$ as shown in figure (4-D), sound waves are deflected toward the shadow region under the plate due to the presence of the velocity discontinuity.

(3) The Transmission and Reflection Coefficients:

In this case the solution of equations (4-1) and (4-2) in the absence of the plate (that is, if the interface $\gamma = 0$ extends from $X = -\infty$ to $X = +\infty$) are considered. The results are used to determine the boundary condition at $\gamma = 0, X > 0$ in the Kirchhoff's integral to solve the two-stream problem.

In the region $\gamma > 0$, the solution of equation (4-1) consists of an incident and a reflected wave while in the region $\gamma < 0$ the solution of equation (4-2) consists of transmitted wave only. If one selects:

$$\phi_1 = \phi_i + \phi_r \quad (4-7)$$

$$\phi_2 = \phi_t$$

where

$$\phi_i = A_i e^{i(k_1 X - k_2 \gamma - \omega t)}$$

$$\phi_r = A_r e^{i(k_1 X + k_2 \gamma - \omega t)}$$

$$\phi_t = A_t e^{i(k_1 X + k_2' \gamma - \omega t)} \quad (4-8)$$

where A_i, A_r, A_t are the wave amplitudes for the incidence, reflection and transmission,

The boundary conditions on the interface ($\gamma = 0$)

require that:

- (i) There must be a pressure balance across the interface;

hence $p_1 = p_2$

where $p_1 = -\rho_0 \left(\frac{\partial}{\partial t} + U_1 \frac{\partial}{\partial x} \right) \phi_1$

and $p_2 = -\rho_0 \left(\frac{\partial}{\partial t} + U_2 \frac{\partial}{\partial x} \right) \phi_2$

or

$$\left(\frac{\partial}{\partial t} + U_1 \frac{\partial}{\partial x} \right) \phi_1 = \left(\frac{\partial}{\partial t} + U_2 \frac{\partial}{\partial x} \right) \phi_2 \quad \text{on } y=0 \quad (4-9)$$

- (ii) The particle displacement of the two streams should

be the same at the interface. This means that

$$\eta_1 = \eta_2 = \eta$$

where the expression of the interface is taken to be:

$$g(x, y, t) = y - \eta(x, t) \quad (4-10)$$

and the equation of $g(x, y, t)$ is:

$$\frac{\partial g}{\partial t} + \vec{u} \cdot \nabla g = 0 \quad (4-11)$$

When this equation is linearized and applied separately

to the upper and the lower streams, the following kinematic

conditions result. $v_1 = \frac{\partial \eta_1}{\partial t} + U_1 \frac{\partial \eta_1}{\partial x}$; $v_1 = \frac{\partial \phi_1}{\partial y}$ on $y > 0$

$$v_2 = \frac{\partial \eta_2}{\partial t} + U_2 \frac{\partial \eta_2}{\partial x}$$
 ; $v_2 = \frac{\partial \phi_2}{\partial y}$ on $y < 0$

On matching these conditions, one obtains:

$$\left(\frac{\partial}{\partial t} + U_2 \frac{\partial}{\partial x}\right) \frac{\partial \phi_1}{\partial y} = \left(\frac{\partial}{\partial t} + U_1 \frac{\partial}{\partial x}\right) \frac{\partial \phi_2}{\partial y} \quad \text{at } y=0 \quad (4-12)$$

On substituting expressions (4-7) into equations (4-9) and (4-12) and setting $y = 0$ in the result, each term in the resulting equations will contain the factor $e^{ik_1 x - i\omega t}$

A necessary condition to obtain a consistent solution is, therefore, to choose the same k_1 for all three wave solutions ϕ_1 , ϕ_r , and ϕ_t . This is what has been used in writing equation (4-10) and in determining \vec{k}_r and \vec{k}_t using the ellipses in section IV-3 (2).

Since the wave number \vec{k}_i of the incident wave is given as a boundary condition, the value \vec{k}_1 , \vec{k}_2 and \vec{k}'_2 for all three expressions in equation (4-8) are determined. The two equalities resulting from the two conditions at the interface, namely, equations (4-9) and (4-12), serve to determine the reflection coefficient $R_c = \frac{A_r}{A_i}$ and the transmission coefficient $T_c = \frac{A_t}{A_i}$. Let $D_1 = \omega + U_1 K_1$ and $D_2 = \omega + U_2 K_1$.

Equations (4-9) and (4-12) yield:

$$\left. \begin{aligned} D_1 (A_i + A_r) &= D_2 A_t \\ K_2 D_2 (A_i - A_r) &= K_2' D_1 A_t \end{aligned} \right\} \quad (4-13)$$

then

$$R_c = \frac{K_2 D_2^2 - K_2^1 D_1^2}{K_2 D_2^2 + K_2^1 D_1^2} \quad (4-14)$$

$$T_c = \frac{2 D_1 D_2 K_2}{K_2 D_2^2 + K_2^1 D_1^2}$$

IV-4 Solution of the Two-Stream Problem:

The interest here is in determining the wave transmission and refraction in the region under the wing (see figure 4-E); for this reason the Kirchhoff's integral is applied using a contour enclosing the lower half plane, and composed of the semi-infinite plate, the interface and a semi-circle of infinite radius. In addition, use is made of the short wave length approximation (that is, $k = \frac{\omega}{a_0} \gg 1$) to find the asymptotic solution of ϕ_2 valid to the order $O\left(\frac{1}{\sqrt{k}}\right)$.

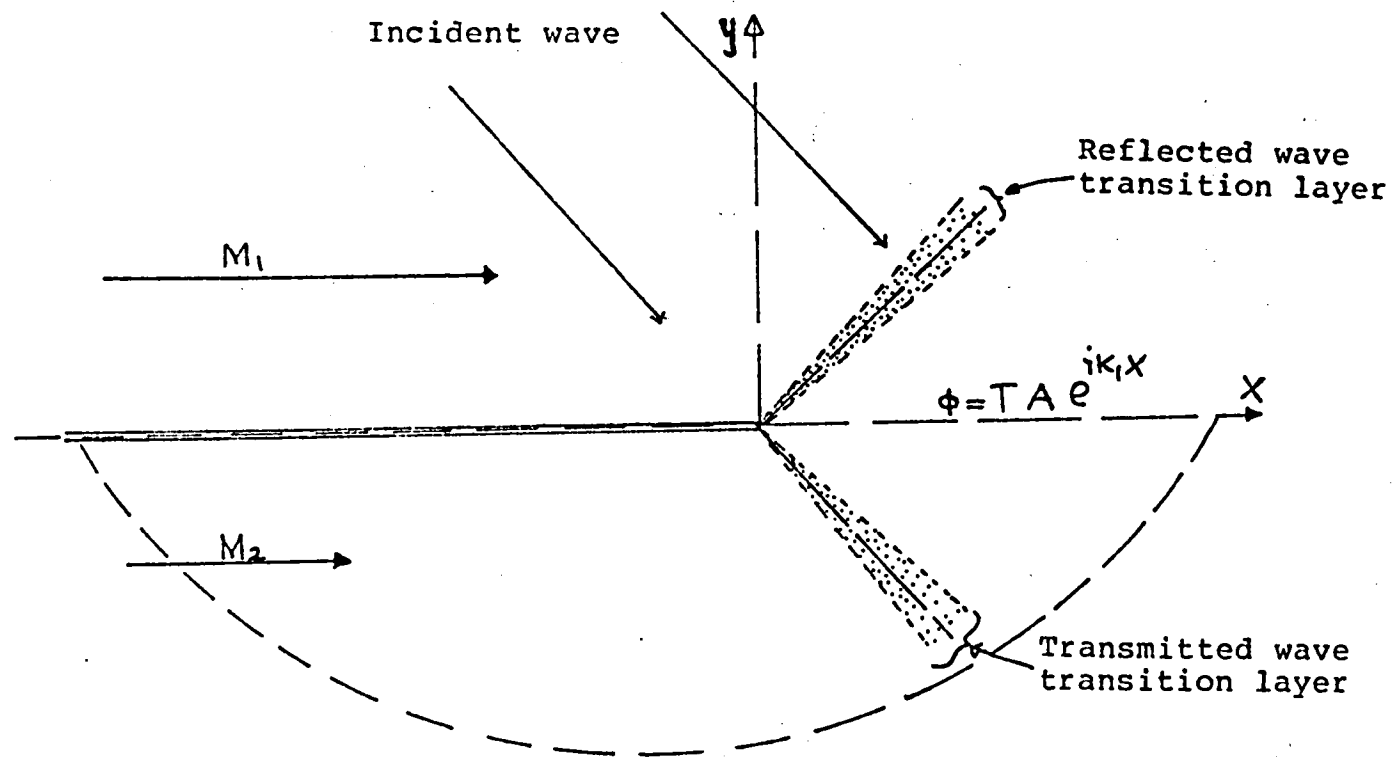


Figure (4-E): Transition zones in ray acoustics.

Two important approximations are then made possible.

These are:

(1) The method of stationary phase can be used to evaluate the Kirchhoff's integral. As shown in chapter III, the point of stationary phase is located on the part of the control surface which lies between the acoustic source and the point of observation. Thus, in the present problem the point of stationary phase lies on the surface composed of the solid plate and the interface. Any contribution from integral over the semi-circular arc is of higher order and need not be considered.

(2) As shown in figure (4-E) the region of the transition layers approach two narrow sectors as k becomes sufficiently large. Outside these two sectors, the solution given by the ray acoustics is accurate to the extent that the neglected error terms are of the order $O\left(\frac{1}{k}\right)$. The solution sought for the transmission transition layer is of lower order (that is $O\left(\frac{1}{\sqrt{k}}\right)$), and hence can be determined by the Kirchhoff's

integral using the boundary value on the $y = 0$ axis given by the ray acoustics.

With these in mind, one may reformulate the problem in a way that one can solve it by the general method outlined in chapter III. Since the interest in this problem is in the transmitted wave across the interface, the field equations will be developed for the lower flow regime.

IV-5 Field equations and solution procedure.

$$(1 - M^2) \frac{\partial^2 \phi}{\partial x^2} + \frac{\partial^2 \phi}{\partial y^2} - 2kM_2 i \frac{\partial \phi}{\partial x} + k^2 \phi = 0 \quad (4-15)$$

where $k = \frac{\omega}{a_0}$

The appropriate boundary conditions are:

(i) At the interface, $y = 0$; $x > 0$, the solution of ϕ_2 is the same as the one given by the ray acoustics, namely, the form expressed in equation (4-7) as discussed in section IV-3.

$$\phi_2 = A_t e^{i(k_1 x + k'_2 y - \omega t)}$$

with A_t and k'_2 likewise determined by the method outlined in that section. Thus:

$$\phi_2 = A_t e^{ik_1 x} \quad \text{and} \quad \frac{\partial \phi_2}{\partial y} = iA_t k'_2 e^{ik_1 x} \quad \text{at} \quad \begin{matrix} y=0 \\ x>0 \end{matrix} \quad (4-16)$$

(ii) At the backside of the plate, (that is, in $\gamma < 0$, $x < 0$), the sound is completely shielded according to the ray acoustics. So,

$$\phi_2 = \frac{\partial \phi_2}{\partial \gamma} = 0 \quad \text{at } \gamma = 0, x < 0 \quad (4-17)$$

(iii) The radiation condition is satisfied at $\gamma = -\infty$.

Let
$$\phi = e^{\frac{ik_M x}{1-M^2}} \psi \quad (4-18)$$

This gives, on substitution into equation (4-3):

$$\frac{\partial^2 \psi}{\partial x^2} + \frac{1}{1-M^2} \frac{\partial^2 \psi}{\partial \gamma^2} + \frac{k^2}{(1-M^2)^2} \psi = 0 \quad (4-19)$$

with the boundary conditions of the form:

$$(i) \quad \psi = A_t e^{i\Omega x} ; \quad \frac{\partial \psi}{\partial \gamma} = i A_t k'_2 e^{i\Omega x} ; \quad \begin{matrix} \gamma=0 \\ x>0 \end{matrix}$$

where
$$\Omega = k_1 - \frac{M_2 k}{1-M_2^2}$$

$$(ii) \quad \psi = \frac{\partial \psi}{\partial \gamma} = 0 \quad \text{on } \gamma = 0, x < 0 \quad (4-21)$$

(iii) The radiation condition at $\gamma = -\infty$

On introducing new variables:

$$\bar{x} = x; \quad \bar{\gamma} = \gamma \sqrt{1-M_2^2}; \quad \bar{k} = \frac{k}{\sqrt{1-M_2^2}}; \quad \bar{k}'_2 = \frac{\bar{k}'_2}{\sqrt{1-M_2^2}}$$

The equation (4-19) reduces to the standard form:

$$\frac{\partial^2 \psi}{\partial \bar{x}^2} + \frac{\partial^2 \psi}{\partial \bar{\gamma}^2} + \bar{k}^2 \psi = 0 \quad (4-22)$$

with the boundary conditions:

$$\left. \begin{aligned}
 \text{(i)} \quad \psi &= A_t e^{i\Omega \bar{x}} \quad ; \quad \frac{\partial \psi}{\partial \bar{y}} = i A_t \bar{k}_2 e^{i\Omega \bar{x}} \quad \text{on} \quad \left. \begin{array}{l} \bar{y} = 0 \\ \bar{x} > 0 \end{array} \right\} \\
 \text{(ii)} \quad \psi = \frac{\partial \psi}{\partial \bar{y}} &= 0 \quad \text{on} \quad \bar{y} = 0, \quad \bar{x} < 0 \\
 \text{(iii)} \quad \text{The radiation condition is satisfied at } \bar{y} &= -\infty
 \end{aligned} \right\} \begin{array}{l} (4-23) \\ (a, b, c) \end{array}$$

Equations (4-22) and (4-23) constitute a standard wave scattering problem which has been discussed thoroughly in chapter III.

The solution of these equations is:

$$\psi(\bar{x}, \bar{y}, \bar{k}) = A_t e^{i(\Omega \bar{x} + k'_2 \bar{y})} F(\bar{\beta}) \quad (4-24)$$

where

$$\bar{k}'_2 = -\sqrt{\sigma^2 - \Omega^2}$$

and

$$F(\bar{\beta}) = \frac{1+i}{\pi} \int_{\bar{\beta}}^{\infty} e^{-u^2} du$$

with

$$\bar{\beta}^2 = \bar{k}^2 [\bar{r}_m - \bar{r}_0]$$

as shown in figure

(4-F) next page. The final solution for θ is obtained by a

direct substitution:

$$\phi = T_c A_i e^{i \left[k_1 \bar{x} - \sqrt{k^2 + 2kM_2 k_1 - (1-M_2^2) k_1^2} \bar{y} \right]} F(\bar{\beta})$$

(4-25)

where \bar{r}_0 , $\bar{\theta}$, $\bar{\Theta}$, σ are defined next page.

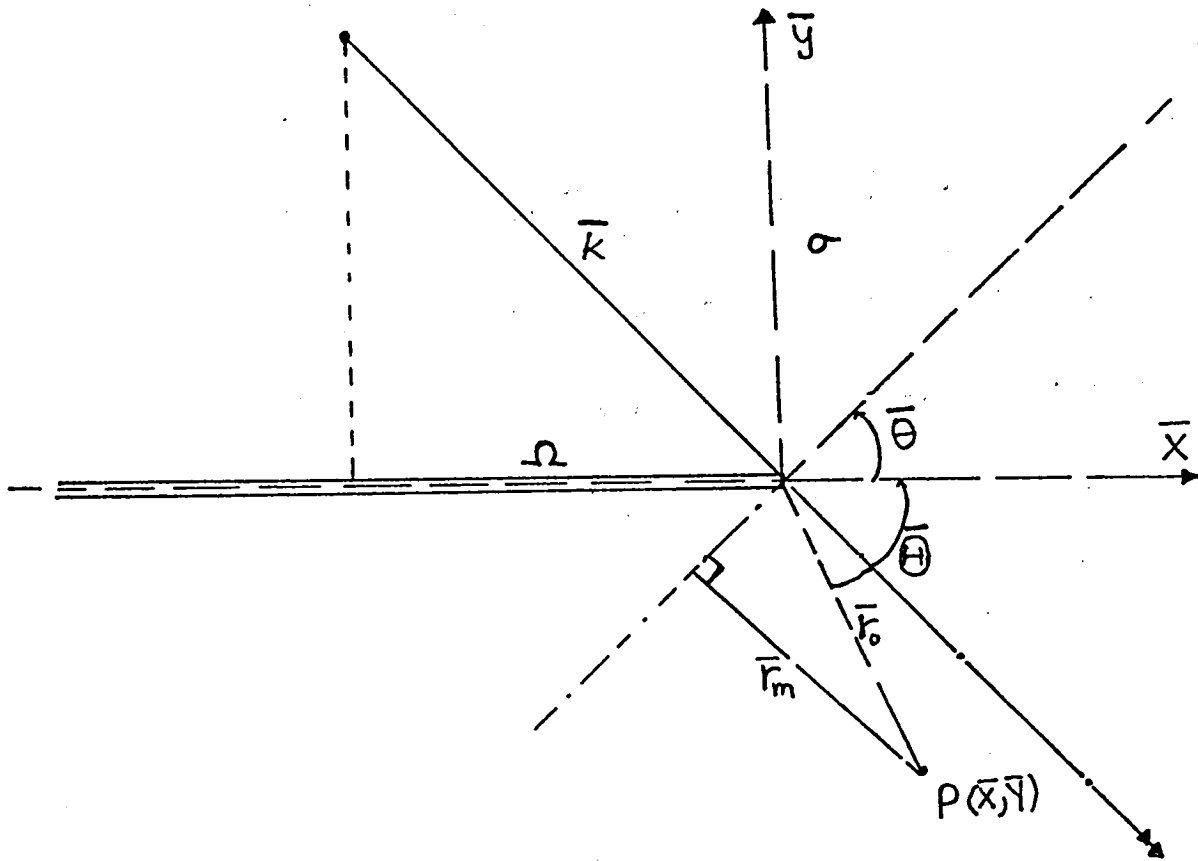


Figure (4-F): The geometry showing the transformation as in the solution in equation (4-25).

$$\bar{b} = \sqrt{\frac{2k\bar{r}_0}{1-M_2^2}} \sin\left(\frac{\bar{\theta} - \hat{\theta}}{2}\right)$$

$$\bar{r}_0 = \sqrt{x^2 + (1-M_2^2)y^2} \quad ; \quad \bar{k} = \frac{k}{1-M_2^2}$$

$$\sin \bar{\theta} = -\frac{\bar{y}}{\bar{r}_0} = -\frac{\sqrt{(1-M_2^2)}y}{\sqrt{x^2 + (1-M_2^2)y^2}}$$

$$\sin \hat{\theta} = \frac{\sigma}{k}$$

$$\sigma = \sqrt{\frac{k^2 + 2k_1kM_2 - (1-M_2^2)k_1^2}{(1-M_2^2)}}$$

Chapter VCONCLUSIONS:

The methodology that has been designed and used in the previous chapter proves extremely powerful in handling the problem of current interest in noise shielding by aircraft wing. Additional features and utility of the mathematical method formulated can be illustrated in the following aspects of noise shielding.

V-1 Shielding by a Finite Plate:

The solution method for a semi-infinite plate can be used to obtain the solution for a finite wing. The following discussion is based on the two-dimensional case. As shown in figure (5-A) next page, the potential $\phi(P)$ at a point P below the semi-infinite plate is due to the direct radiation and given by:

$$\phi(P) = + \phi_0 F(\bar{\beta}) \quad (5-1)$$

where $F(\bar{\beta})$ is the diffraction factor, and

$$\bar{\beta}^2 = k \left[\vec{SO} + \vec{OP} - \vec{SP} \right] \quad (5-2) (a)$$

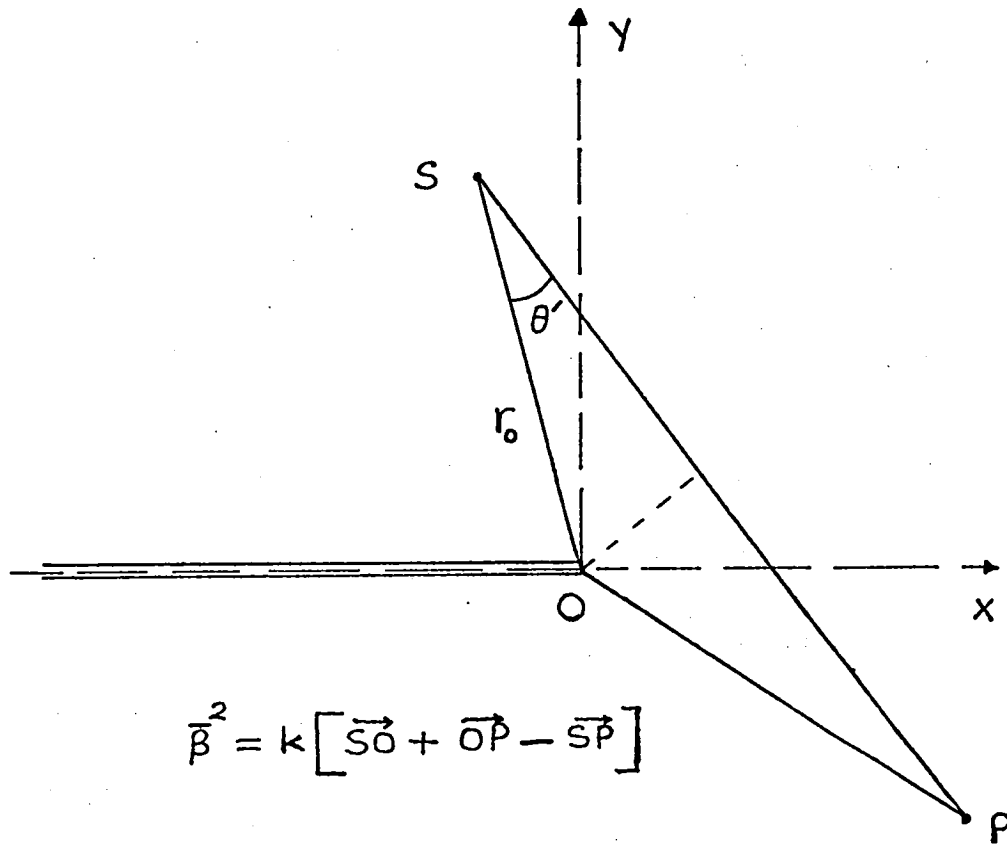


Figure (5-A): Geometry defining the diffraction factor for the two-dimensional case.

When P is very far away, $\bar{\beta}$ is given approximately by:

$$\bar{\beta}^2 = k [r_0 - r_0 \cos \theta'] = 2k r_0 \sin^2 \frac{\theta'}{2} \quad (5-2) (b)$$

or

$$\bar{\beta} = -\sqrt{2k r_0} \sin \frac{\theta'}{2} \quad (5-3)$$

In this formula, θ' is the angle between the line \overrightarrow{SP} and the line \overrightarrow{OS} figure (5-B).

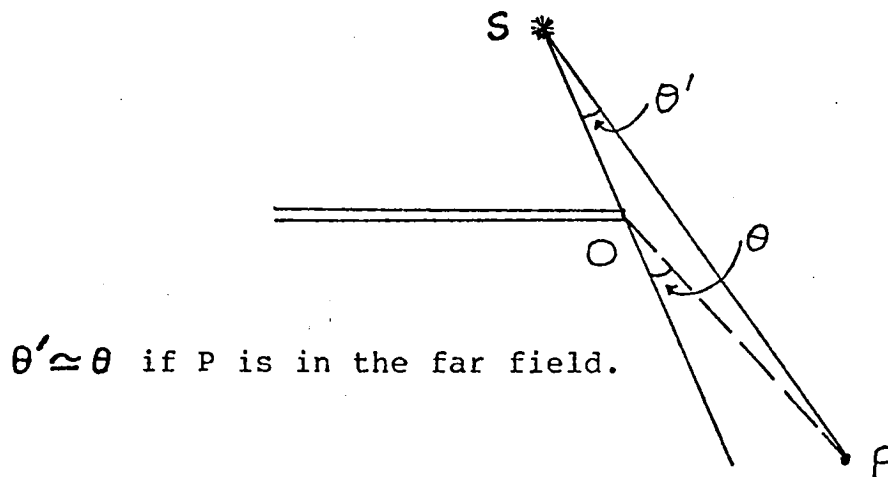


Figure (5-B): Far field approximation of wave reception at P.

When P is very far away, this angle becomes approximately equal to θ , which is the angle between the line \overrightarrow{OP} and a line passing through the two points S and O. According to

ray acoustics, the line OP defines the boundary line between the propagation and the shadow regions.

The potential at P, to the first order of accuracy, may be written as:

$$\phi = +\phi_0 F(\bar{\beta})$$

with

$$\bar{\beta} = -\sqrt{2kr_0} \sin \frac{\theta}{2}$$

As shown in figure (5-C) next page, the transition from full transmission to complete blockage takes place inside a sector centred at the trailing edge of the plate. The angular width of the sector decreases as the wave number K increases.

Figure (5-D) next page shows the acoustic field due to the reflected wave. Again for large K, the transition takes place within a narrow sector.

The implication of the above observation is that for the case of large K, the solution of $\phi(P)$ for a finite plate can be obtained by combining two solutions: one solution corresponds to waves diffracted around the trailing edge and the other corresponds to waves diffracted around the leading edge.

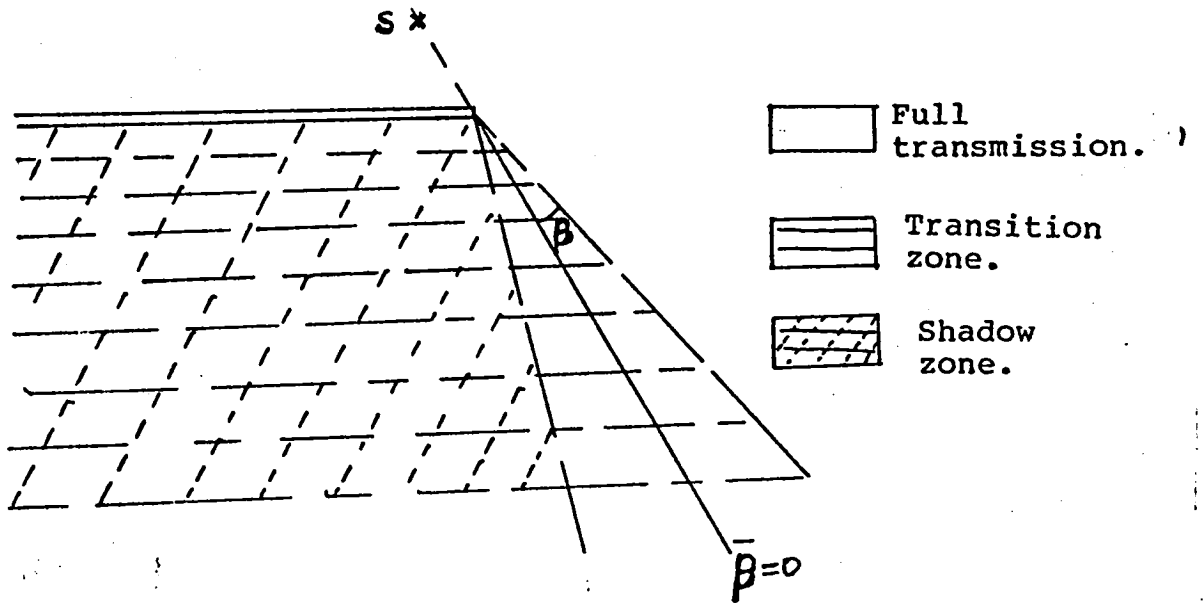


Figure (5-C): Incident wave field variation.

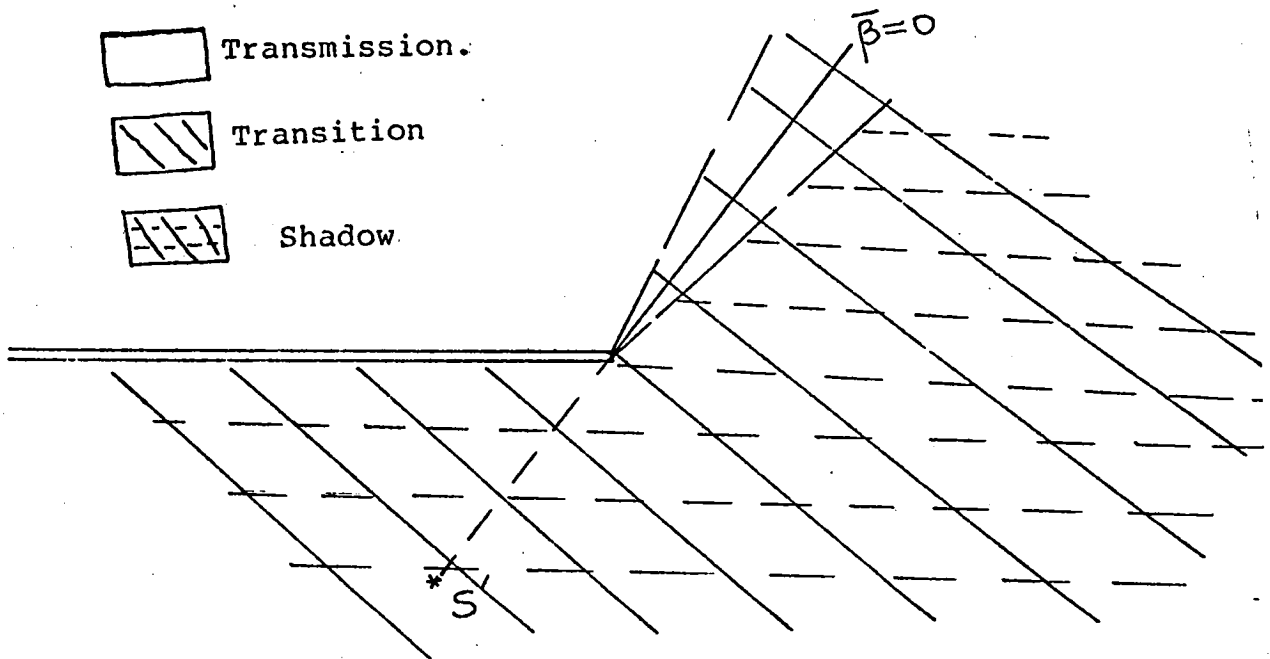


Figure (5-D): Reflected wave field variation.

It can be shown that, for a long plate, the resulting solution will not significantly violate the boundary conditions imposed on the problem (figure 5-E) below. Using this approach the diffracted field around a plate of finite length has been calculated numerically. Figures (5-F, 5-G and 5-H) next three pages show the results of such calculations.

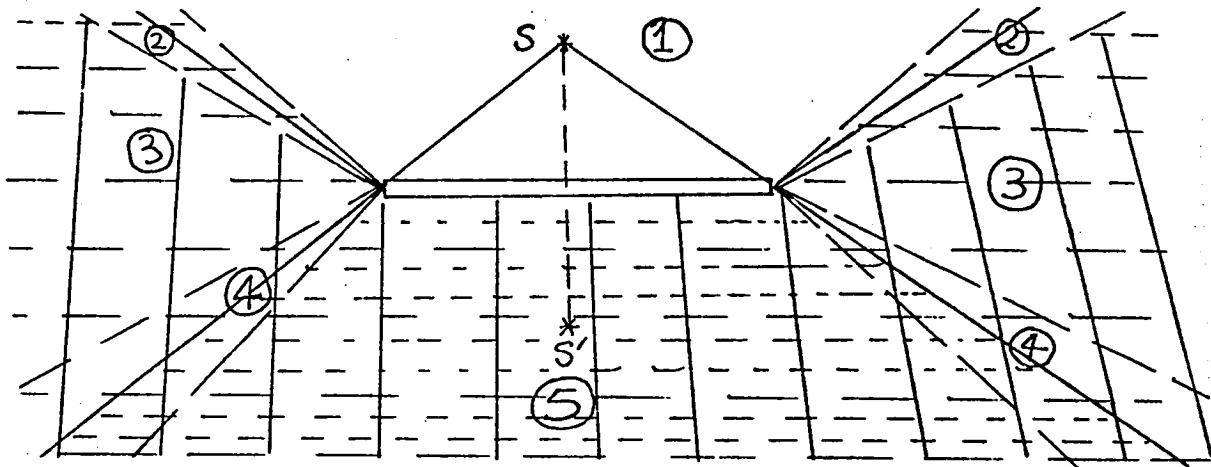
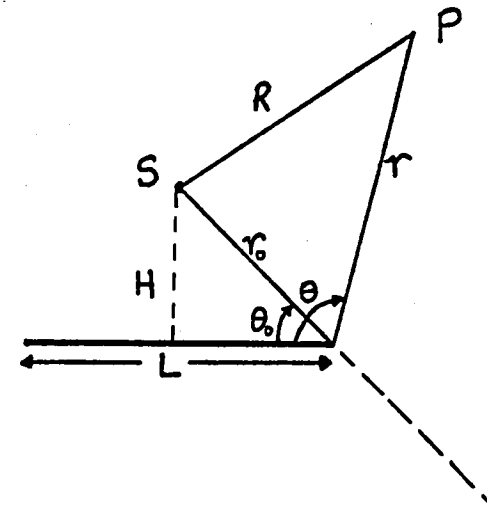
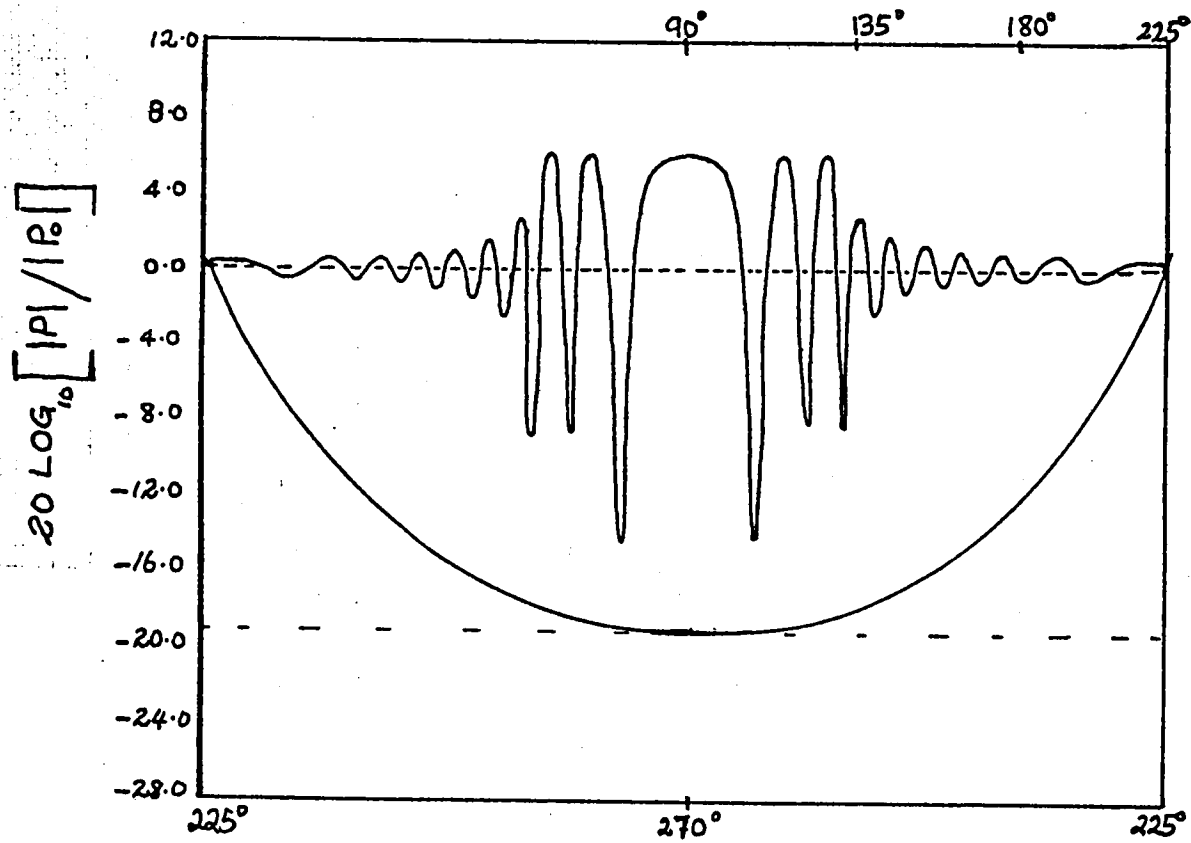


Figure (5-E): Configuration of a finite plate and a simple source above it.

1. Incident and Reflected wave.
2. Transition between 1 and 3.
3. Incident wave only.
4. Transition between 3 and 5
5. Complete shadow.



$H = 5.0$
 $\lambda = 1.0$
 $L = 10.0$
 $r = 1000.0$
 $\theta_0 = 45^\circ$

Figure (5-F): Finite plate solution for $\lambda = 1$, with the source centrally located.

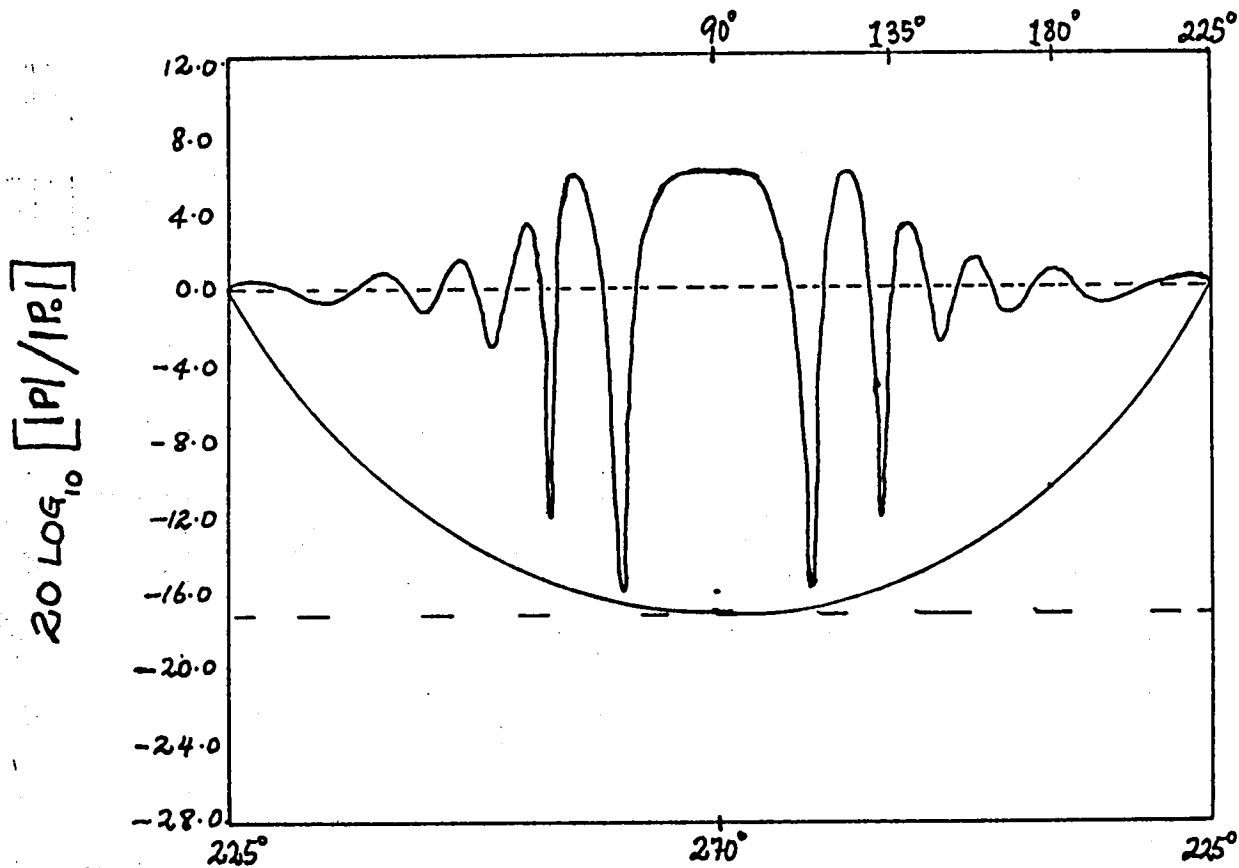
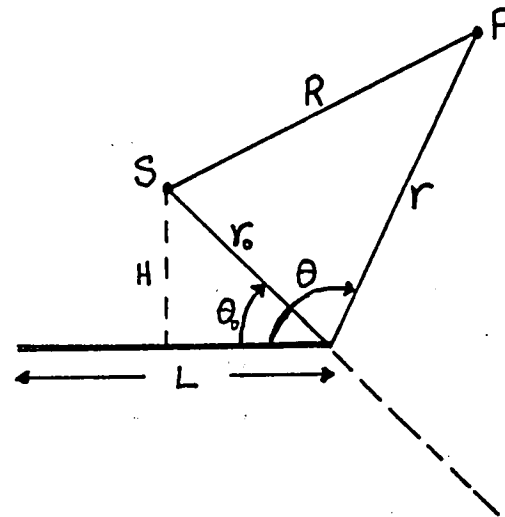


Figure (5-G): Finite plate solution for $\lambda = 2$ with the source centrally located.



$H = 5.0$
 $\lambda = 2.0$
 $L = 10.0$
 $r = 1000.0$
 $\theta_0 = 45^\circ$

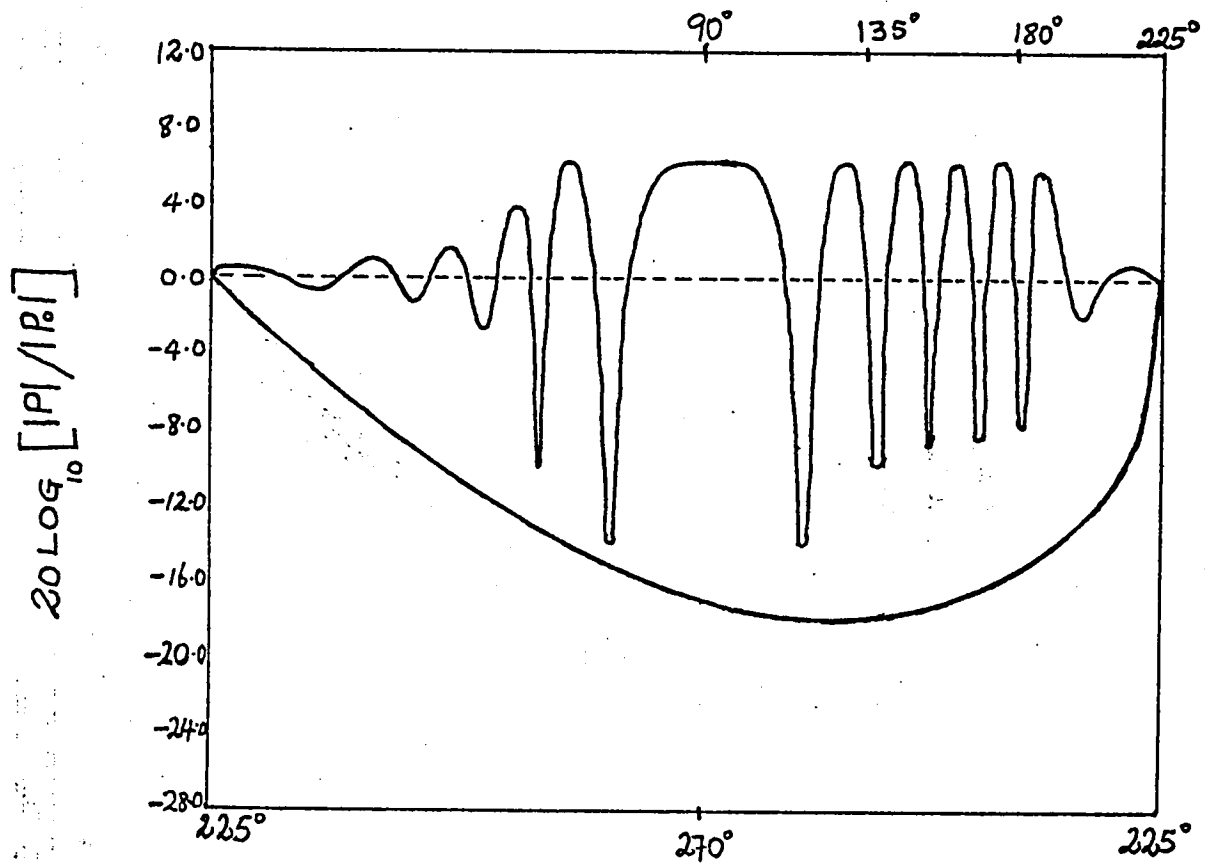
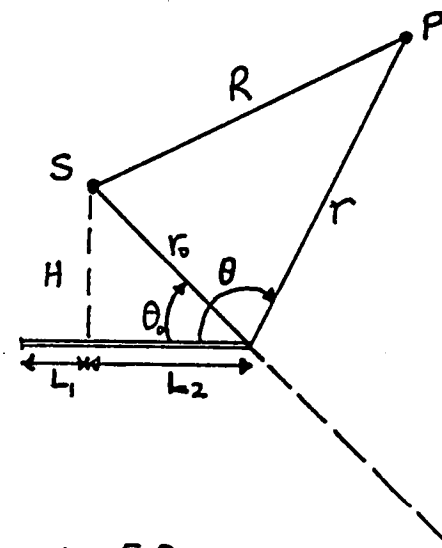


Figure (5-H): Finite plate solution for $\lambda = 2$ with the source not centrally located.



$H = 5.0$
 $L_1 = 5.0$
 $L_2 = 20.0$
 $\lambda = 2.0$
 $r = 1000.0$

V-2 Effect due to Gaps, Angular Deflection and otherGeometrical Variation of the Wing Surface:

The audible range of the aircraft sound lies essentially between 20 to 20,000 Hz, corresponding to wave length of about 16 metres to 2 centimetres. If the dimension of any geometrical variation for the assumed plate and a gap on the plate surface is less than the dominant wave length of the sound, the fluid pressure and velocity variation over that part of the wing surface is nearly simultaneous. Therefore, the solution to the region of the acoustic field may be approximated by the solution of the steady compressible flow equation. A local solution obtained by this equation is needed in order to smooth out any discontinuities in velocity pressure or mass flow due to ignoring such geometrical variation in the first approximation. In the gap problem discussed in chapter II, for example, the tangent velocity over the upper and the lower surface given by the wave equation and neglecting the presence of the gap will be

discontinuous and a local solution near the gap is necessary to remove this discontinuity. In the far field, this local steady solution around the gap acts like localized acoustic poles. The strength and phase of these induced poles depend on the nature of the original sound source.

V-3 Effect of Source Distribution on Power Radiation:

The problems of acoustic interactions with barriers poses the more fundamental question of the nature the acoustic power is distributed in the region of interest. The clear understanding of this will facilitate the approach to the noise shielding.

It is known that the interaction of acoustic waves by any barrier has the effect of inducing distributed sources on the surface of the barrier and hence the problem then becomes one of understanding the nature of interactions from such sources and the effect these have on the power generated from the original source. The study on such problems is nearly a century old beginning with the study of such problems

in the field of radio waves. Recently, however, the effect of a boundary on the radiated power has been studied by Thiessen (41), Embleton (12) and Levine (27). In such studies, it has been indicated that the distribution of sources affects the impedance of the power transmission. In this study, the radiative power of a three-dimensional monopole source placed in a stationary medium in the presence of a semi-infinite plate will be briefly discussed. The mathematical expressions given below are in terms of the spherical coordinates whose centre is the point on trailing edge that lies in the same plane as the source point S (figure 5-I). The line through the point O into the paper is chosen as the polar axis whose azimuth and polar angles are θ and ν respectively.

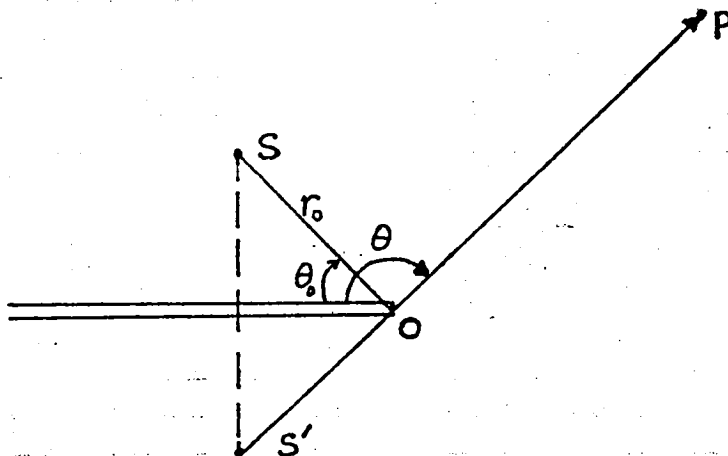


Figure (5-I): Spherical geometry for source distribution solution.

The ranges of such angles are:

$$0 \leq \theta \leq 2\pi ; \quad 0 \leq \nu \leq \pi/2$$

The potential $\phi(p, t)$ at a point $P(r, \psi, \theta)$ is obtained

as in chapter III as:

$$\phi = -\frac{e}{4\pi r_1} e^{i(kr_1 - \omega t)} F(\bar{\beta}_1) - \frac{e}{4\pi r_2} e^{i(kr_2 - \omega t)} F(\bar{\beta}_2) \quad (5-4)$$

where r_1 and r_2 are the distances from the point P to the points S and S' . $F(\bar{\beta}_1)$ and $F(\bar{\beta}_2)$ are the diffraction factors with $\bar{\beta}_1$ and $\bar{\beta}_2$ given by the expressions (assuming r very large):

$$\left. \begin{aligned} \bar{\beta}_1 &= -\sqrt{2kr_0 \sin \nu} \cos \left(\frac{\theta - \theta_0}{2} \right) \\ \bar{\beta}_2 &= +\sqrt{2kr_0 \sin \nu} \cos \left(\frac{\theta + \theta_0}{2} \right) \end{aligned} \right\} \quad (5-5)$$

The function F may be written in the form $F = A_1 e^{i\alpha_1}$.

Let $A_1(\bar{\beta}_1)$ and $\alpha_1(\bar{\beta}_1)$ be denoted by A_1 and α_1 ; and $A_2(\bar{\beta}_2)$

$\alpha_2(\bar{\beta}_2)$ by A_2 and α_2 . Then the following expressions for

large r may be easily obtained:

$$p' = -\frac{i\rho_0 \omega A_1}{4\pi r} e^{i(kr_1 - \omega t + \alpha_1)} - \frac{i\rho_0 \omega A_2}{4\pi r} e^{i(kr_2 - \omega t + \alpha_2)} \quad (5-6)$$

$$\bar{I} \approx \frac{1}{\rho_0 a_0} \langle p'^2 \rangle = \frac{\rho_0 \omega^2}{32\pi^2 a_0 r} \left[A_1^2 + A_2^2 + A_1 A_2 \cos \left[k(r_1 - r_2) + (\alpha_1 - \alpha_2) \right] \right] \quad (5-7)$$

where, for large r : $r_1 - r_2 \approx -2r_0 \sin \theta_0 \sin \nu \sin \theta$

The total radiated power W is then given by the expression:

$$W = \frac{\rho_0 \omega^2}{32\pi^2 a_0} \int_{\nu=0}^{\pi} \int_{\theta=0}^{2\pi} \left[A_1^2 + A_2^2 + A_1 A_2 \cos \left[k(r_1 - r_2) + (\alpha_1 - \alpha_2) \right] \right] \sin \nu d\nu d\theta \quad (5-8)$$

which may be evaluated numerically. For the purpose of the present discussion, it suffices to comment on the following simple example. Consider the source to be at a distance h above the edge of the plate (figure 5-J).

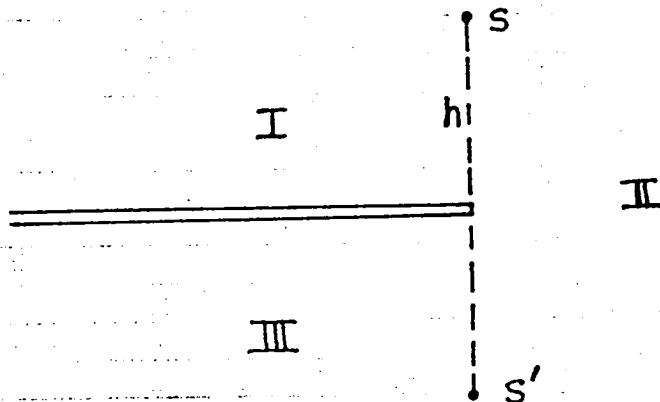


Figure (5-J): Set up for power approximation for distributed sources.

Assuming the wave number is very large, then the ray acoustic solution gives a good approximate solution.

The acoustic field then comprises of three regions with sharp boundaries. In region I, which is the region of direct radiation and reflection, sound is received from both the original source S and its image S' so that:

$$\phi = - \frac{e^{i(kr_1 - \omega t)}}{4\pi r_1} - \frac{e^{i(kr_2 - \omega t)}}{4\pi r_2} \quad (5-9)$$

The total radiated power from two identical sources with a separation distance $2h$ in a free space without boundaries can be easily be found.

$$W_{SS'} = \frac{\rho_0 \omega^2}{4\pi a_0} \left[1 + \frac{1}{2} \frac{\sin \mu}{\mu} \right]$$

where $\mu = 2kh$

The power radiated in region I is 1/4 of this value and is hence equal to:

$$W_I = \frac{\rho_0 \omega^2}{16\pi a_0} \left[1 + \frac{1}{2} \frac{\sin \mu}{\mu} \right] \quad (5-10) (a)$$

In region II, which is the region of direct radiation with no reflection, the radiated power is equal to 1/2 of the

power radiated by a source in the free space and is given by:

$$W_{II} = \frac{\rho_0 \omega^2}{16\pi a_0} \quad (5-10) (b)$$

In region III, where there is no radiation

$$W_{III} = 0 \quad (5-10) (c)$$

The total power radiated by the simple source in the presence of the plate is then:

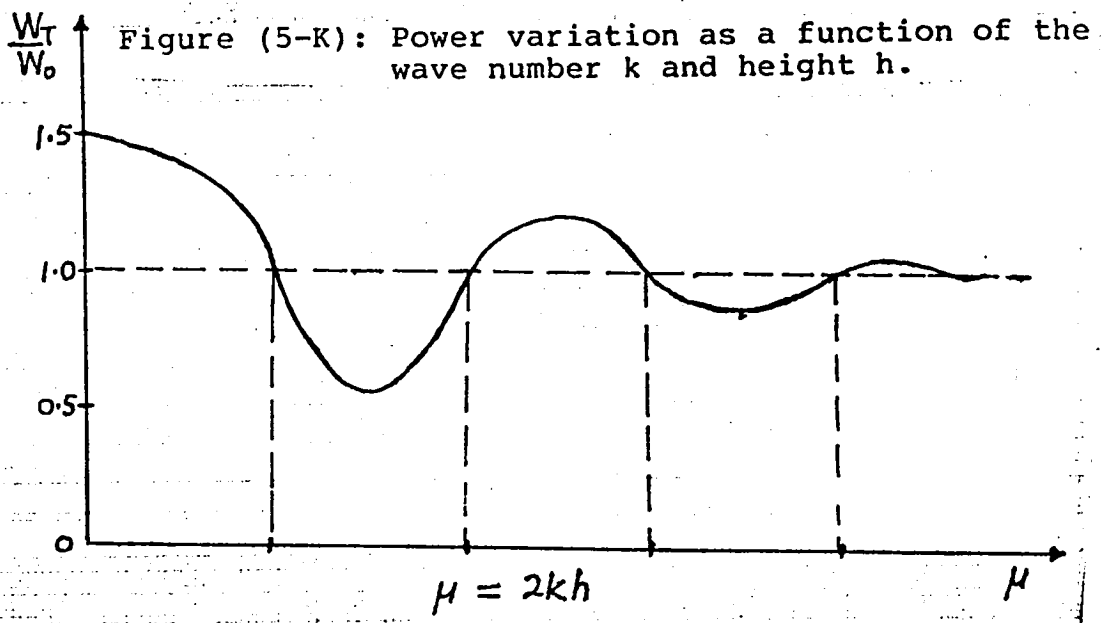
$$\begin{aligned} W_t &= W_I + W_{II} + W_{III} \\ &= \frac{\rho_0 \omega^2}{8\pi a_0} \left[1 + \frac{1}{2} \frac{\sin \mu}{\mu} \right] \end{aligned} \quad (5-11)$$

so that $\frac{W_T}{W_0} = 1 + \frac{1}{2} \frac{\sin \mu}{\mu}$

where $W_0 = \frac{\rho_0 \omega^2}{8\pi a_0}$ is the power radiated by a simple source

in the free space. In figure (5-K), the variation of $\frac{W_T}{W_0}$

is plotted as a function of μ .



It is seen that, as the source approaches the plate (that is $h \rightarrow 0$ or $\mu \rightarrow 0$), the radiated power approaches a value which is 50% greater than the value for the source without the plate, so that

$$\frac{W_T}{W_0} \rightarrow 1.5 \quad \text{as} \quad \mu \rightarrow 0$$

On the other hand, when h is much larger than the acoustic wave length, then

$$\frac{W_T}{W_0} \rightarrow 1 \quad \text{as} \quad \mu \rightarrow \infty$$

Between these two limits, the value of $\frac{W_T}{W_0}$ oscillates through a series of maxima and minima about the value $\frac{W_T}{W_0} = 1$

The crossover points with $\frac{W_T}{W_0} = 1$ are $\mu = n\pi$ where $n = 1, 2, \dots$

The corresponding values of h is ($\lambda = \frac{2\pi}{k} = \text{wave length}$)

$$\text{with } h_n = n\lambda/4, \quad (n = 1, 2, \dots)$$

As h is increased, $\frac{W_T}{W_0}$ changes from greater than unit 1 to less than 1 as h passes the series of values h_n ,

$$n = 1, 2, \dots$$

The acoustic impedance as seen by the source is, therefore, greater or smaller than that in the absence of the plate depending on where the position of the source is. This effect

on the radiating power is due to the reflection effect of the plate.

V-4 The Effect of the Uniform Flow:

Consider a monopole in a uniform flow in the presence of a semi-infinite plate as shown in figure (5-L).

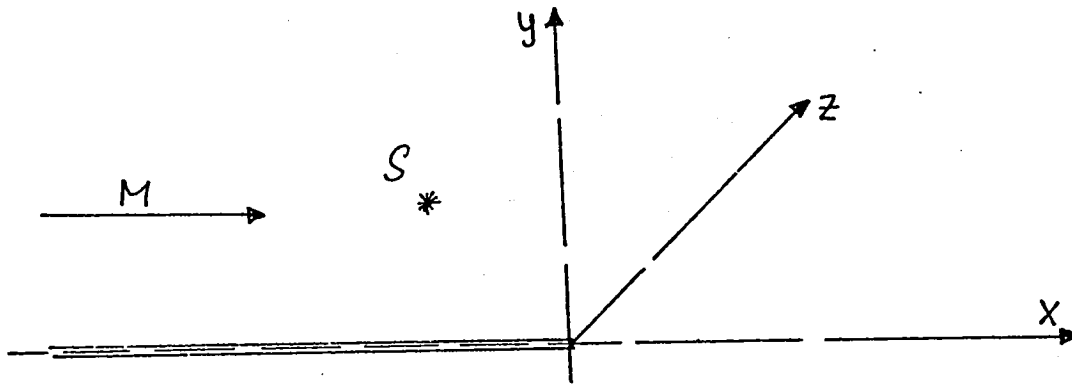


Figure (5-L): A monopole in a uniform flow in the presence of a semi-infinite plate.

The governing differential equation and the boundary conditions for the potential ϕ are given by

$$(1-M^2) \frac{\partial^2 \phi}{\partial x^2} + \frac{\partial^2 \phi}{\partial y^2} + \frac{\partial^2 \phi}{\partial z^2} - 2ikM \frac{\partial \phi}{\partial x} + k^2 \phi = \delta(x-x_0) \delta(y-y_0) \delta(z-z_0) \quad (5-12)$$

where $k = \frac{\omega}{a_0}$

The boundary conditions are:

- (i) $\frac{\partial \phi}{\partial y} = 0$ at $y = 0$; $x < 0$
- (ii) ϕ and its derivatives are continuous elsewhere.
- (iii) The Sommerfeld radiation condition at infinity is satisfied.

This problem can be reduced to the standard form by

letting

$$\phi = e^{-\frac{j k M x}{(1-M^2)}} \psi(\bar{x}, \bar{y}, \bar{z}, \bar{k}) \quad (5-13)$$

where: $\bar{x} = x$; $\bar{y} = y \sqrt{1-M^2}$; $\bar{z} = z \sqrt{1-M^2}$; $\bar{k} = \frac{k}{1-M^2}$

The equation and the boundary conditions for ψ are then:

$$\frac{\partial^2 \psi}{\partial \bar{x}^2} + \frac{\partial^2 \psi}{\partial \bar{y}^2} + \frac{\partial^2 \psi}{\partial \bar{z}^2} + \bar{k}^2 \psi = \delta(\bar{x}-\bar{x}_0) \delta(\bar{y}-\bar{y}_0) \delta(\bar{z}-\bar{z}_0) \quad (5-14)$$

- (i) $\frac{\partial \psi}{\partial \bar{y}} = 0$ at $\bar{y} = 0$; $\bar{x} < 0$
- (ii) ψ and its derivatives are continuous elsewhere.
- (iii) Sommerfeld radiation condition at infinity is satisfied.

Therefore, the diffraction problem for ψ in the new variables is identical to that for a monopole source in a stationary medium.

If the potential due to the incident wave only is considered the solution of Ψ is

$$\Psi = \Psi_0 F(\bar{\beta}) \quad (5-15)$$

where $\Psi = -\frac{e^{i\bar{k}\bar{r}}}{4\pi\bar{r}}$ and $F(\bar{\beta})$ is the diffraction factor.

Assuming, for simplicity, that both the source and the observation point lie on the X-Y plane, then $\bar{\beta}$ is given by the relation (figure 5-A):

$$\bar{\beta}^2 = \bar{k} (\vec{SO} + \vec{OP} - \vec{SP})$$

In term of the original variables, the expression is

$$\bar{\beta}^2 = \frac{\bar{k}}{1-M^2} \left[\sqrt{x_0^2 + (1-M^2)y_0^2} + \sqrt{x^2 + (1-M^2)y^2} - \sqrt{(x-x_0)^2 + (1-M^2)(y-y_0)^2} \right] \quad (5-16)$$

It will first be shown that along the straight line SOP' shown in figure (5-M) the value of $\bar{\beta}$ is equal to zero for all values of K and M .

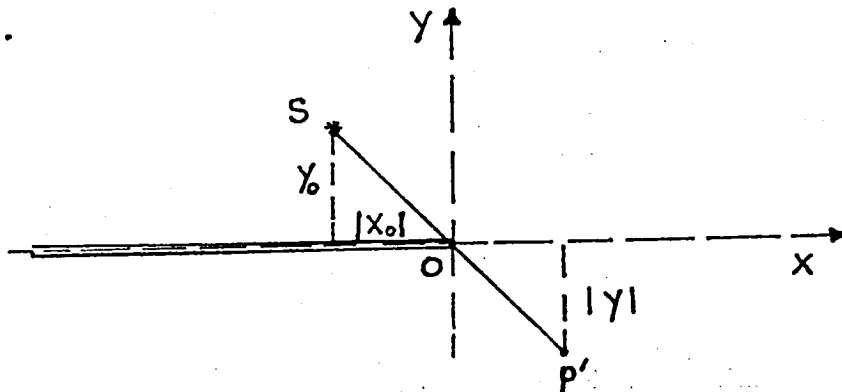


Figure (5-M): Geometry to show the boundary according to ray acoustics.

Obviously, if SOP' is a straight line, its end point (X_0, Y_0) and (X, Y) satisfy the relations:

$$X = -\Gamma X_0 \quad ; \quad Y = -\Gamma Y_0$$

where Γ is a positive constant. By a direct substitution, it is found that:

$$\begin{aligned} & \sqrt{X_0^2 + (1-M^2)Y_0^2} + \sqrt{X^2 + (1-M^2)Y^2} - \sqrt{(X-X_0)^2 + (1-M^2)(Y-Y_0)^2} \\ & \hspace{20em} (5-17) \\ & = \sqrt{X_0^2 + (1-M^2)Y_0^2} + \Gamma \sqrt{X_0^2 + (1-M^2)Y_0^2} - \sqrt{(1-\Gamma^2)[X_0^2 + (1-M^2)Y_0^2]} = 0 \end{aligned}$$

This proves that $\bar{\beta}$ has a zero value everywhere on the line SOP' for all values of the wave number k and flow Mach number M . When, in particular, the wave number becomes very large ($k \rightarrow \infty$), then the transition layer collapses onto this line SOP' . Therefore, the line SOP' is the boundary line between the regions of transmission and the shadow according to ray acoustics for all Mach numbers as long as the wave number k is large. Latter in this section, the effect of the Mach number on the transition layer thickness will be shown.

From this, it is concluded that the line drawn from the source to the trailing edge of the plate completely defines the position of the ray acoustics boundaries irrespective of whether the medium is stationary or moving figure (5-N). In the special case of a plane wave incident on the plate, the above conclusion agrees with the result of Candel (5) as shown below.

The incident field due to a monopole at (r_0, θ_0) and $z = 0$ is given by the expression:

$$\phi_i = -\frac{e^{-ikM \left[(x + r_0 \cos \theta_0) - \sqrt{(x + r_0 \cos \theta_0)^2 + (1-M^2)(y - r_0 \sin \theta_0)^2} \right]}}{\sqrt{(x + r_0 \cos \theta_0)^2 + (1-M^2)(y - r_0 \sin \theta_0)^2}} \quad (5-18)$$

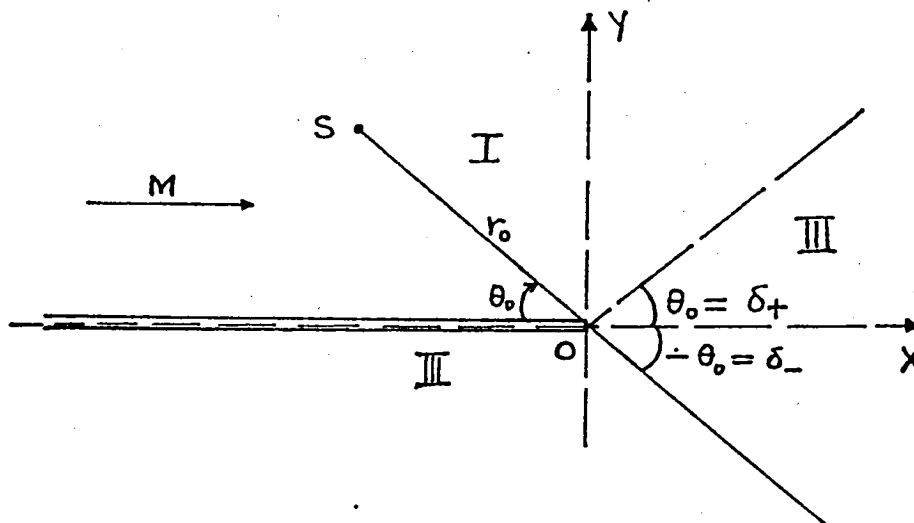


Figure (5-N): A monopole source field in two-dimensional geometry in the presence of a uniform flow.

When the source is moved to infinity along the line OS figure (5-N), the incident wave on the plate due to the concentrated source becomes identical to that of a plane wave with its potential given by the asymptotic expression of equation (5-18) with $r_o \rightarrow \infty$ as:

$$\phi_i \approx e^{-ik \left[\frac{x}{1-M^2} \left(M - \frac{\cos \theta_o}{\sqrt{1-M^2 \sin^2 \theta_o}} \right) + \frac{y \sin \theta_o}{\sqrt{1-M^2 \sin^2 \theta_o}} \right]} \quad (5-19)$$

The potential due to a plane wave of incidence angle Θ figure (5-0) is given by the expression in the equation 19 of Candel (5) as:

$$\phi_i = e^{-ik \left[\frac{x \cos \Theta}{1-M \cos \Theta} + \frac{y \sin \Theta}{1-M \cos \Theta} \right]} \quad (5-20)$$

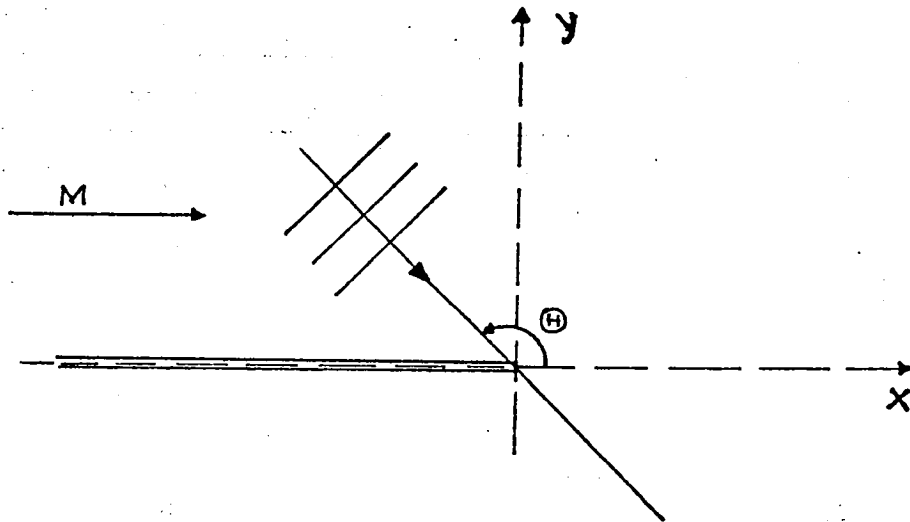


Figure (5-0): A plane wave field in two-dimensional geometry in the presence of a uniform flow.

Comparing equation (5-19) and (5-20) it is seen that the incidence angle Θ is equal to $\pi - \theta_0$ only when $M = 0$. In general, when $M \neq 0$, the incidence angle Θ of the plane wave given by equation (5-20) is a function of θ_0 and the relationship is obtained by comparing the exponents contained in equations (5-19) and (5-20) thus:

$$\frac{1}{1-M} \left[M \frac{\cos \theta_0}{\sqrt{1-M^2 \sin^2 \theta_0}} \right] = \frac{\cos \Theta}{1-M \cos \Theta} \quad (5-21)(a)$$

and

$$\frac{\sin \theta_0}{\sqrt{1-M^2 \sin^2 \theta_0}} = \frac{\sin \Theta}{1-M \cos \Theta} \quad (5-21)(b)$$

The following relation is then obtained from equation (5-21)

(b) as:

$$\tan \theta_0 = \frac{\sin \Theta}{M - \cos \Theta} \quad (5-22)$$

This relation is also found to satisfy equation (5-21)(a).

According to the conclusion mentioned above, the angle θ_0 is also the angle of the ray acoustic boundaries which were determined and denoted as δ_+ and δ_- by Candel (5), figure (5-N). Thus:

$$\tan \delta_{\pm} = \tan (\pm \theta_0) = \pm \frac{\sin \Theta}{M - \cos \Theta} \quad (5-23)$$

This relationship between δ_{\pm} and Θ derived by the present general method is identical to equation 35 obtained by Candel (5) for the case of the plane wave.

The effect of the Mach number on the thickness of the transition layer is now examined. An angle α is introduced, for this purpose, using the line $\bar{\beta} = 0$ as the baseline (figure 5-P). The angle α is defined as positive on the side adjacent to the radiation zone, and is negative on the shadow region.

In terms of α , the asymptotic expression of $\bar{\beta}^2$ for large r is obtained by a lengthy but straightforward calculation.

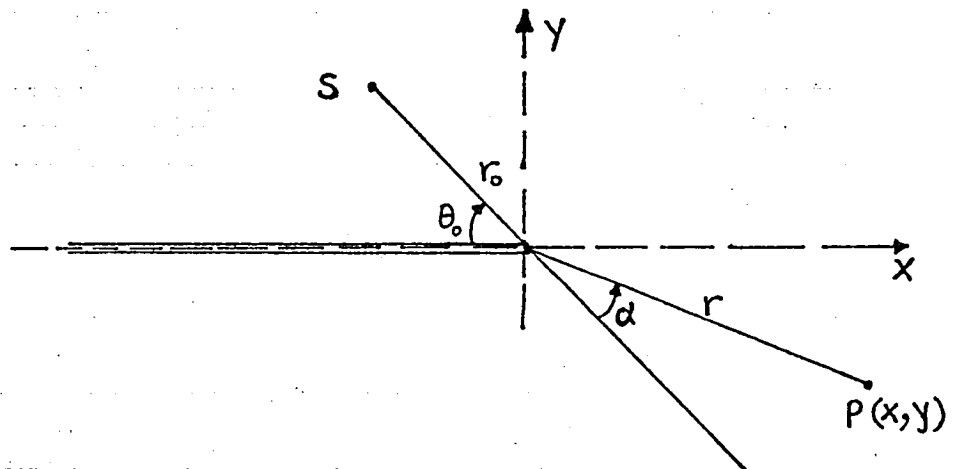


Figure (5-P): Transition zone layout.

The final result is given as:

$$\bar{\beta}^2 = \frac{kr_0}{1-M^2} \left[\sqrt{1-M^2 \sin^2 \theta_0} + \frac{M^2 \sin(\theta_0 - \alpha) \sin \theta_0 - \cos \alpha}{\sqrt{1-M^2 \sin^2(\theta_0 - \alpha)}} \right] \quad (5-24)$$

$$+ O(r_0/r)$$

This result is derived by assuming **S** and **P** are in the same plane. The sign of $\bar{\beta}$ is chosen so that $\bar{\beta} < 0$ when $\alpha > 0$ and $\bar{\beta} \geq 0$ when $\alpha < 0$. It follows from this choice that:

- (i) $\bar{\beta} \rightarrow -\infty$ and $F(\bar{\beta}) \rightarrow 1$ as $\alpha \rightarrow \infty$
- (ii) $\bar{\beta} = 0$, $F(\bar{\beta}) = 1/2$ at $\alpha = 0$ (5-25)
- (iii) $\bar{\beta} \rightarrow +\infty$, $F(\bar{\beta}) \rightarrow 0$ as $\alpha \rightarrow -\infty$

From the mathematical table of $F(\bar{\beta})$ (Ref. 1), it is found that $F(\bar{\beta})$ is practically equal to 1 when $\bar{\beta} \simeq -20$. The corresponding value of α , denoted by α_+ defines the position of the "bright" edge of the transition layer.

Similarly, when $\bar{\beta} \simeq +20$, $F(\bar{\beta})$ is practically equal to zero, and the corresponding α , denoted by α_- , defines the position of the "dark" edge of the transition layer.

As one can see from the expression for $\bar{\beta}^2$, α_+ and α_-

are functions of kr_0 , θ_0 and M . In table I and figure (5-Q) next page, the values of α_+ and α_- are listed. These values are calculated by assuming $kr_0 = 2500$, $\theta_0 = \pi/4$ for various values of the Mach numbers.

From this example, it is seen that the thickness of the transition layer at the trailing edge of the plate becomes narrower when the Mach number increases, and the decrease in thickness is more pronounced on the side adjacent to the shadow region (under the plate). The effect of the Mach number is, therefore, to increase the size of the shadow region and hence make the shielding more effective. Table II shows such calculations.

Table I

Transition layer thickness as a function of the Mach number.

Mach number (M)	0	0.2	0.4	0.6	0.8	0.95
α_+ (degrees)	32.9	32.7	32.2	31.2	29.5	27.7
α_- (degrees)	-32.9	-32.0	-29.5	-25.5	-20.3	-15.7
Layer thickness (degrees)	65.8	64.7	61.7	56.7	49.8	43.4

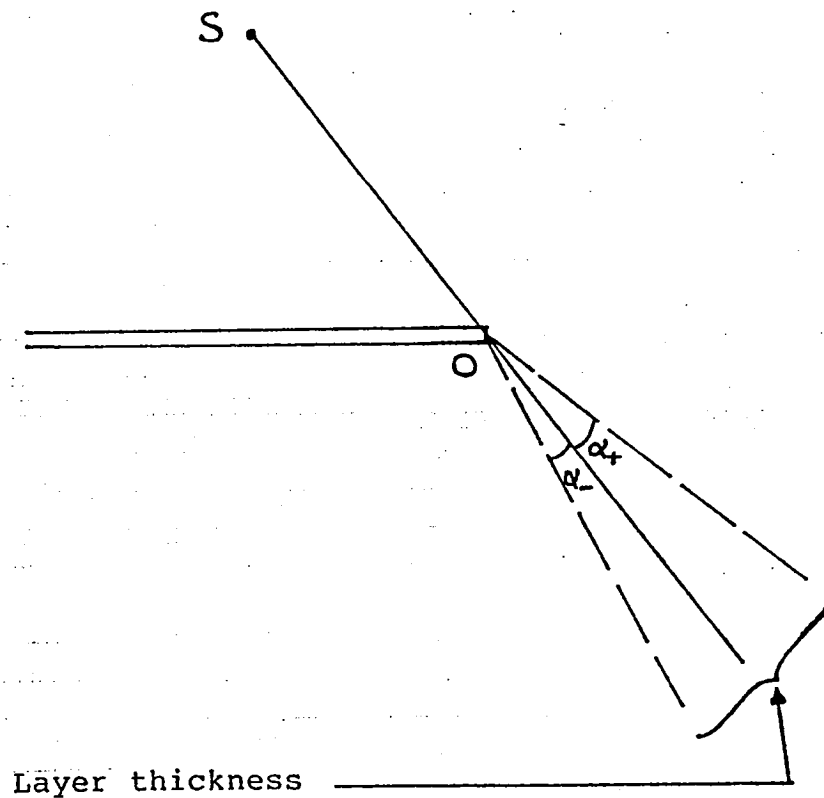


Figure (5-Q): Transition layer thickness.

Table II

Values of $\bar{\beta}$ when $kr_0 = 2500$ and $\theta_0 = \pi/4$

α	M = 0	M = .2	M = .4	M = .6	M = .8	M = .95
-35	21.263	21.820				
-30	18.301	18.759	20.318	23.763		
-25	15.304	15.667	16.891	19.546	25.706	
-20	12.278	12.551	13.463	15.402	19.670	
-15	9.229	9.419	10.049	11.358	14.096	
-10	6.162	6.279	6.660	7.437	8.982	
-5	3.084	3.137	3.308	3.649	4.297	
0	0	-1.456 ⁻⁰³	-1.019 ⁻⁰³	-1.651 ⁻⁰³	-2.543 ⁻⁰³	-3.863 ⁻⁰³
5	-3.084	-3.125	-3.258	-3.512	-3.959	-4.522
10	-6.162	-6.235	-6.464	-6.894	-7.628	-8.514
15	-9.229	-9.322	-9.614	-10.154	-11.053	-12.105
20	-12.278	-12.382	-12.708	-13.304	-14.277	-15.388
25	-15.304	-15.411	-15.747	-16.355	-17.335	-18.439
30	-18.301	-18.405	-18.732	-19.321	-20.264	-21.307
35	-21.263	-21.361	-21.666	-22.216		

BIBLIOGRAPHY:

1. Abramowitz, M. and Stegun, I.A.
"Handbook of Mathematical Functions"
U.S. Department of Commerce (National Bureau of Standards).
2. Broadbent, E.G.
"Noise Shielding for Aircraft."
Progress in Aerospace Sciences, Vol. 17, (1977).
3. Broadbent, E.G.
"Acoustic ray theory applied to vortex refraction."
J. Inst. of Math. Applications Vol. 19 (1977).
4. Broadbent, E.G. and Butler, G.F.
"The Calculation of noise shielding by a delta wing."
Royal Aircraft Establishment (RAE) Tech. Report 70116
(1970).
5. Candel M.S.
"Diffraction of a plane wave by a half plane in a subsonic
and supersonic medium."
J. Acoustic Soc. Am. Vol. 54, (1973).
6. Clapper, W.S.; Mani, R.; Stringas, E.J. and Banerian, G.
"Development of a Technique for Inflight Jet Noise
Simulation - Part I."
Journal of Aircraft (1978).
7. Conticelli, V.M.; Di Blasi, A. and O'Keefe, J.V.
"Noise Shielding Effects for Engine-over-the-wing
Installations."
AIAA 2nd Aero-Acoustics Conference (1975).

8. Cooke, J.C.
"Refraction of Sound by a Vortex."
Royal Aircraft Establishment (RAE) Tech. Report 67175
(1967).
9. Cooke, J.C.
"Notes on the Diffraction of Sound."
Royal Aircraft Establishment (RAE) Tech. Report 69283
(1969).
10. Curle, N.
"The Influence of Solid Boundaries Upon Aerodynamic
Sound."
Proc. Roy. Soc. Lond. A 231 pp. 505-514.
11. Davis, S.S.
"Theory of Discrete Vortex Noise."
AIAA Journal Vol. 13, No. 3, Mar. 1975.
12. Embleton, T.F.W.
"Line integral theory of barrier attenuation."
J. Acoust. Soc. Am. 67, 42-45 (1980).
13. Falarski, M.D.; Aoyagi, K. and Koenig, D.G.
"Acoustic Characteristics of Large-scale STOL Models at
Forward Speeds."
NASA SP-320
14. Ffowcs-Williams and Hawkings.
"Sound generation by turbulence and surfaces in arbitrary
motion."
Phil. Trans. R. Soc. A 264, 321 (1969).

15. Fink, M.
"Forward flight effects on externally blown flap noise."
J. of Aircraft Vol. 15, No. 9 (1978).
16. Hoch, R.G.
"Use of the Bertin Aerotrainer for investigating forward flight effects on aircraft engine noise."
3rd AIAA Aero-Acoustics Conference; AIAA paper 76-534 (1976).
17. Howe, M.S.
"The Generation of Sound by Aerodynamic source in an inhomogeneous steady flow."
J. Fluid Mech. (1975) Vol. 67, Part 3, pp. 597-610.
18. Jeffery, R.W.; Broadbent, E.G. and Hazell, A.F.
"A wind tunnel investigation of vortex refraction effects on aircraft noise propagation."
3rd AIAA Aero-Acoustics Conference; AIAA paper, 76-588 (1976).
19. Jeffery, R.W. and Holbeche, T.A.
"An experimental investigation of noise shielding effects for a Delta-winged aircraft in flight, wind-tunnel and anechoic room."
2nd AIAA Aero-Acoustics Conference, AIAA paper, 75-513 (1975).
20. Jones, D.S.
"The effect of radiation due to a moving source on a vortex sheet."
Proc. Roy. Soc. Edinburgh (A) 72, 14, 1973/4.

21. Kelvin, Lord
"On the waves produced by a single impulse in water of any depth, or a dispersive medium."
Phil. Mag. (5), 23, 1887 pp. (252-5).
22. Lan, C.E. and Campbell, J.F.
"A Wing-jet interaction theory for USB configurations,"
J. of Aircraft, Vol. 13, No. 9, Sept. (1976) pp. 718-726.
23. Larson, R.S. ; McColgan C.J.; and Packman, A.B.
"Jet noise source modification due to forward flight."
AIAA Journal Vol. 16, No. 3 (1978).
24. Lasagna, P.L. and Putnam, T.W.
"Externally Blow Flap Impingement Noise."
NASA SP-320.
25. Leppington, F.G.
"Curvature effects in the diffraction of short waves into a shadow."
Royal Aircraft Establishment (RAE) Tech. Report 70183
(1970).
26. Levine, H.
"On source radiation."
JIAA TR-29 (1980).
27. Levine, H.
"A note on sound radiation from distributed sources."
Journal of Sound and Vibrations 68(2) page 203-207
(1979).
28. Lighthill, M.J.
"On sound generated aerodynamically I."
Pro. Roy. Soc. A 211, 564 (1952).

29. Lighthill, M.J.
"on sound generated aerodynamically II."
Pro. Roy. Soc. A 222, 1 (1954).
30. Lush, P.A.
"Measurements of subsonic jet noise and comparison with theory."
J. Fluid Mech. (1971), Vol. 46, Part 3, pp. 477-500.
31. MacDonald, H.M.
"A class of diffraction problems."
Pro. Lond. Math. Soc. (2) 14, 410 (1915).
32. Maekawa, Z.
"Noise reduction by Screens."
Appl. Acoustics 1, pp. 157-173 (1969).
33. Morse, P.M. and Feshbach, H.
"Methods of Mathematical Physics." Vol. I pp. 403.
McGraw-Hill (1953).
34. Noble, B.
"Methods based on the Wiener-Hopf Technique." (1958)
35. Orszag, S.A. and Crow, S.C.
"Instability of a vortex sheet leaving a semi-infinite plate."
Stud. Appl. Maths. 49, 167 (1970).
36. Powell, A.
"On the aerodynamic noise of a rigid flat plate moving at zero incidence."
J. of the Acoustical Soc. of America. Vol. 31, No. 12 (1959).

37. Rawlins, A.D.
"The engine-over-the-wing noise problem."
Journal of Sound and Vibrations (1977) 50 (4), 553-569.
38. Reshotko, M ; Goodykoontz, J.H. and Dorsch, R.G.
"Engine-over-the-wing noise research."
AIAA 6th Fluid and Plasma Dynamics Conference,
AIAA paper 73-631 (1973).
39. Ribner, H.S.
"Reflection, Transmission and Amplification of sound by
a moving medium."
J. Acoust. Soc. America, Vol. 29, 1957, pp. 435-441.
40. Strout, F.G. and Atencio, A.
"Flight effects on JTBD engine jet noise measured in a
40' x 40' tunnel."
J. of Aircraft Vol. 14, No. 8 (1976).
41. Thiessen, G.J.
"On the efficiency of an acoustic line source with
progressive phase shift."
Applied physics; Canadian National Research Council
(1955).
42. Ting, L.
"Radiation of an acoustic source near the trailing edge
of a wing in forward motion."
AIAA Journal Vol. 18. No. 3.

